

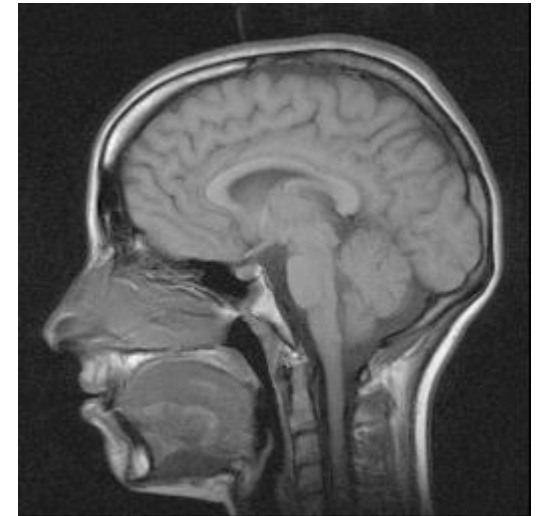
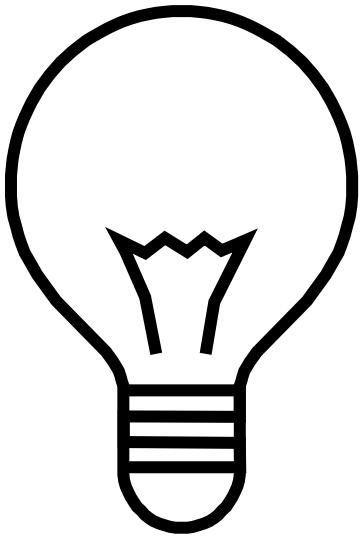


Oxford School on Neutron Scattering

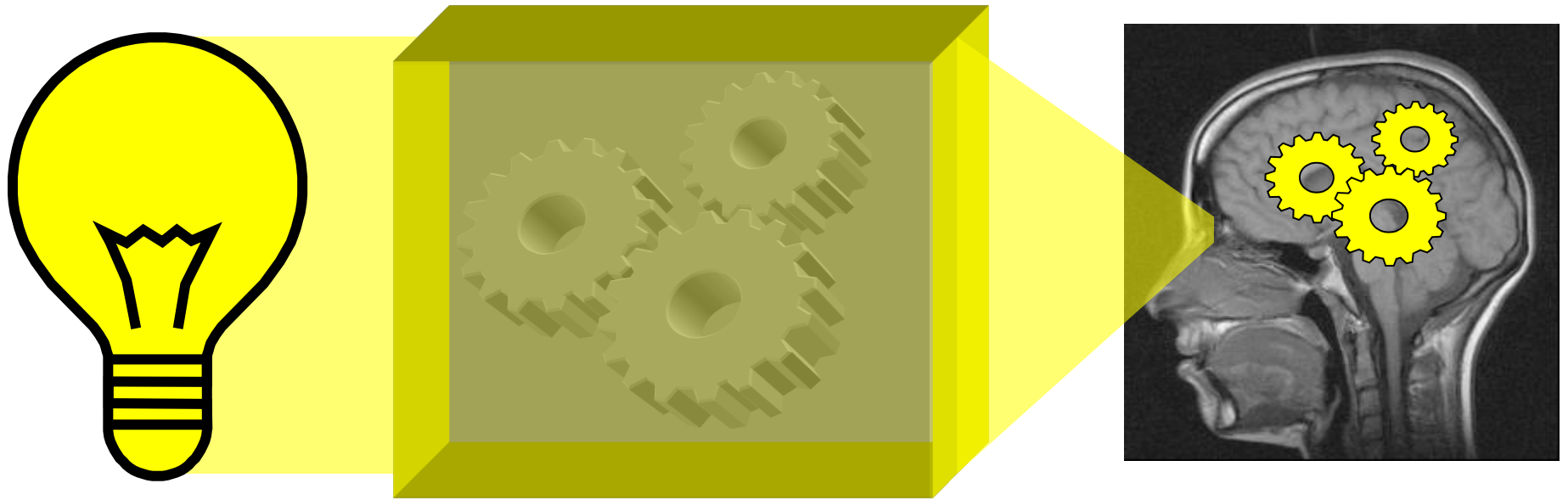
Neutron imaging

Nikolay Kardjilov

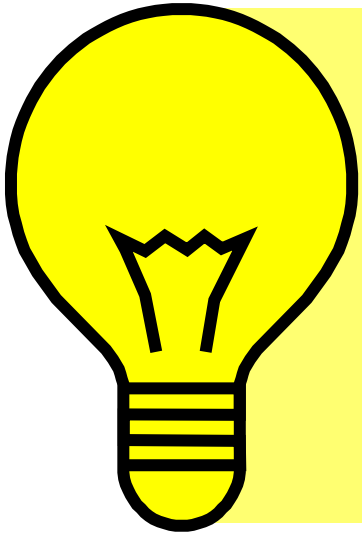
Neutron imaging



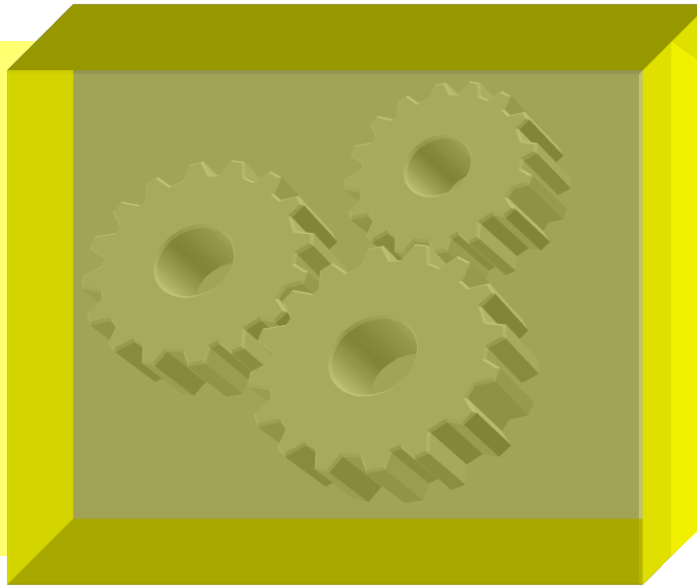
Neutron imaging



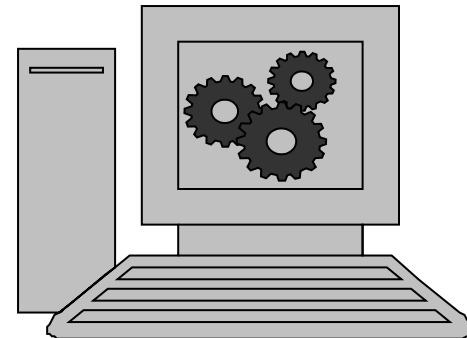
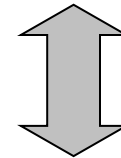
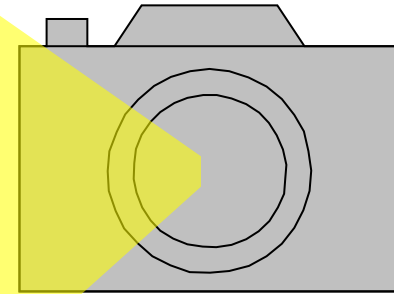
Source



Sample



Detector



Neutron imaging

Introduction



One of the first X-ray experiments late in 1895 performed by [Konrad Röntgen](#) was a film of a hand.

The bones and also finger rings deliver much higher contrast than the soft tissue.

Neutron imaging

Introduction

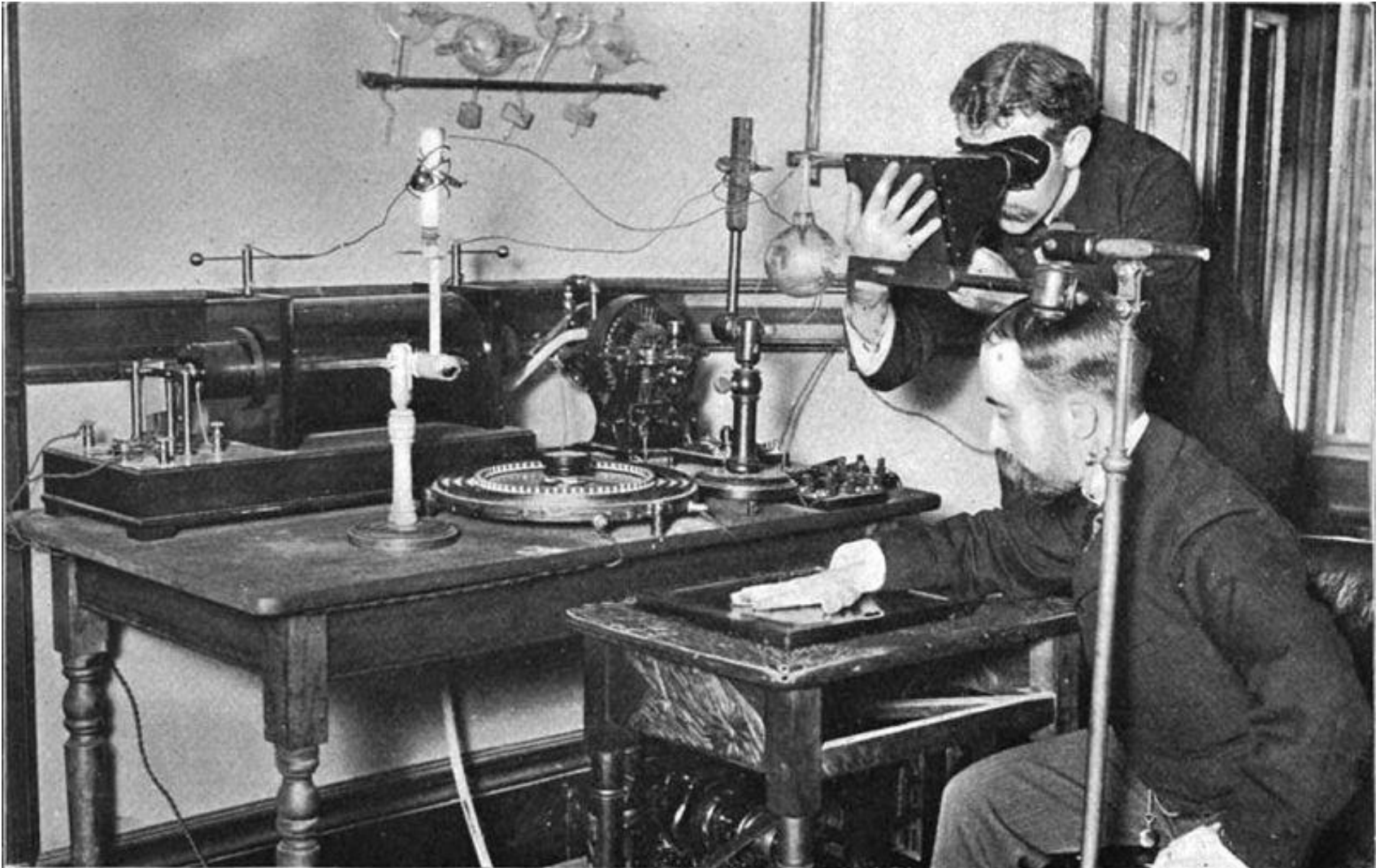


Photo of experimenters taking an X-ray with an early Crookes tube apparatus, from the late 1800s.

Neutron imaging

Roots of neutron radiography

Comparison between x-ray
and neutron images

x-rays



Berlin, 1935 – 1938

H. Kallmann & Kuhn with Ra-Be
and neutron generator

neutrons



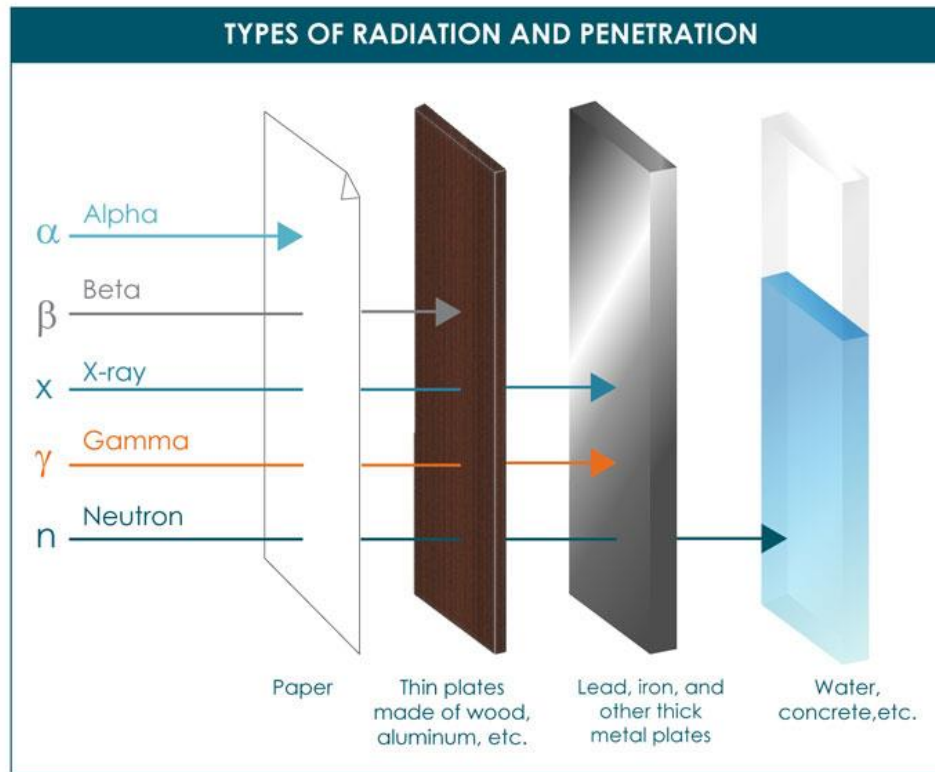
Berlin until Dec. 1944

O. Peter with an
accelerator neutron source

But the real programs with neutrons started after World War II at research reactors

Physical Background

- Free neutrons are able to penetrate matter of relevant thickness (several μm to dm)

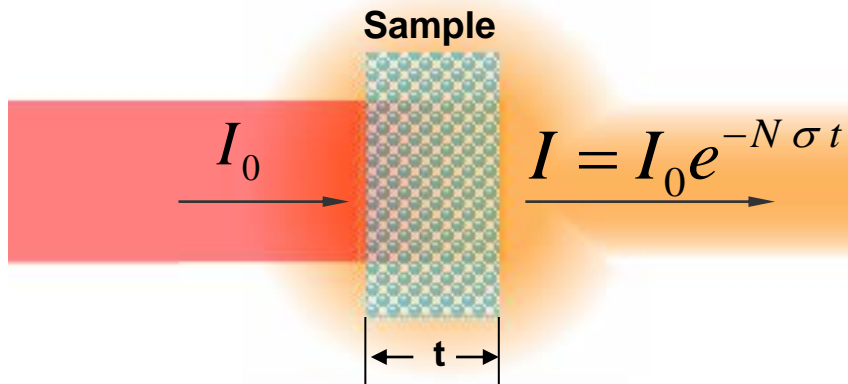


<https://www.mirion.com/learning-center/radiation-safety-basics/types-of-ionizing-radiation>

Interaction principle of neutrons with matter

- Neutrons interact with the **nuclei** of the atoms only
- The probability for interaction with matter is expressed by „*microscopic cross-sections*“ – σ , the unit is „barn = 10^{-24} cm²“
- For each type of interaction a microscopic cross-section can be defined: $\sigma_{\text{absorption}}$, $\sigma_{\text{scattering}}$, $\sigma_{\text{total}} = \sigma_{\text{abs.}} + \sigma_{\text{scatt.}}$.
- The “*macroscopic cross-section*” Σ , also called “*attenuation coefficient*” is defined as : $\Sigma = N^* \sigma_{\text{tot}}$, the unit is cm⁻¹
- N = nuclear density = $(\rho^* A)/M$ (A =Avogadro’s number, M =mass)
- $\Sigma = N^* \sigma_{\text{tot}} = \sigma_{\text{tot}}^* (\rho^* A)/M \rightarrow \Sigma \sim \rho$

Attenuation in transmission mode



- N – numerical density of sample atoms per cm^3
- I_0 - incident neutrons per second per cm^2
- σ - neutron cross section in $\sim 10^{-24} \text{ cm}^2$
- t - sample thickness

**Transmission
(Beer-Lambert's law)**

$$T = \frac{I}{I_0} = e^{-\Sigma * d} = e^{-\sigma * \frac{A}{M} * \rho}$$

and inverted ...

$$\Sigma * d = \ln\left(\frac{I_0}{I}\right)$$



Thickness d can be
obtained when
 Σ is known

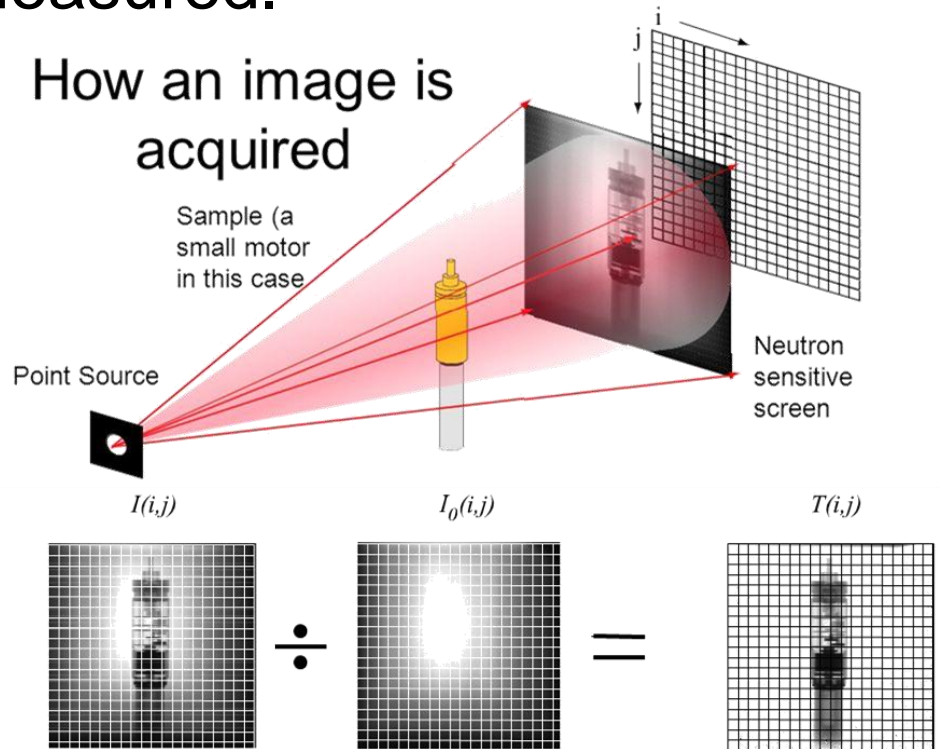
Density or composition
derived if thickness
 d is known

Physical Background

- Neutrons can be detected with suitable devices (neutron imaging detectors)
- The distribution of the neutrons without a sample (unperturbed, «open» beam) I_0 and after interaction within the sample I are measured.

- The ratio of the two images gives the neutron transmission in the beam direction $T(i,j)$

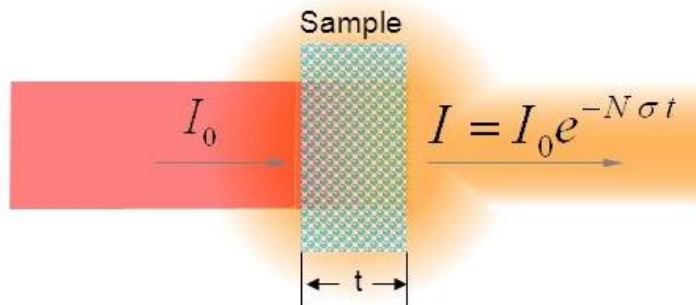
$$T = \frac{I}{I_0} = e^{-\Sigma * d}$$



Physical Background

- The neutron beam can penetrate matter of relevant thickness of several μm to dm.
- The transmission of neutrons through materials can be described by Beer-Lambert law.

- Contrast is due to attenuation of radiation
- Scattering density of material can be extracted
- N - density of sample atoms per cm^3
- I_0 - incident neutrons per second per cm^2
- σ - neutron cross section in $\sim 10^{-24} \text{ cm}^2$



courtesy: Dr. David L. Jacobson (NIST)
<https://slideplayer.com/slide/9149496/>

Physical Background

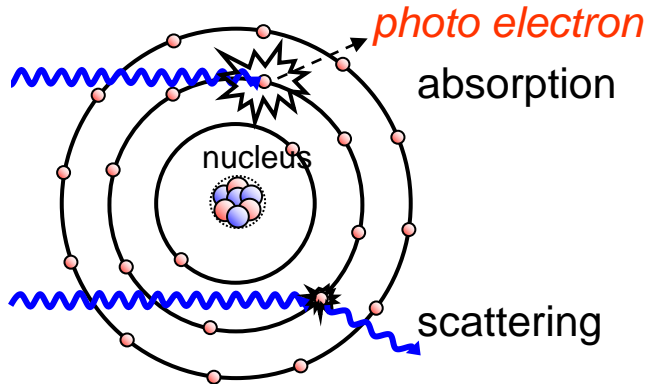
- The neutron beam can penetrate matter of relevant thickness of several μm to dm.
- The transmission of neutrons through materials can be described by Beer-Lambert law.
- The neutron transmission depends on the properties of the material and neutron energy
- Neutrons «distinguish» not only materials but also particular isotopes (e.g. $^{10}\text{B}/^{11}\text{B}$; $^6\text{Li}/^7\text{Li}$)

- **Neutrons** interact with the **nuclei** of the sample materials
- **X rays** only interact with the **electrons** of the atomic shell

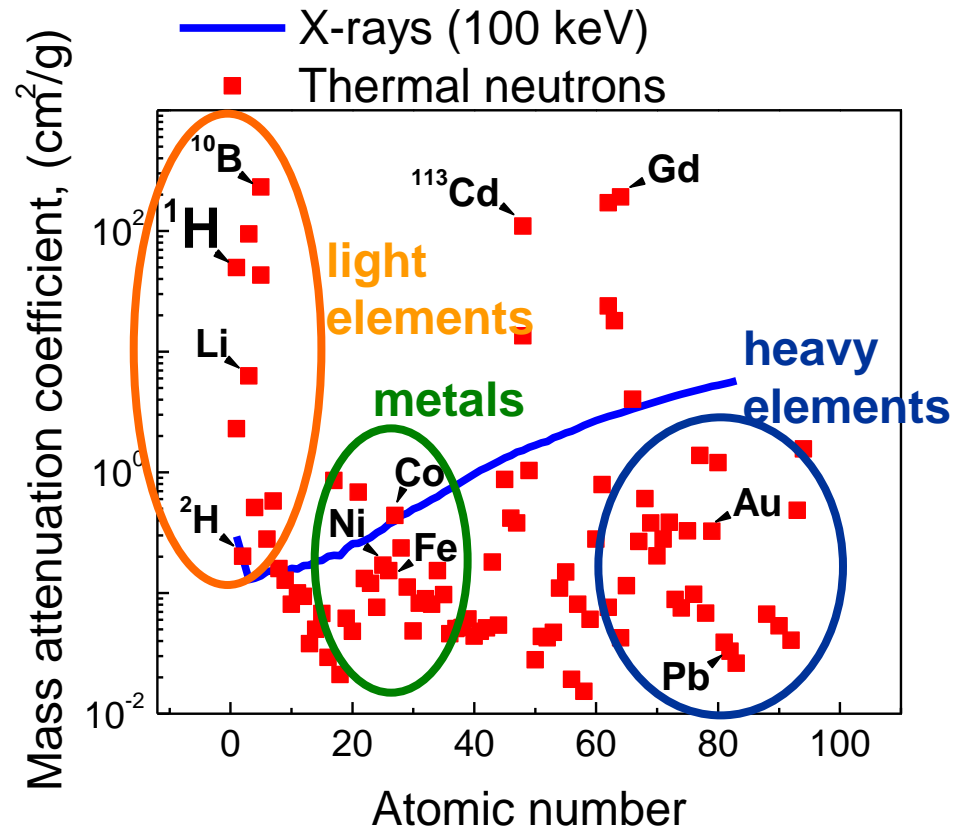
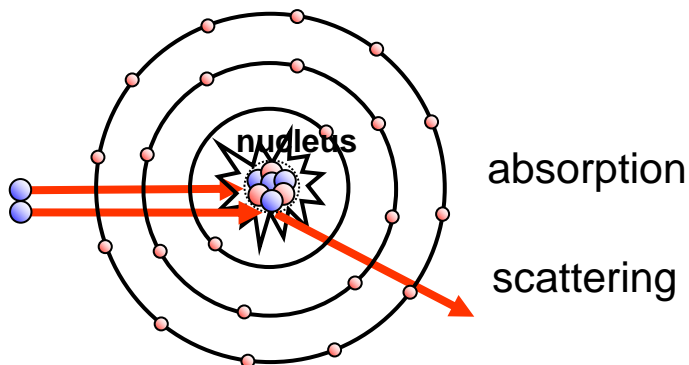
Neutron imaging

Neutron interaction with matter

X-rays



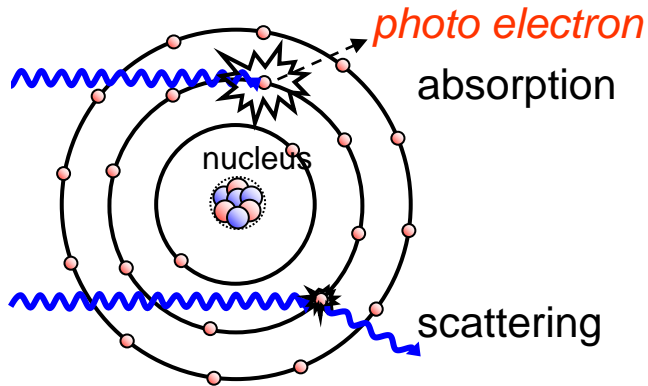
neutrons



Neutron imaging

Neutron interaction with matter

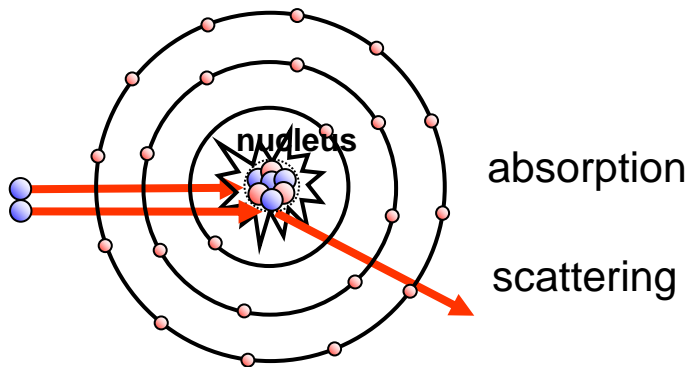
X-rays



Attenuation coefficients with X-ray [cm²g⁻¹]

| | 1a | 2a | 3b | 4b | 5b | 6b | 7b | 8 | 1b | 2b | 3a | 4a | 5a | 6a | 7a | 0 | | |
|-------------|------|-------------|-------------|-------------|-------------|------------|-------------|-------------|-------------|-------------|-------------|-------------|-------------|-------------|-------------|-------------|------------|------------|
| H | 0.02 | | | | | | | | | | | | | | | He 0.02 | | |
| Li | 0.06 | Be 0.22 | | | | | | | | | B 0.28 | C 0.27 | N 0.11 | O 0.16 | F 0.14 | Ne 0.17 | | |
| Na | 0.13 | Mg 0.24 | | | | | | | | | Al 0.38 | Si 0.33 | P 0.25 | S 0.30 | Cl 0.23 | Ar 0.20 | | |
| K | 0.14 | Ca 0.26 | Sc 0.48 | Ti 0.73 | V 1.04 | Cr 1.29 | Mn 1.32 | Fe 1.57 | Co 1.78 | Ni 1.96 | Cu 1.97 | Zn 1.64 | Ga 1.42 | Ge 1.33 | As 1.50 | Se 1.23 | Br 0.90 | Kr 0.73 |
| Rb | 0.47 | Sr 0.86 | Y 1.61 | Zr 2.47 | Nb 3.43 | Mo 4.29 | Tc 5.06 | Ru 5.71 | Rh 6.08 | Pd 6.13 | Ag 5.67 | Cd 4.84 | In 4.31 | Sn 3.98 | Sb 4.28 | Te 4.06 | I 3.45 | Xe 2.53 |
| Cs | 1.42 | Ba 2.73 | La 5.04 | Hf 19.70 | Ta 25.47 | W 30.49 | Re 34.47 | Os 37.92 | Ir 39.01 | Pt 38.61 | Au 35.94 | Hg 25.88 | Tl 23.23 | Pb 22.81 | Bi 20.28 | Po 20.22 | At | Rn 2.53 |
| Fr | | Ra 11.80 | Ac 24.47 | Rf | Ha | | | | | | | | | | | | | |
| Lanthanides | | Ce 5.79 | Pr 6.23 | Nd 6.46 | Pm 7.33 | Sm 7.68 | Eu 5.66 | Gd 8.69 | Tb 9.46 | Dy 10.17 | Ho 10.91 | Er 11.70 | Tm 12.49 | Yb 9.32 | Lu 14.07 | | | |
| Actinides | | Th 28.95 | Pa 39.65 | U 49.08 | Np | Pu | Am | Cm | Bk | Vf | Es | Fm | Md | No | Lr x-ray | | | |

neutrons

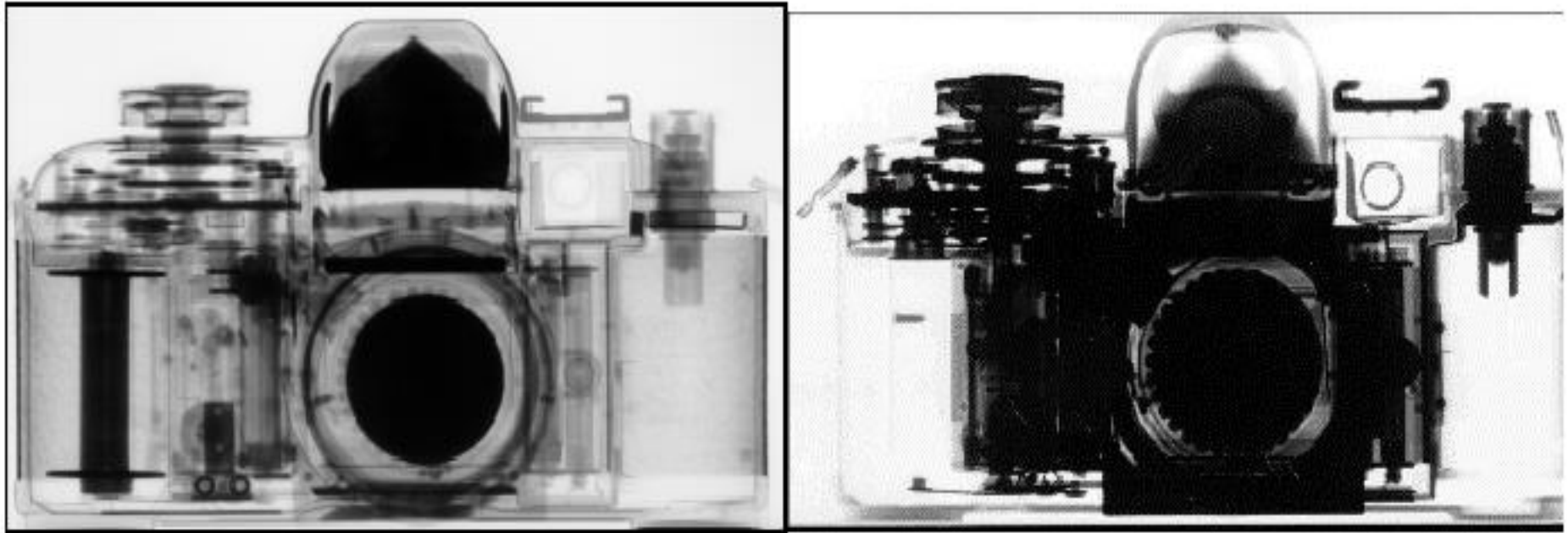


Attenuation coefficients with neutrons [cm²g⁻¹]

| | 1a | 2a | 3b | 4b | 5b | 6b | 7b | 8 | 1b | 2b | 3a | 4a | 5a | 6a | 7a | 0 | | |
|-------------|------|------------|------------|------------|------------|--------------|-------------|---------------|-------------|-------------|-------------|--------------|------------|------------|-------------|------------|------------|------------|
| H | 3.44 | | | | | | | | | | | | | | | He 0.02 | | |
| Li | 3.30 | Be 0.79 | | | | | | | | | B 101.60 | C 0.56 | N 0.43 | O 0.17 | F 0.20 | Ne 0.10 | | |
| Na | 0.09 | Mg 0.15 | | | | | | | | | Al 0.10 | Si 0.11 | P 0.12 | S 0.06 | Cl 1.33 | Ar 0.03 | | |
| K | 0.06 | Ca 0.08 | Sc 2.00 | Ti 0.60 | V 0.72 | Cr 0.54 | Mn 1.21 | Fe 1.19 | Co 3.92 | Ni 2.05 | Cu 1.07 | Zn 0.35 | Ga 0.49 | Ge 0.47 | As 0.67 | Se 0.73 | Br 0.24 | Kr 0.61 |
| Rb | 0.08 | Sr 0.14 | Y 0.27 | Zr 0.29 | Nb 0.40 | Mo 0.52 | Tc 1.76 | Ru 0.58 | Rh 10.88 | Pd 0.78 | Ag 4.04 | Cd 115.11 | In 7.58 | Sn 0.21 | Sb 0.30 | Te 0.25 | I 0.23 | Xe 0.43 |
| Cs | 0.29 | Ba 0.07 | La 0.52 | Hf 4.99 | Ta 1.49 | W 1.47 | Re 6.85 | Os 2.24 | Ir 30.46 | Pt 1.46 | Au 6.23 | Hg 16.21 | Tl 0.47 | Pb 0.38 | Bi 0.27 | Po | At | Rn |
| Fr | | Ra 0.34 | Ac | Rf | Ha | | | | | | | | | | | | | |
| Lanthanides | | Ce 0.14 | Pr 0.41 | Nd 1.87 | Pm 5.72 | Sm 171.47 | Eu 94.58 | Gd 1479.04 | Tb 0.93 | Dy 32.42 | Ho 2.25 | Er 5.48 | Tm 3.53 | Yb 1.40 | Lu 2.75 | | | |
| Actinides | | Th 0.59 | Pa 8.46 | U 0.82 | Np 9.80 | Pu 50.20 | Am 2.86 | Cm | Bk | Cf | Es | Fm | Md | No | Lr neut. | | | |

Neutron imaging

Neutron radiography - examples




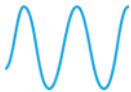

The example for a camera helps to explain differences in neutron (left) and X-ray (right) radiography. Whereas the hydrogen containing parts can be visualised with neutron even at thin layers, thicker metallic components are hard to penetrate with X-rays.

Images courtesy: Dr. Eberhard Lehmann (Paul-Scherrer-Institute, Switzerland)

Resolution

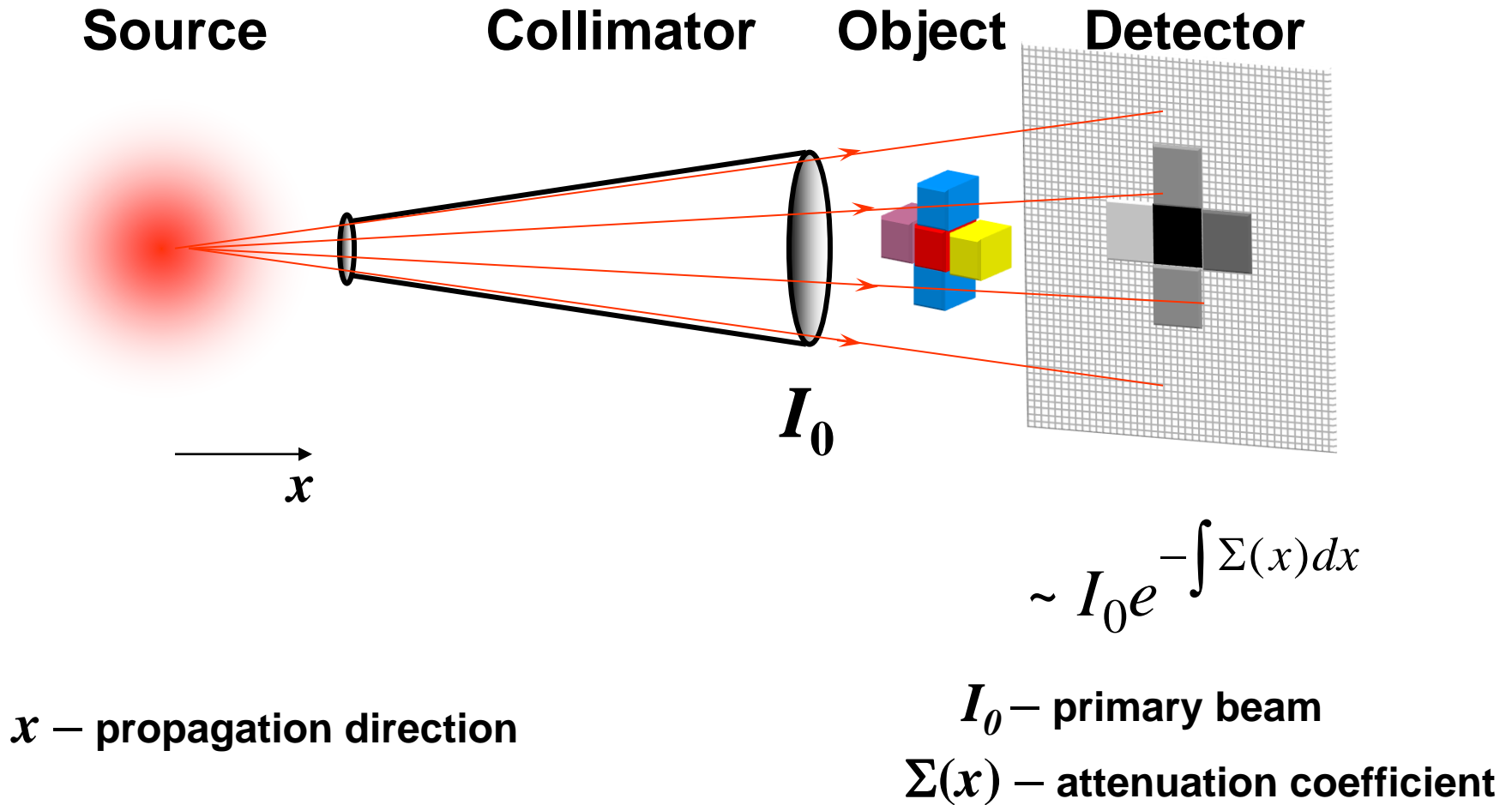
- Beam optimisation ←
- Detector development

Contrast

- Neutron interaction with matter
 -  - absorption
 -  - scattering
 -  - magnetic interaction

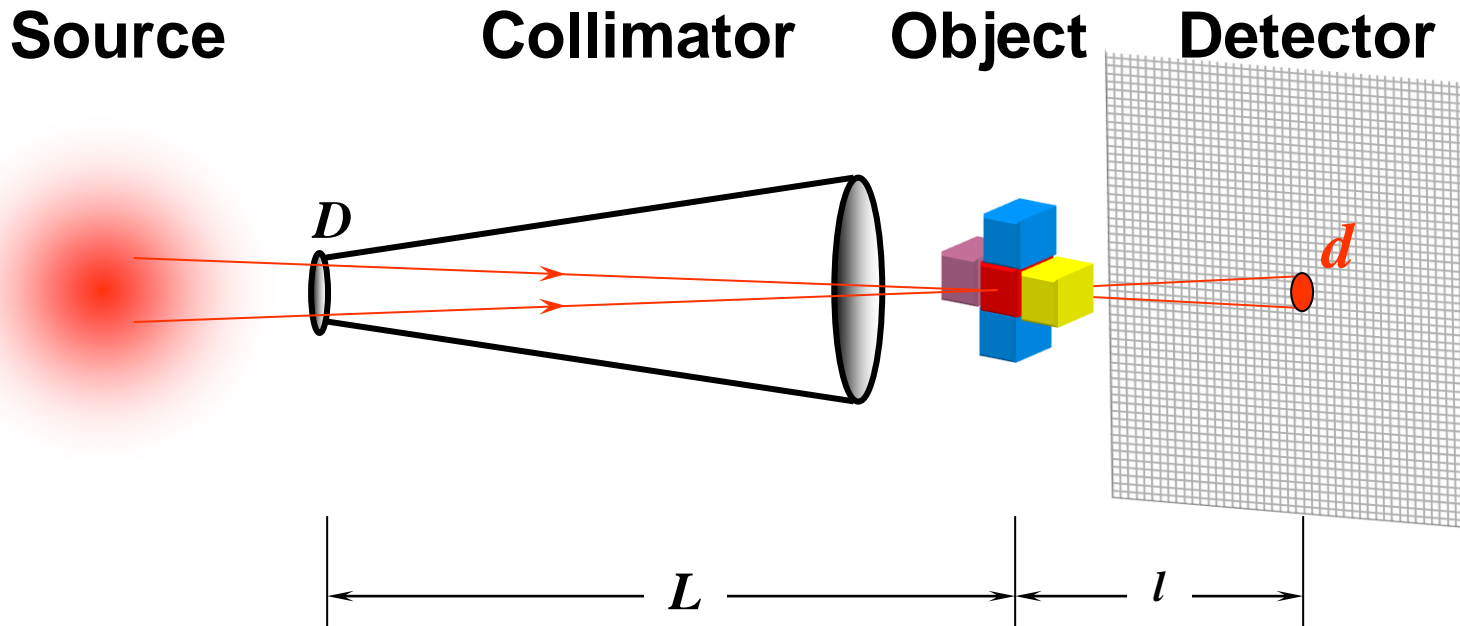
Neutron imaging

Beam optimisation



Neutron imaging

Beam optimisation



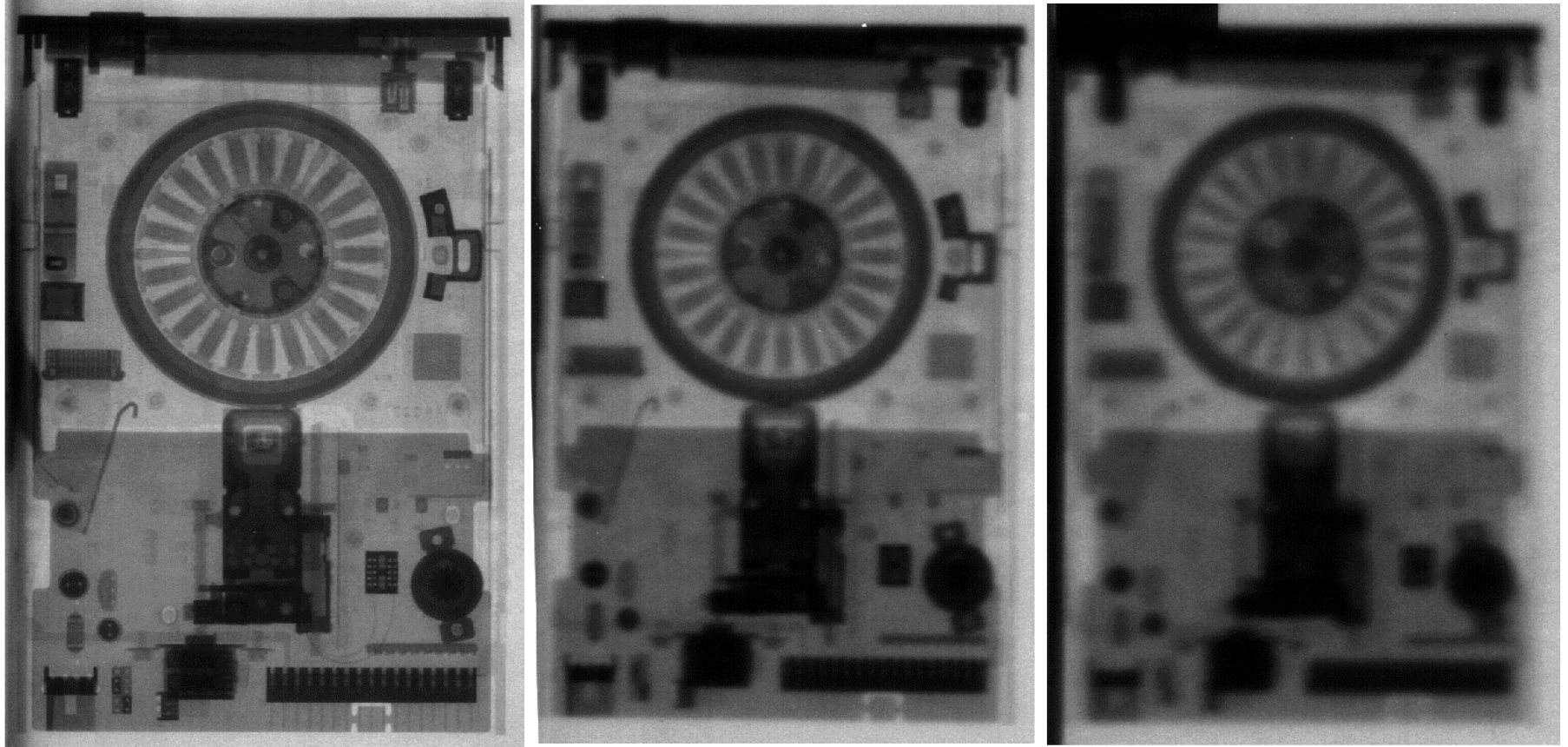
D – Collimator aperture

L – Distance Collimator-Object

l – Distance Object-Detector

$$d = \frac{l}{L/D}$$

Neutron imaging

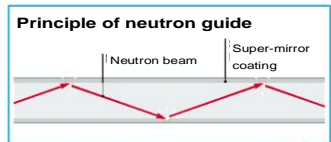
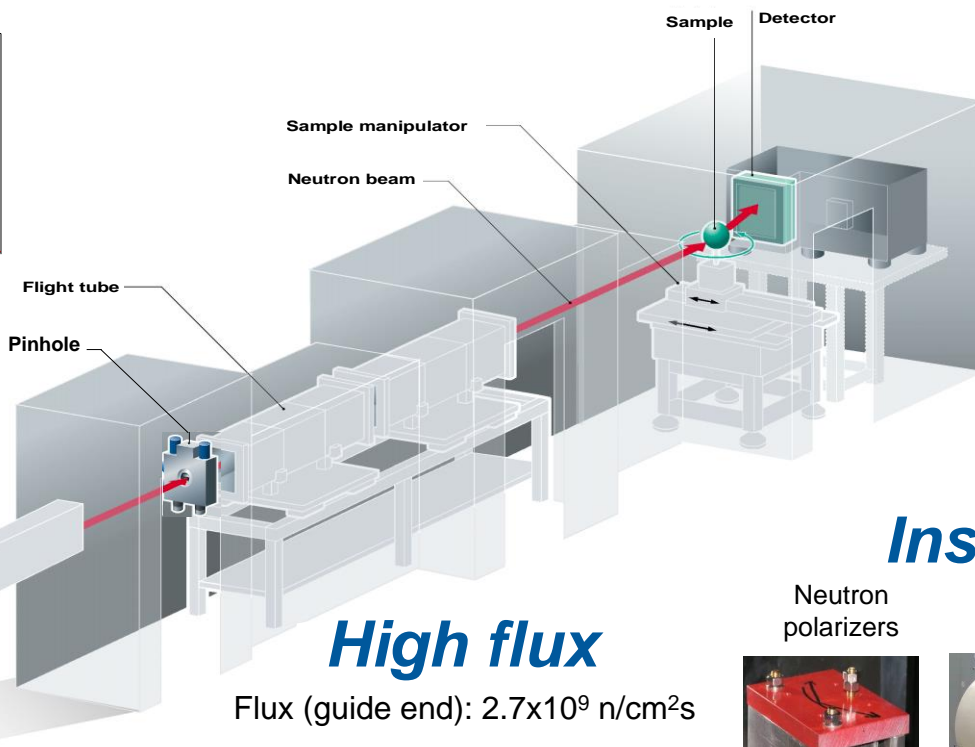
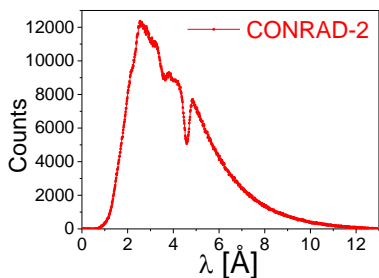


Radiographs of a 3,5" floppy drive in 0 cm, 10 cm and 20 cm distance from a film + Gd sandwich taken at a cold neutron guide with $L/D=71$.

B. Schillinger, Estimation and measurement of L/D on a cold and thermal neutron guide, in: Nondestructive Testing and Evaluation, World Conference on Neutron Radiography, vol. 16, Osaka, 1999, pp. 141–150

Cold neutrons

Wavelength range: 1.5 Å – 10 Å



Guide system: super-mirror coated neutron guide (M=3) with a curvature of 750 m and length of 15 m followed by linear guide section (M=2) with a length of 10 m.

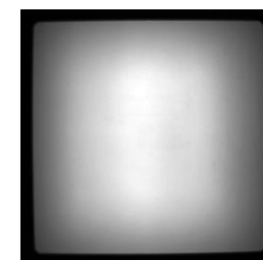
High flux

Flux (guide end): 2.7×10^9 n/cm²s

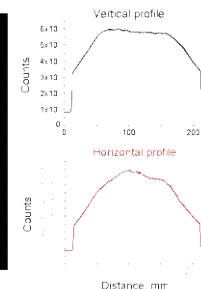


Large beam

Beam size: 20 cm x 20 cm



20 cm



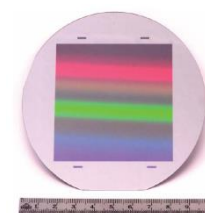
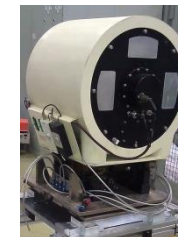
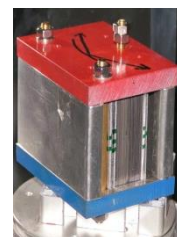
Instrumentation

Neutron polarizers

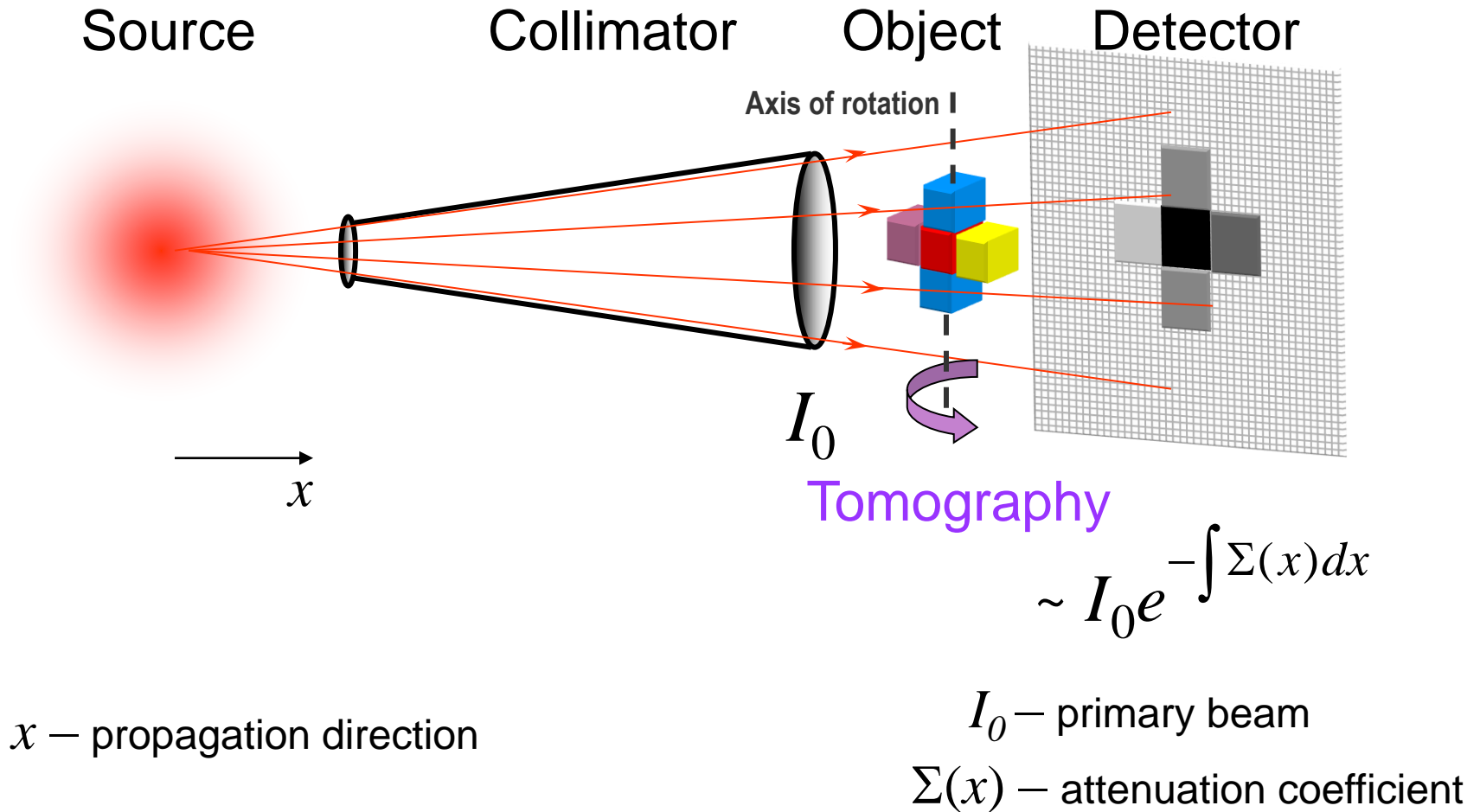
Velocity selector

Double-crystal monochromator

Grating interferometry

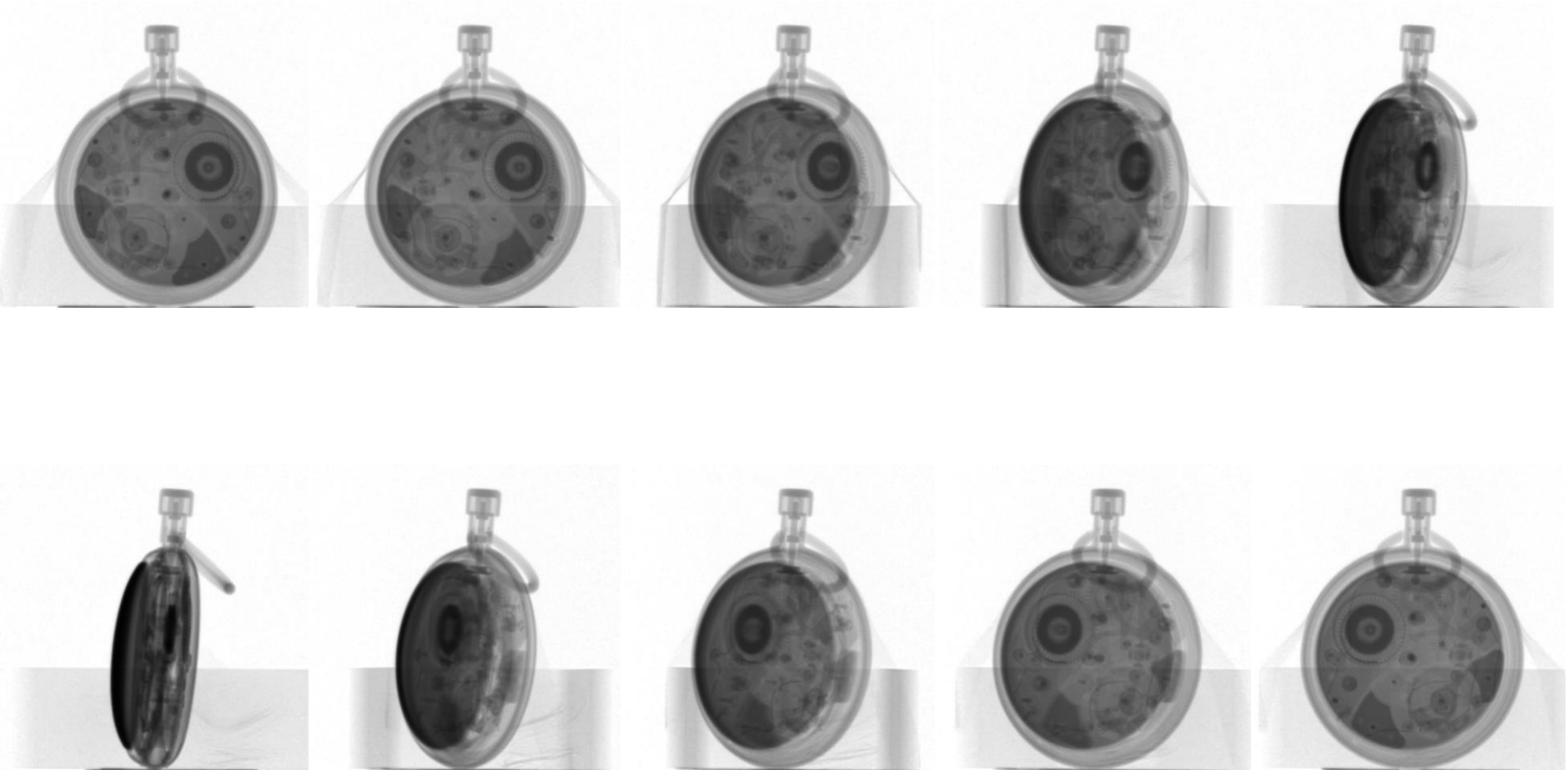


Tomography



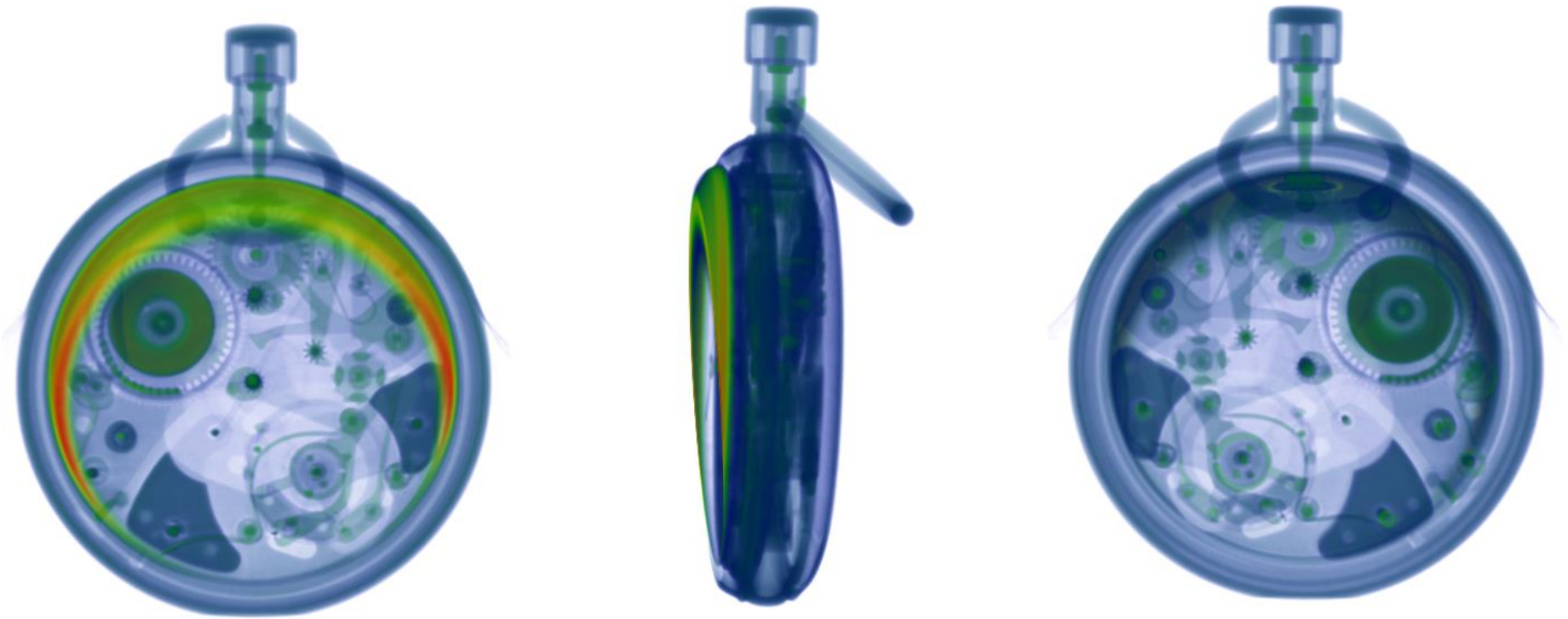
Neutron imaging

Single tomographic projections

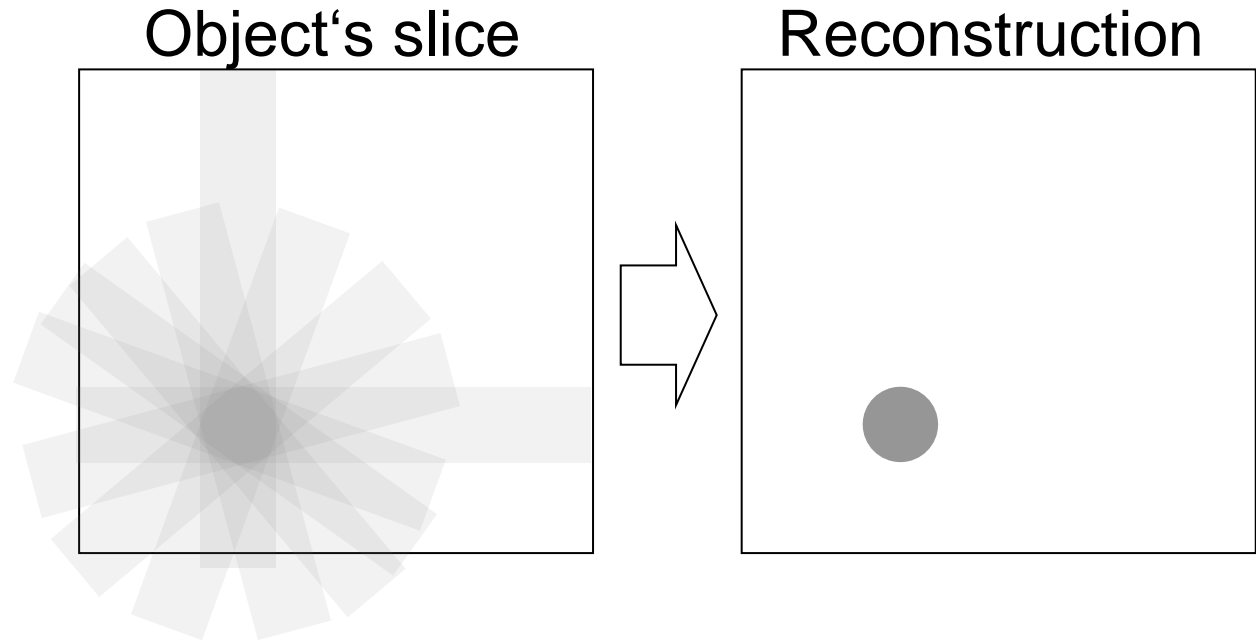


Neutron imaging

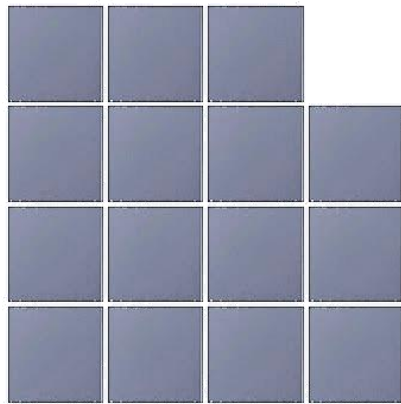
Tomographic reconstruction



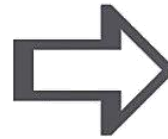
Backprojection



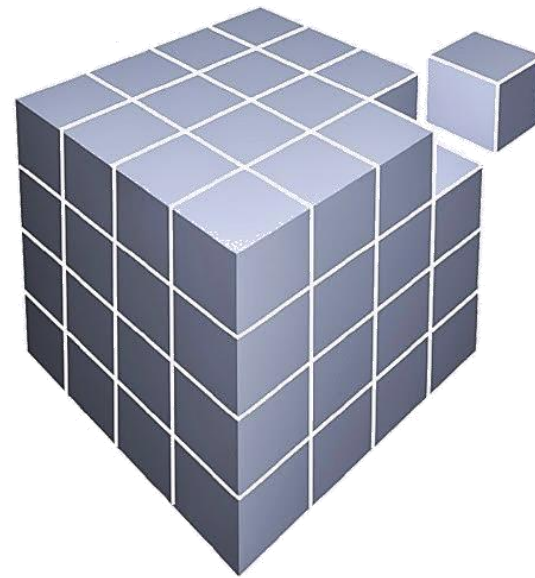
Pixel



Radiography
(2D image of the
transmission $\sim e^{-\Sigma d}$)



Voxel


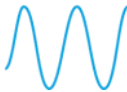



Tomography
(3D matrix of the attenuation
coefficients Σ)

Resolution

- Beam optimisation
- Detector development ←

Contrast

- Neutron interaction with matter
 -  - absorption
 -  - scattering
 -  - magnetic interaction

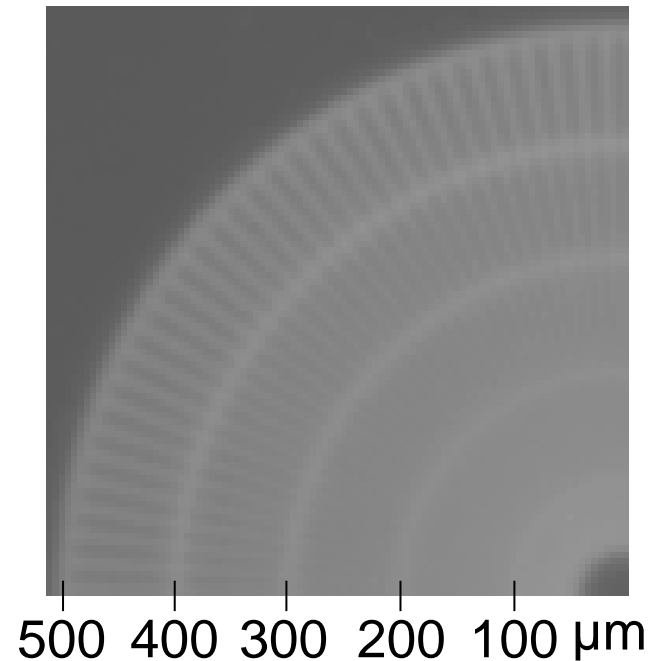
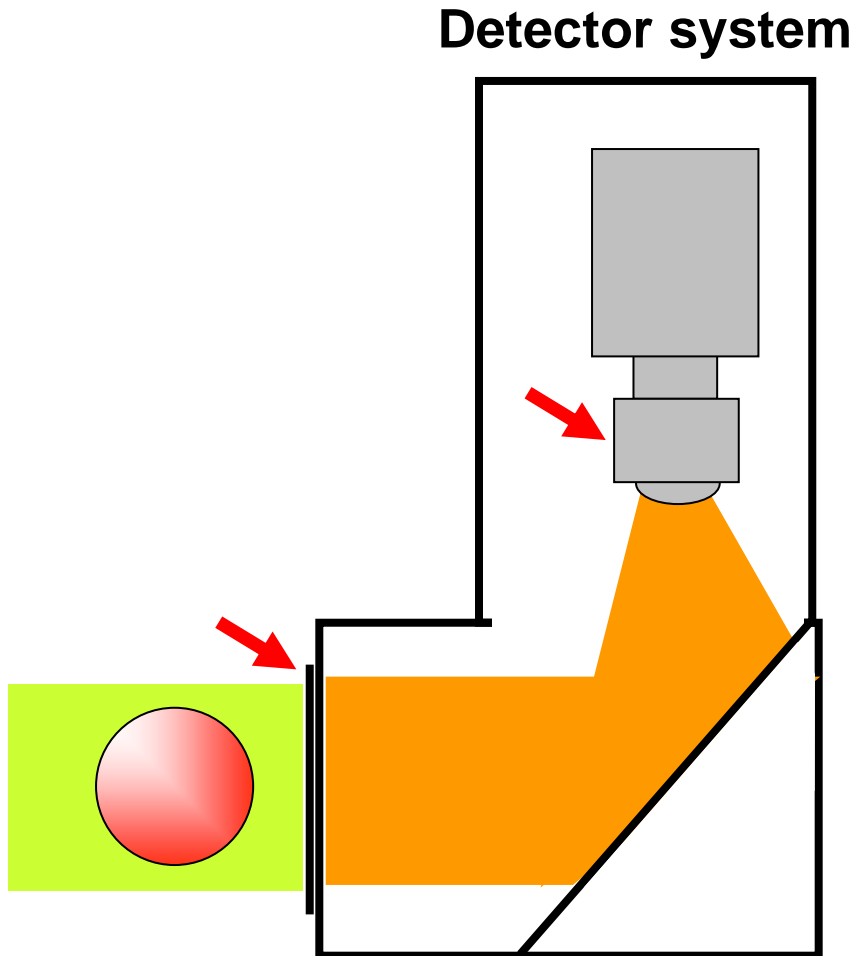
Standard setup

Scintillator: 200 μm 6LiF

Lens system: 50 mm

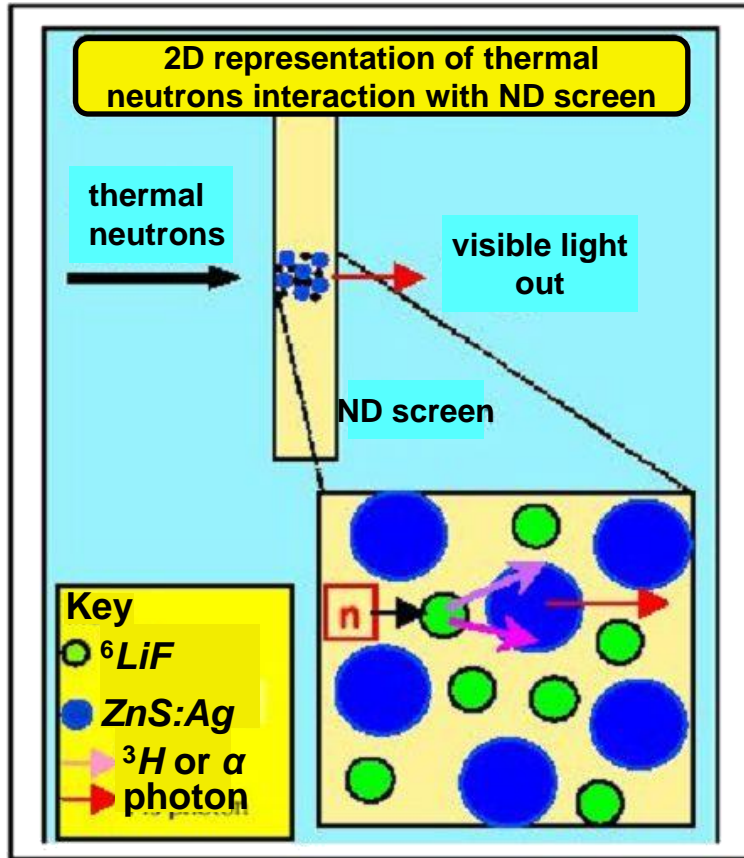
Pixel size: 100 μm

Exposure time: 20 s

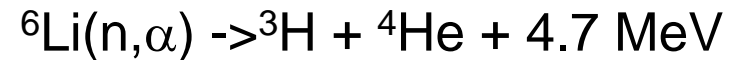


Detector development

The ZnS+⁶LiF scintillation screen is the limit of resolution.



The reaction products of



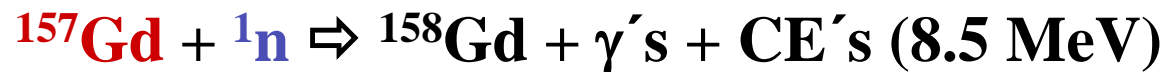
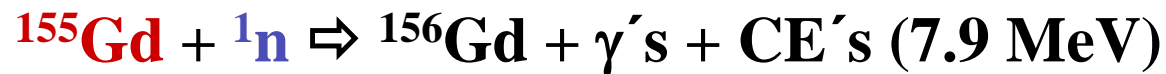
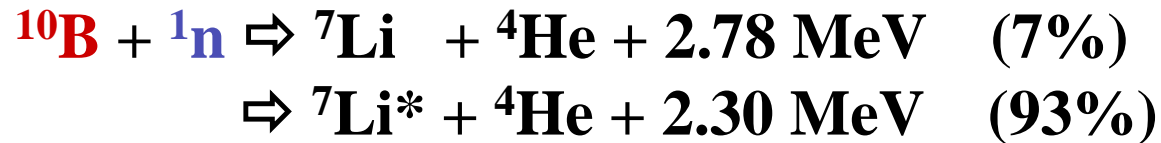
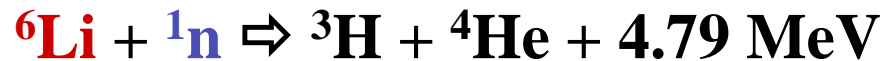
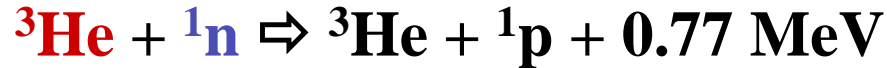
have to be stopped in the ZnS scintillation screen.

Their average range is in the order of 50-80 μm .

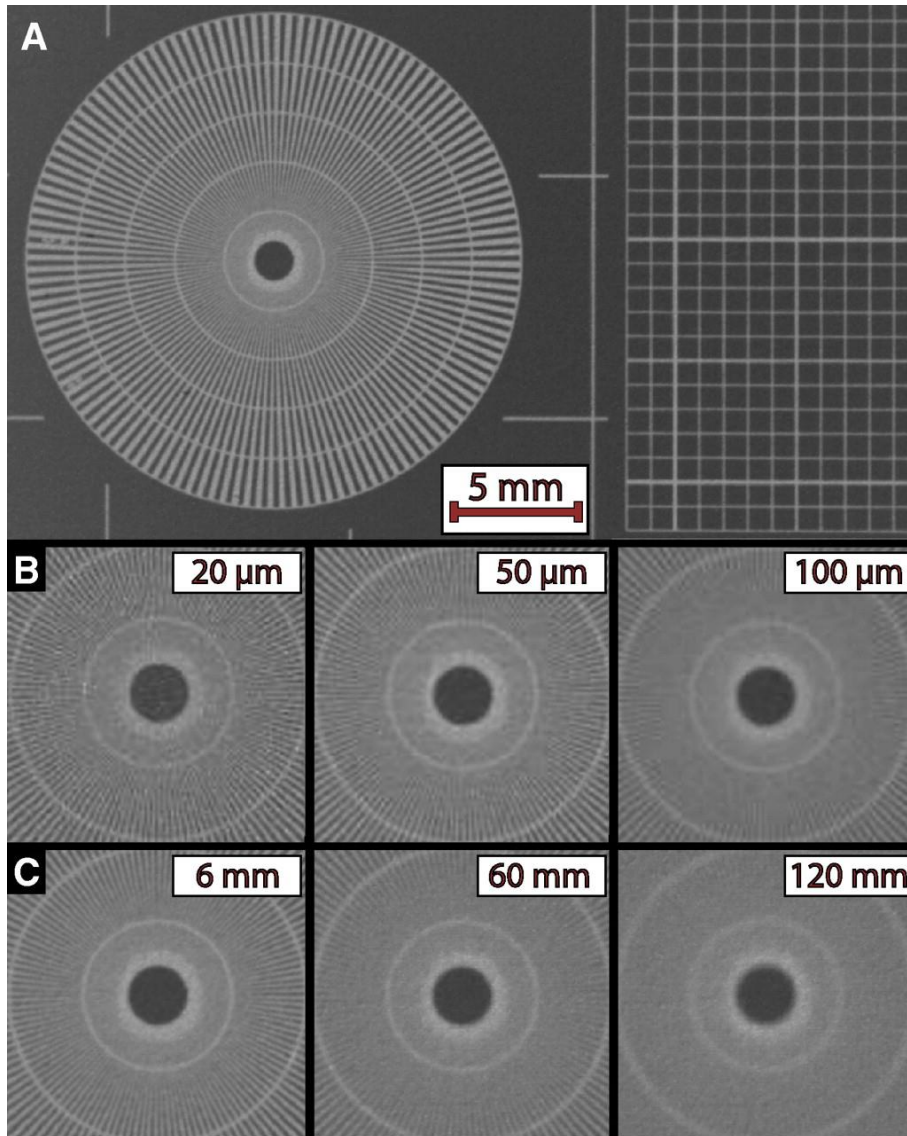
About 177,000 photons are generated per detected neutron.

With thinned scintillation screens, we can achieve resolution in the order of 20-30 μm .

Capture reactions for thermal / cold neutrons



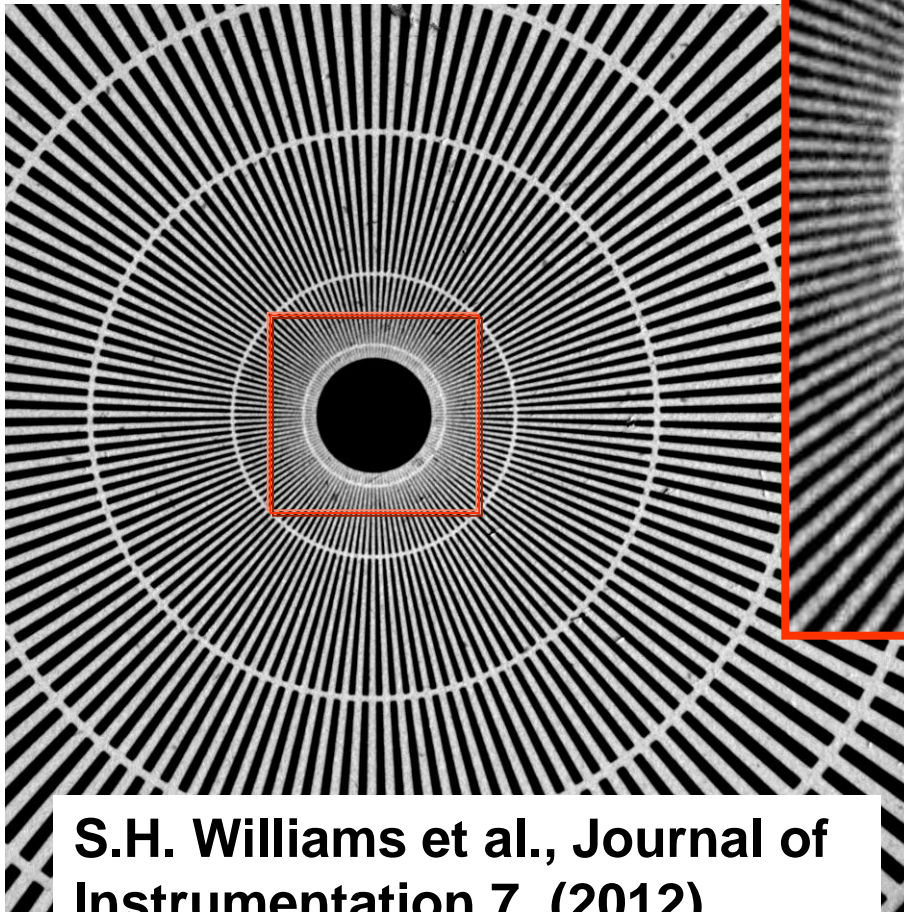
Scintillators, effect of thickness



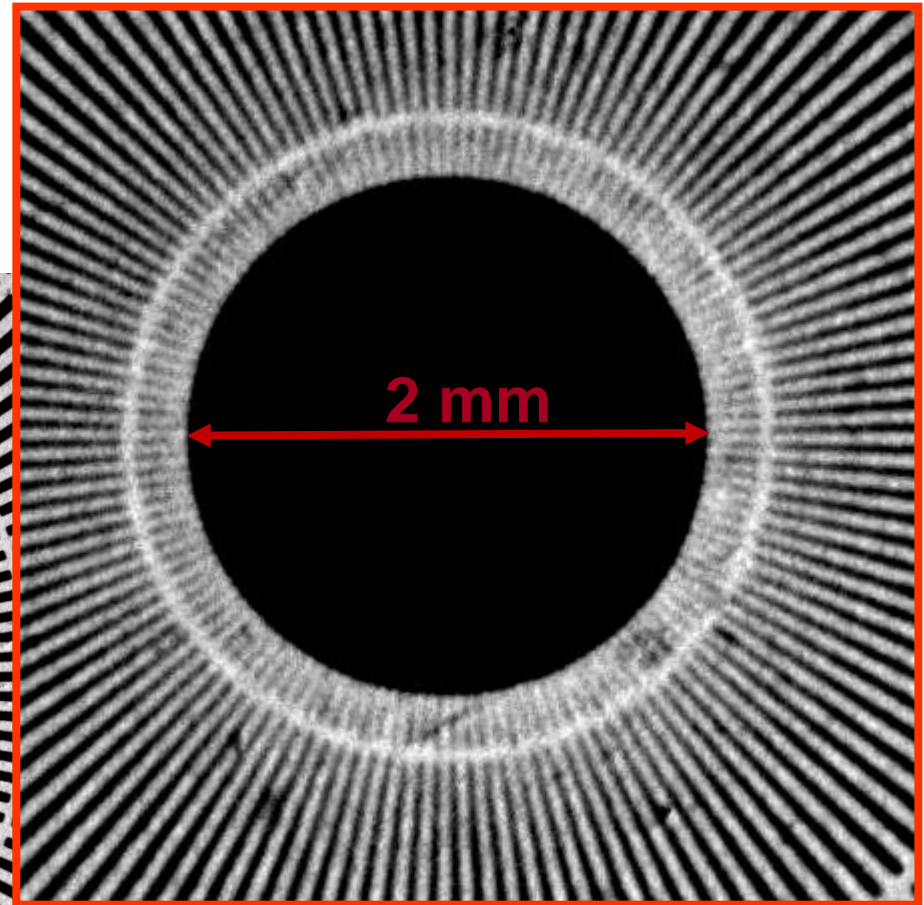
- (A) A radiograph of the Siemens star test pattern used to study the effect of scintillator thickness, exposure time, and impact of geometrical blurring.
- (B) Images showing the center of the Siemens star for scintillators of different thicknesses.
- (C) The same region imaged by a scintillator of 50 μm thickness. In each image the test pattern is placed further away from the scintillator, resulting in increased geometrical blurring.

K.-U. Hess et al., Advances in high-resolution neutron computed tomography: Adapted to the earth sciences , Geosphere (2011) 7 (6): 1294-1302.

Adaptive high-resolution imaging

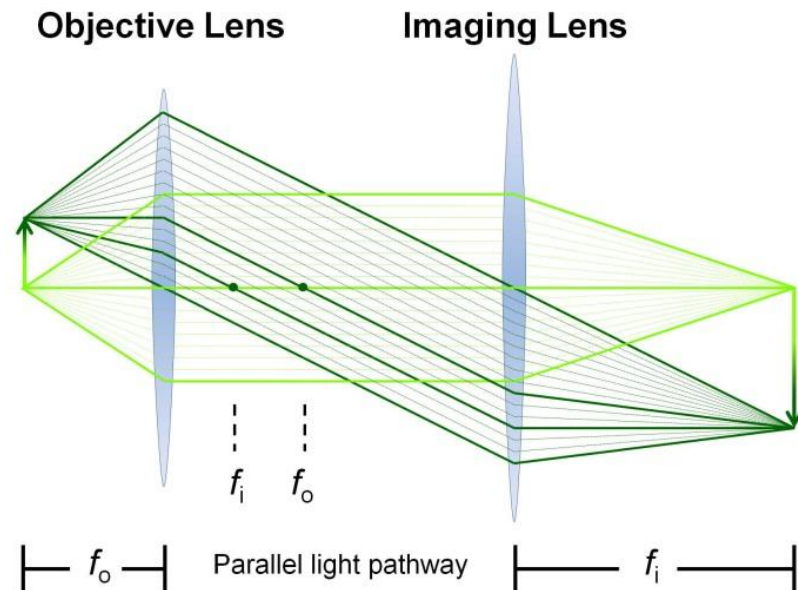
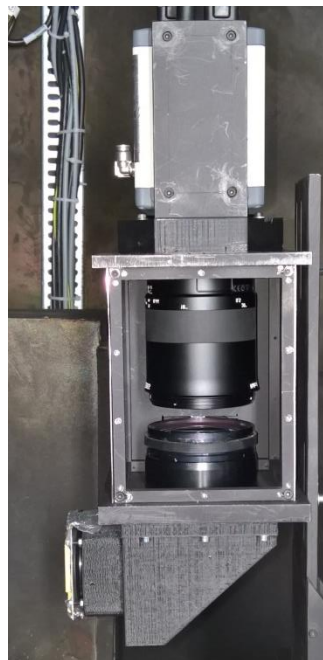
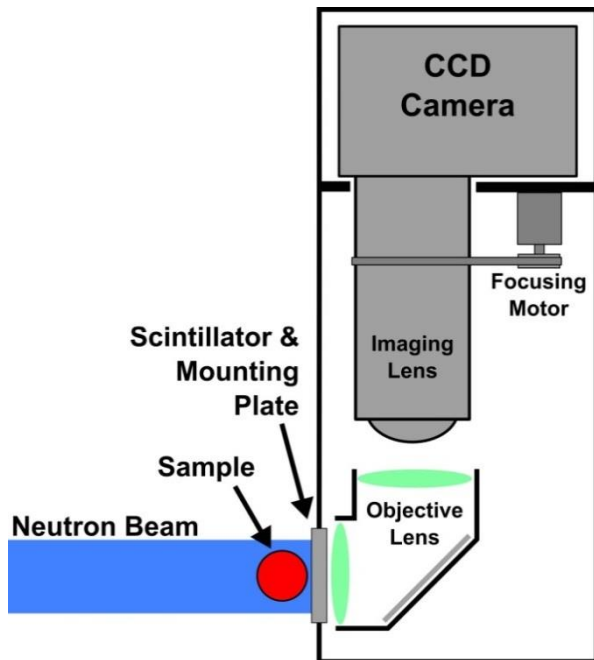


S.H. Williams et al., Journal of Instrumentation 7, (2012)



Camera: Andor DW436
Lens system: Magnification
Pixelsize = $3.375 \mu\text{m}$
Szintillator: GGG
Resolution: $7.9 \mu\text{m}$ (63.2 lp/mm)

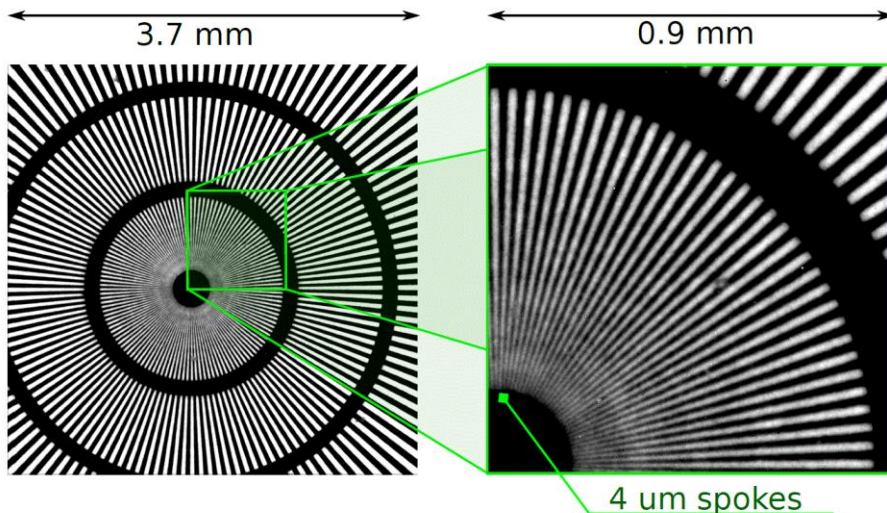
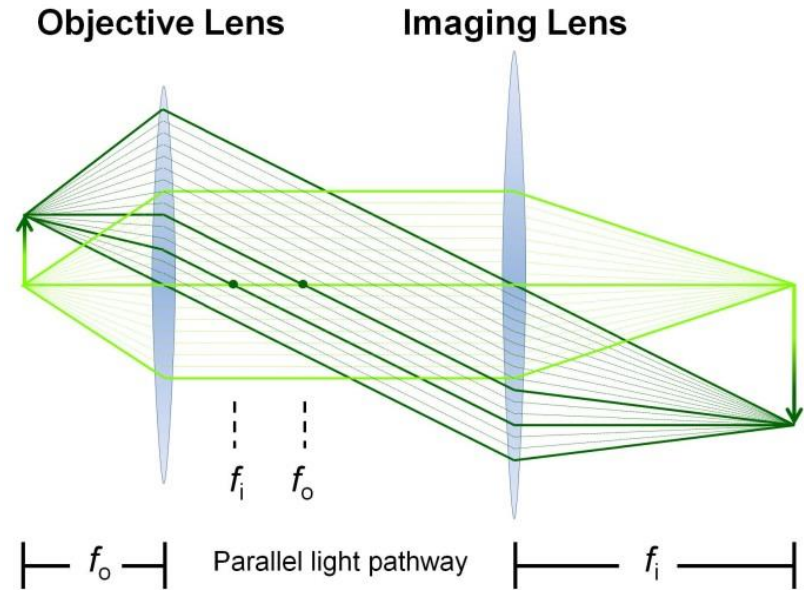
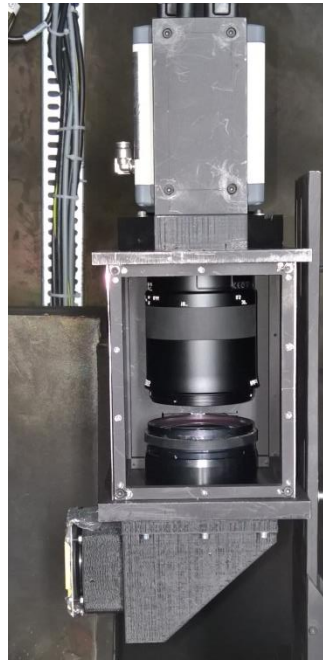
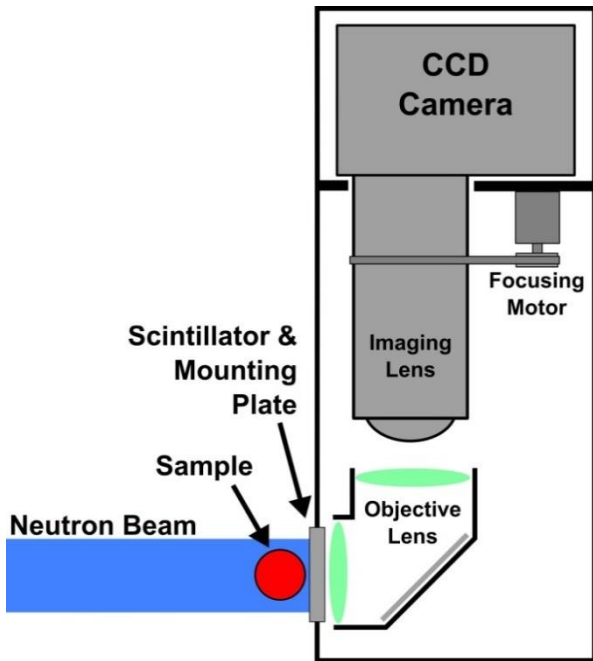
High resolution



| <i>Obj. Lens/Img. Lens</i> | <i>M</i> | <i>P_{eff} (μm)</i> | <i>FOV (mm)</i> |
|----------------------------|----------|-----------------------------|-----------------|
| 105 mm / 50 mm | 2.10 | 6.429 | 13.2 × 13.2 |
| 200 mm / 100 mm | 2.00 | 6.750 | 13.8 × 13.8 |
| 200 mm / 50 mm | 4.00 | 3.375 | 6.9 × 6.9 |

S. H. Williams et al, J. of Instrumentation (2012)

High resolution



spatial resolution
better than 5 μm

Tengattini, Alessandro, et al.
Optics Express 30.9 (2022)

Resolution

- Beam optimisation
- Detector development

Contrast

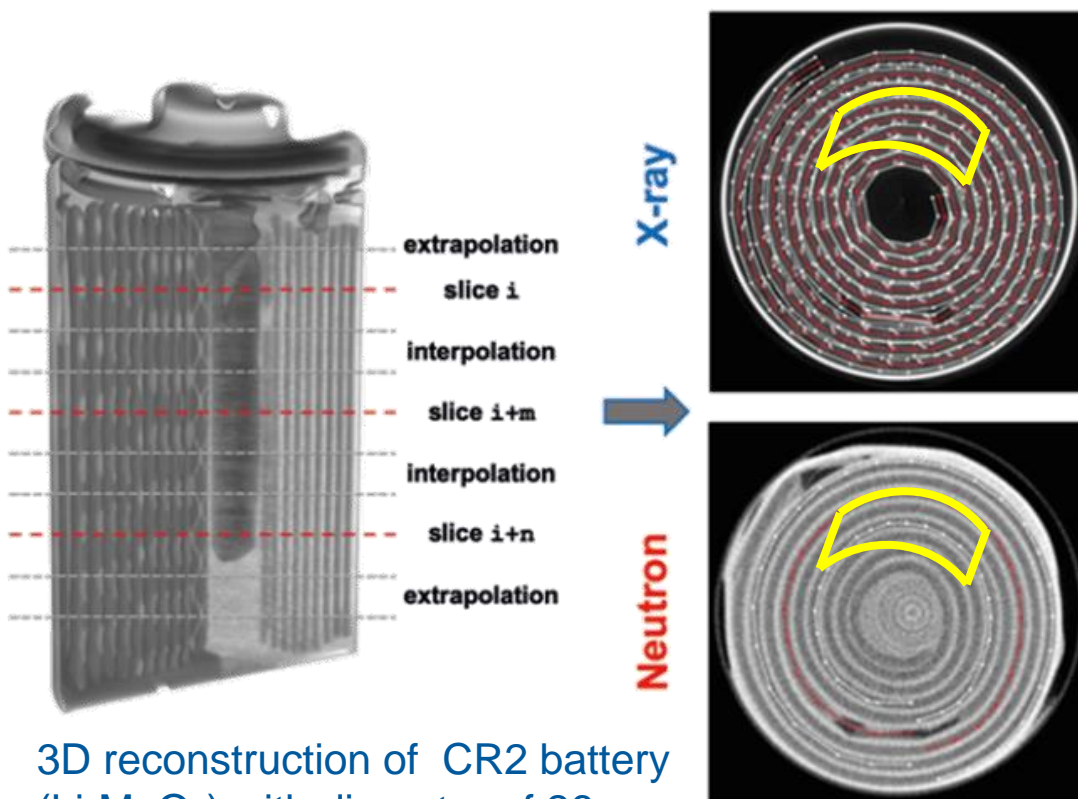
- Neutron interaction with matter

 - absorption 

 - scattering

 - magnetic interaction

How to characterize lithium intercalation in batteries?



3D reconstruction of CR2 battery (Li_xMnO_2) with diameter of 26 mm.

(neutron tomography: pixel size: 13 μm , 600 projections /360°, time: 8 h)

- 3D+T investigation of batteries by dual-mode (X-ray/Neutron) tomography

Virtual unrolling of the electrodes for different discharge times.

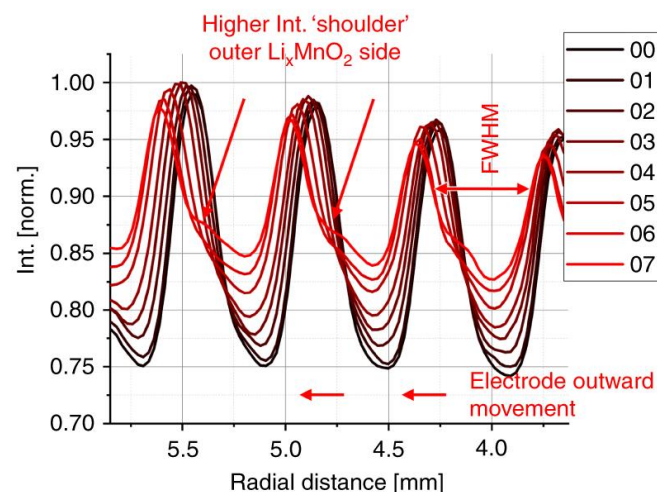
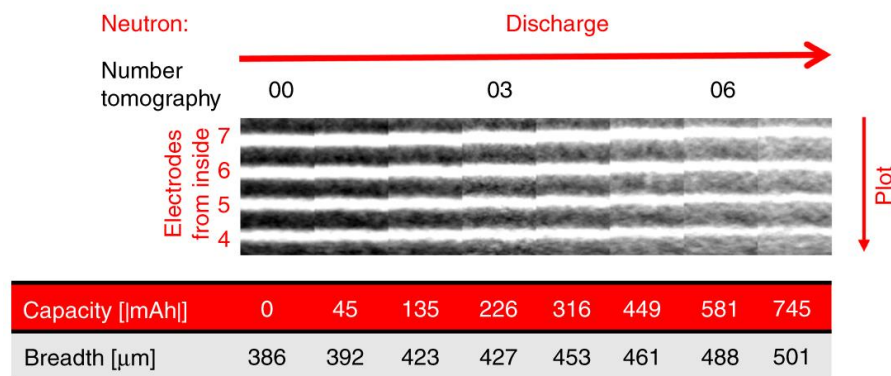
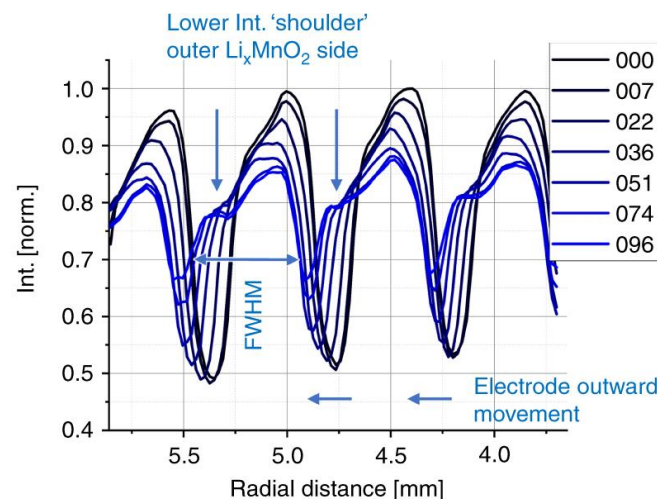
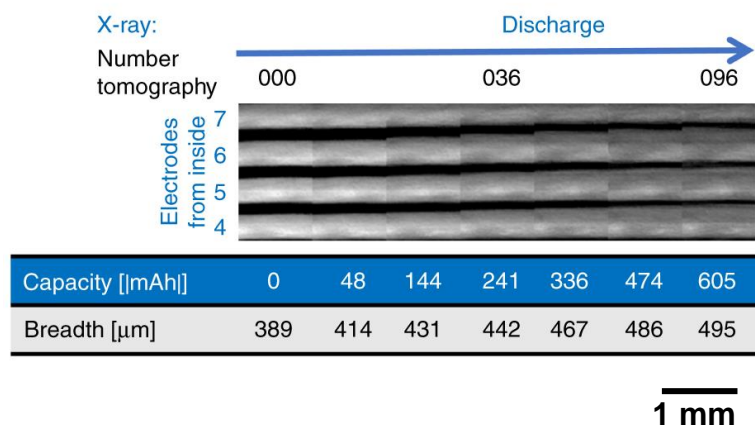
Lithium intercalation can be analyzed dynamically.

R. Ziesche *et al.*,
Nature communications 11.1 (2020): 1-11.

→ Analysis of the dual-mode tomography data

➡ Temporally and spatially resolved tracking of lithium intercalation.

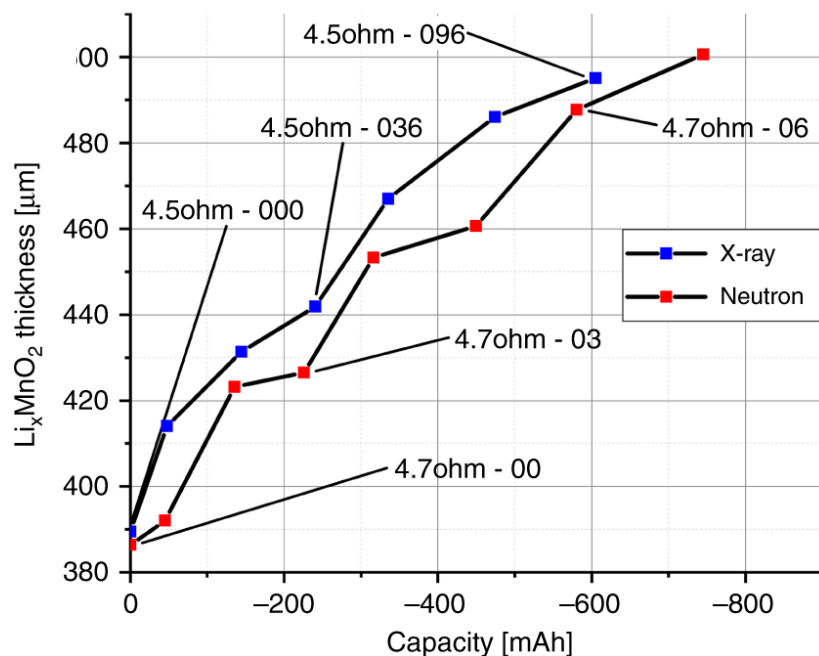
How to characterize lithium intercalation in batteries?



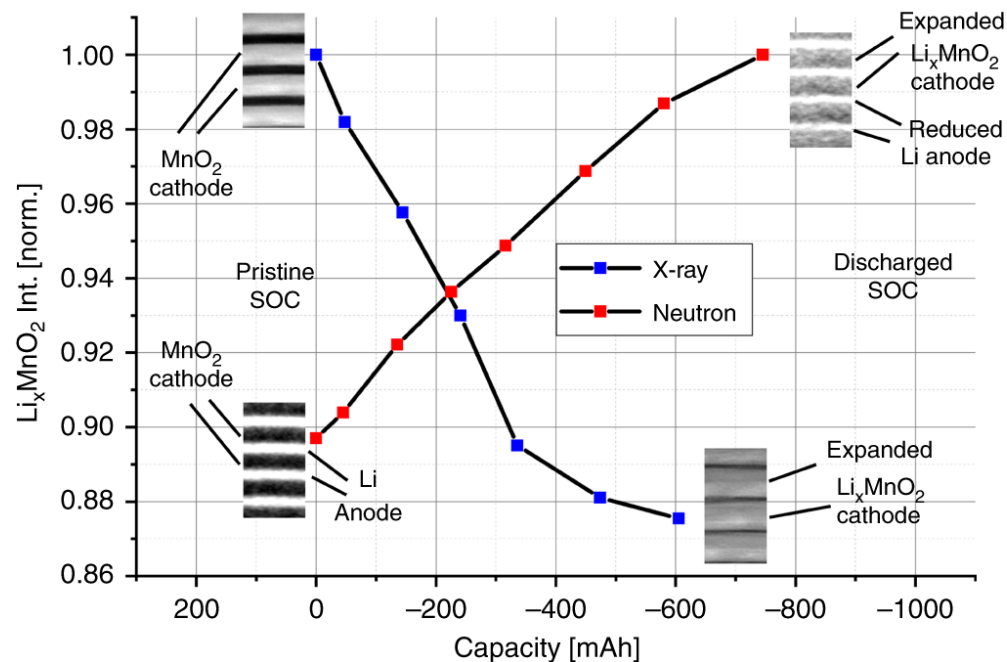
R. Ziesche *et al.*, Nature communications 11.1 (2020): 1-11.

How to characterize lithium intercalation in batteries?

Electrode thickness dependence

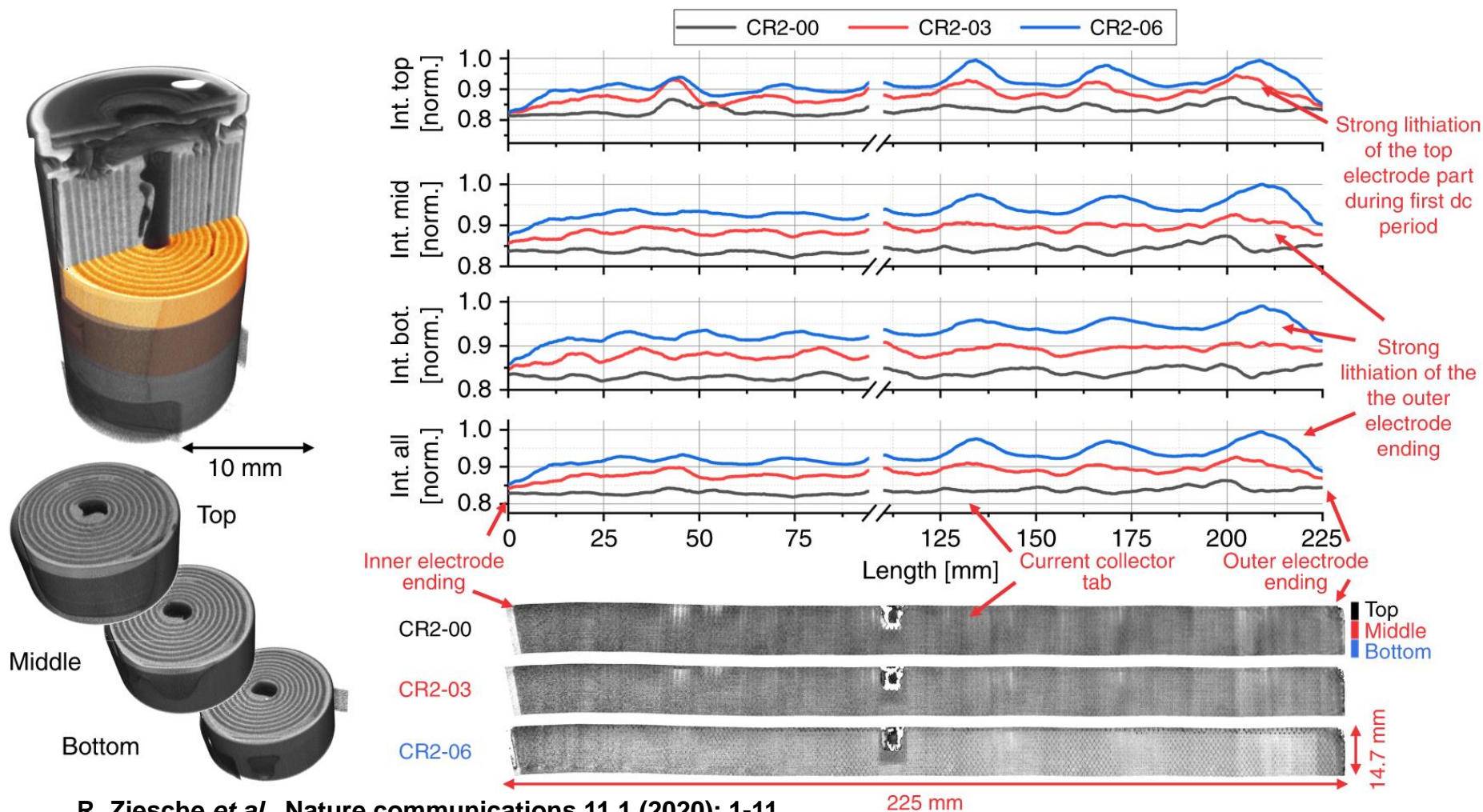


Lithium consumption



R. Ziesche *et al.*, Nature communications 11.1 (2020): 1-11.

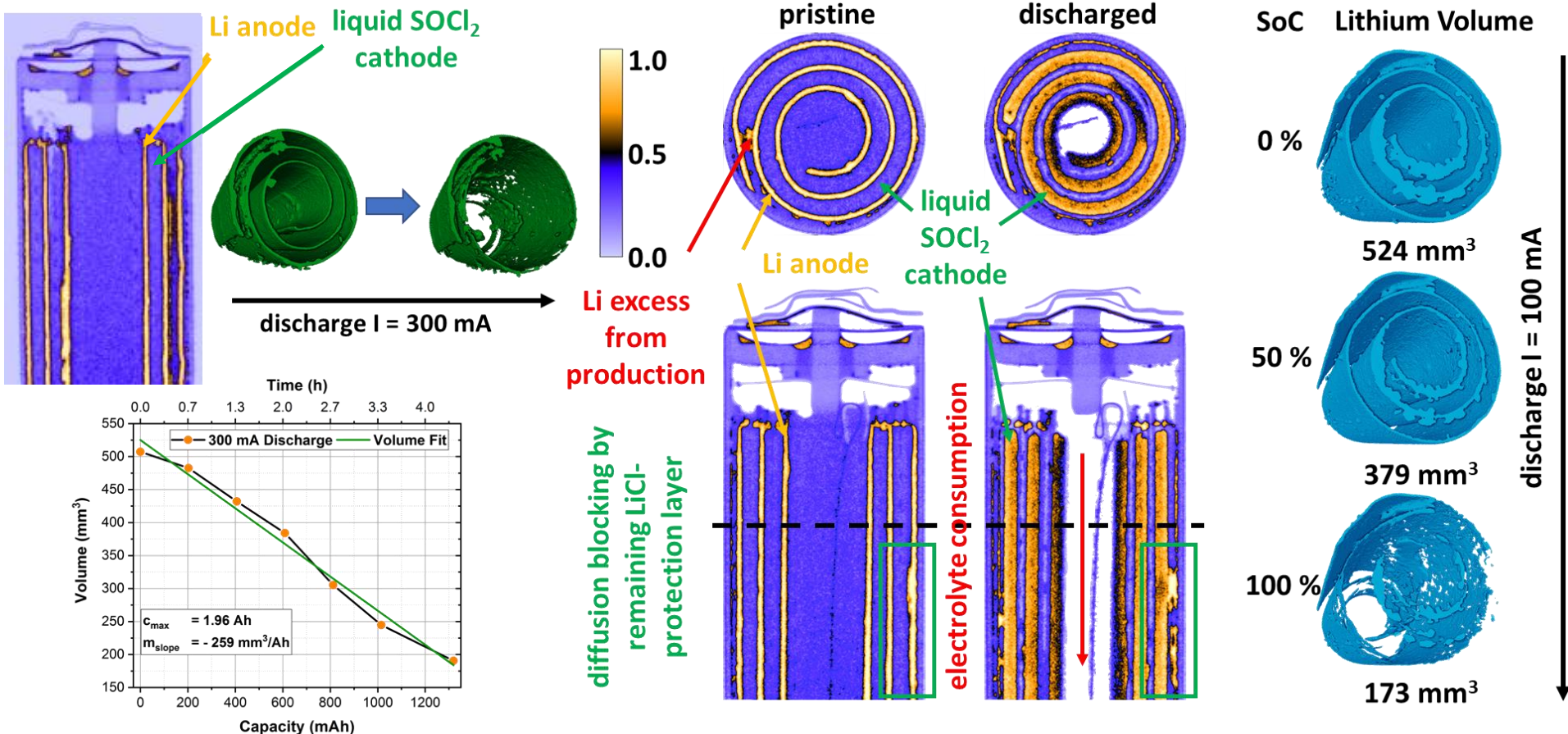
How to characterize lithium intercalation in batteries?



R. Ziesche *et al.*, Nature communications 11.1 (2020): 1-11.

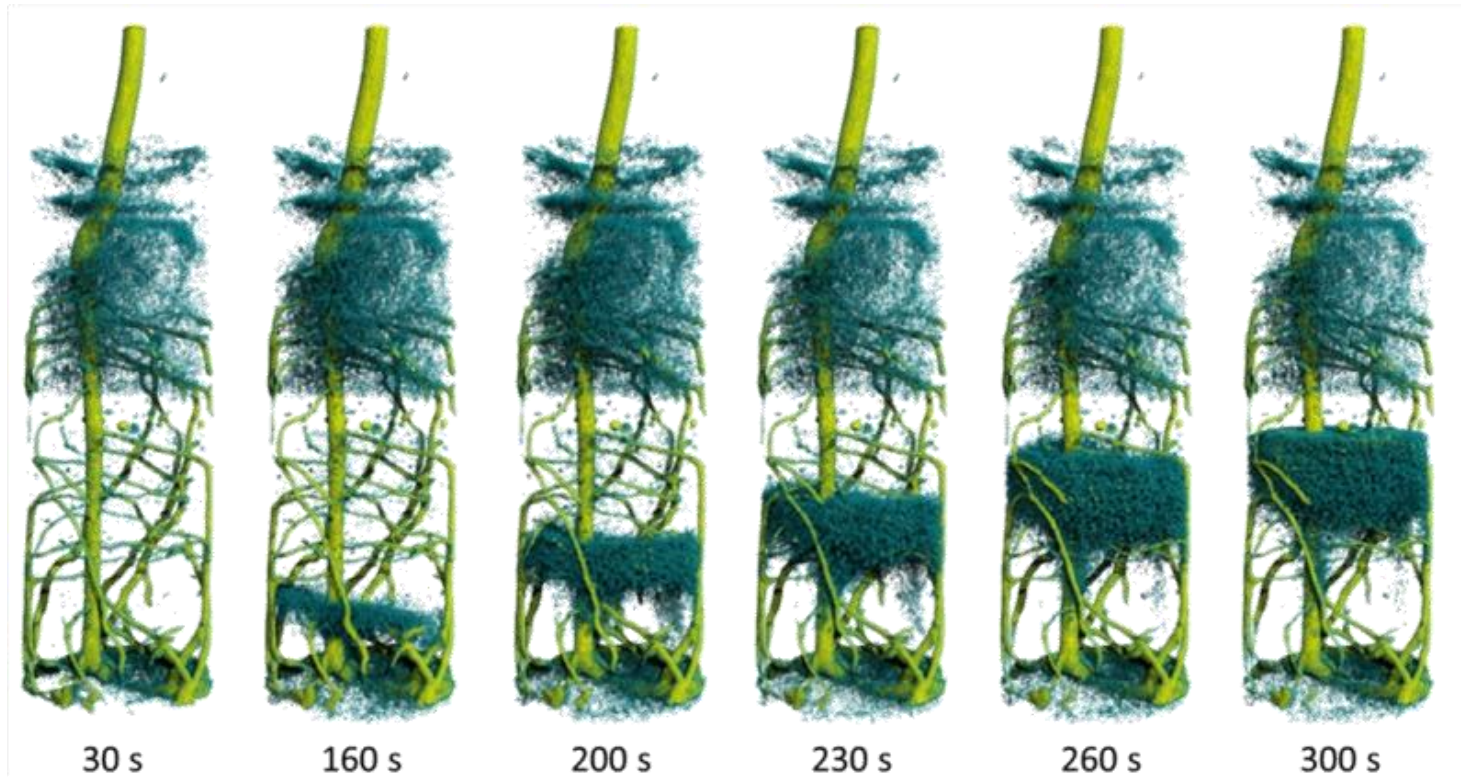
How to characterize lithium diffusion in batteries?

4D Study of SOCl_2 Battery (pixel size: 8 μm , time step: 7.5 min)



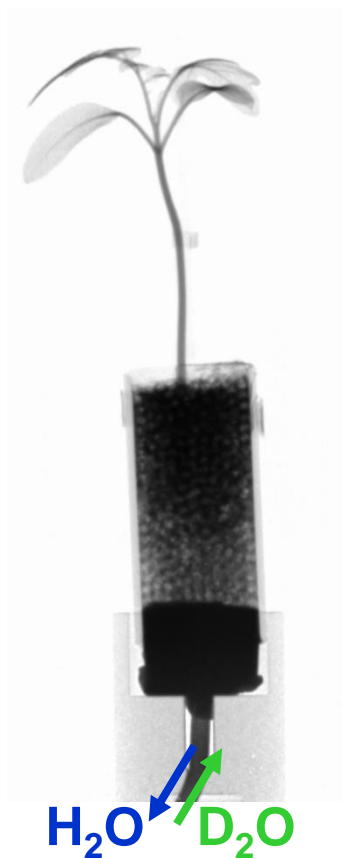
R. Ziesche *et al.*, Journal of Electrochemical Society 167 (2020)

High-speed tomography



C. Tötze *et al.* Scientific Reports 7, 61924, (2017)

How to observe the water uptake in plant's root



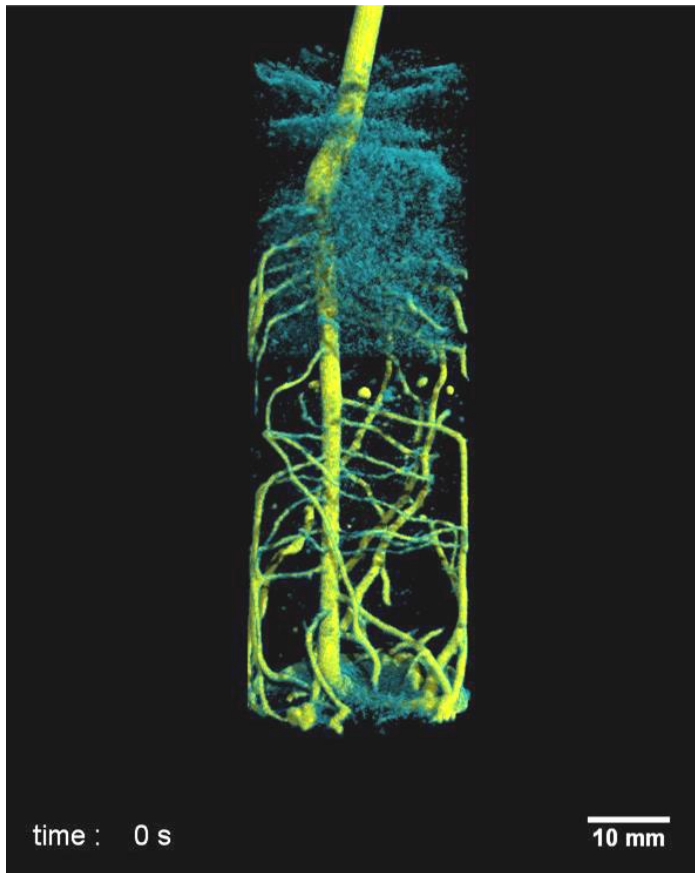
- *In-operando* 3D visualization of water distribution

Water uptake dynamics revealed with D-H contrast

Insights in the water uptake mechanisms in the root system

- Observation of the dynamic processes in root system
- ➡ Learning about the root-soil interaction mechanisms

How to observe the water uptake in plant's root



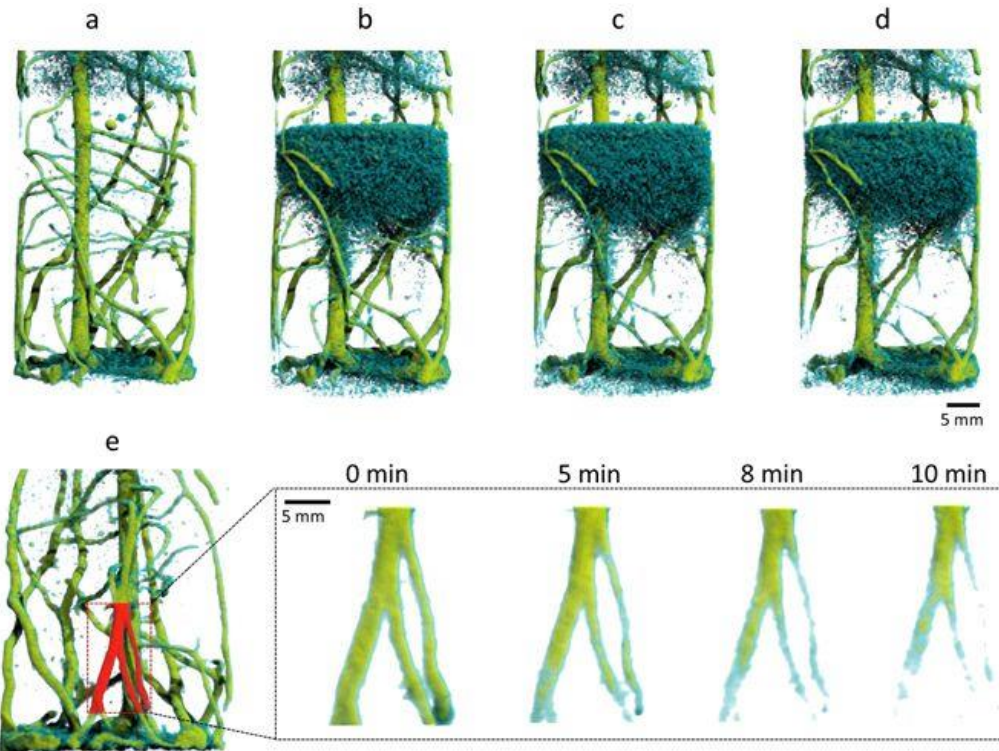
High-speed (on-the-fly) neutron tomography

resolution: 150 μm
exposure: 0.05 s
200 projections/180°

10 s / tomography

- Observation of the dynamic processes in root system
- ➡ Learning about the root-soil interaction mechanisms

How to observe the water uptake in plant's root



High-speed (on-the-fly) neutron tomography

resolution: 150 μm
exposure: 0.05 s
200 projections/180°

10 s / tomography

Time series of neutron tomograms at (a) 0 min; (b) 5 min; (c) 8 min and (d) 10 min after feeding D₂O.

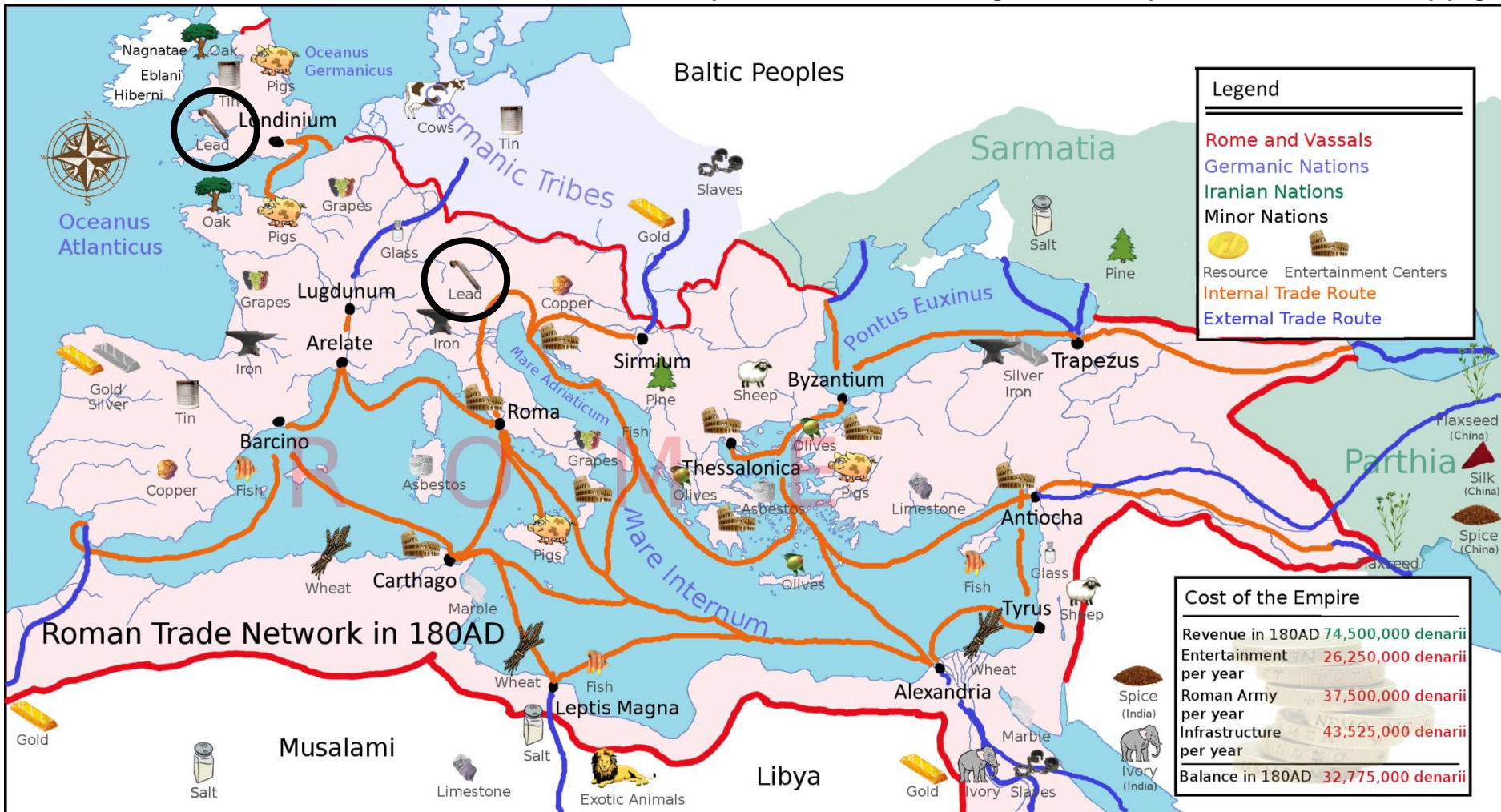
Ch. Tötze, et al. *Scientific reports* 7.1 (2017): 6192.

- Observation of the dynamic processes in root system
- ➡ Learning about the root-soil interaction mechanisms

Attenuation Contrast

Shipwrecks

https://commons.wikimedia.org/wiki/File:Europe_180ad_roman_trade_map.png

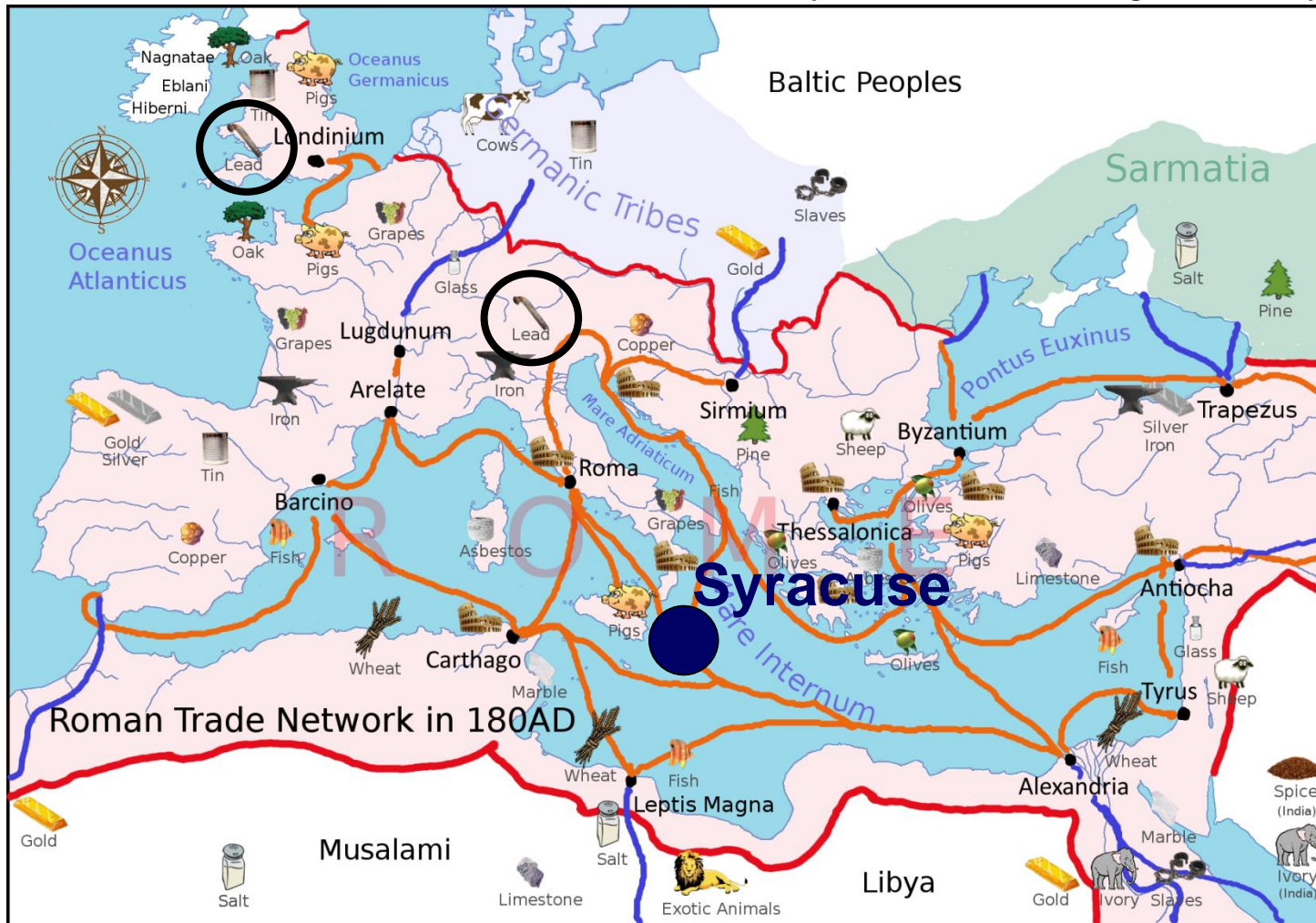


All routes lead to Rome: A map of Roman ports and trade routes

Attenuation Contrast

Shipwrecks

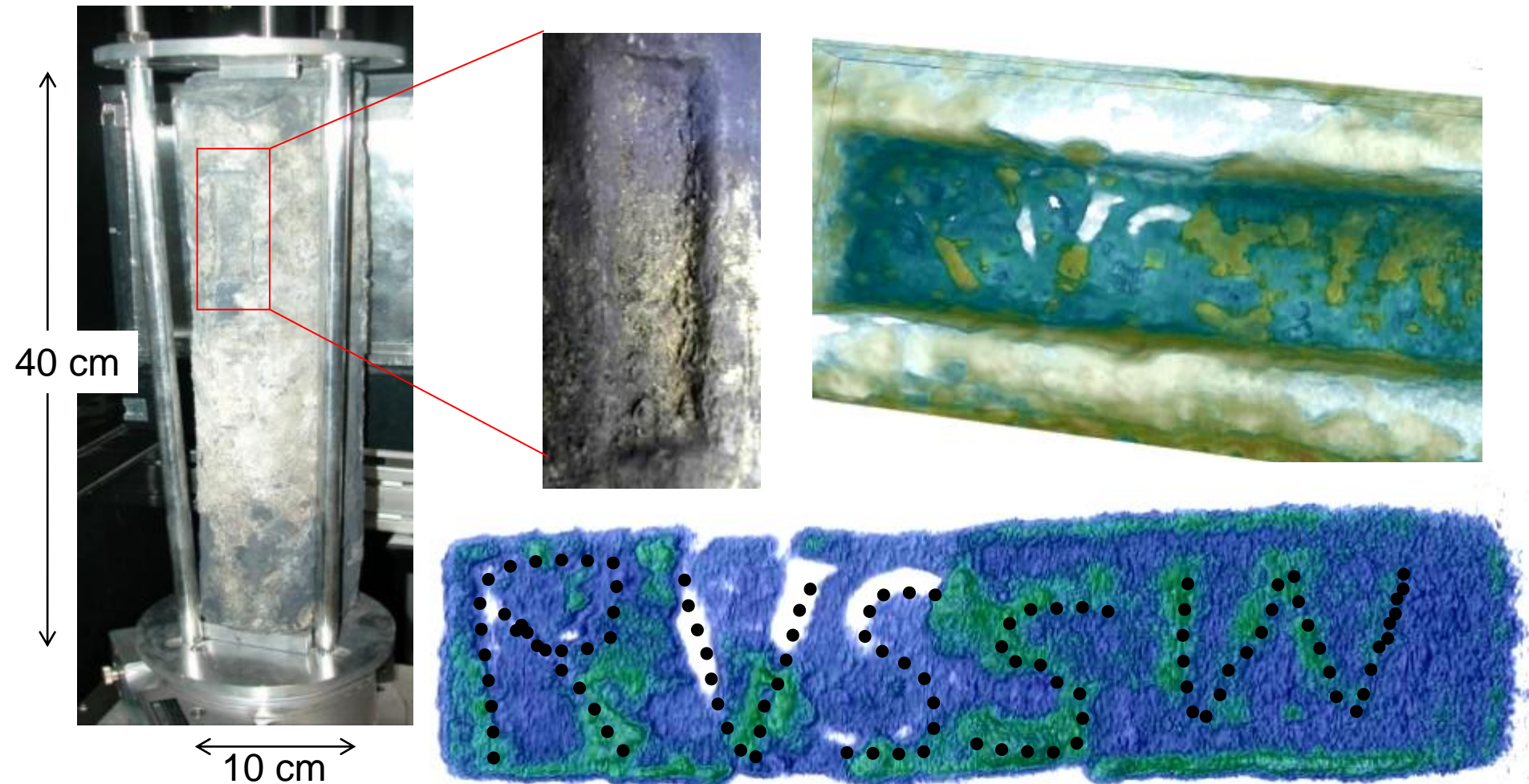
https://commons.wikimedia.org/wiki/File:Europe_180ad_roman_trade_map.png



All routes lead to Rome: A map of Roman ports and trade routes

Attenuation Contrast

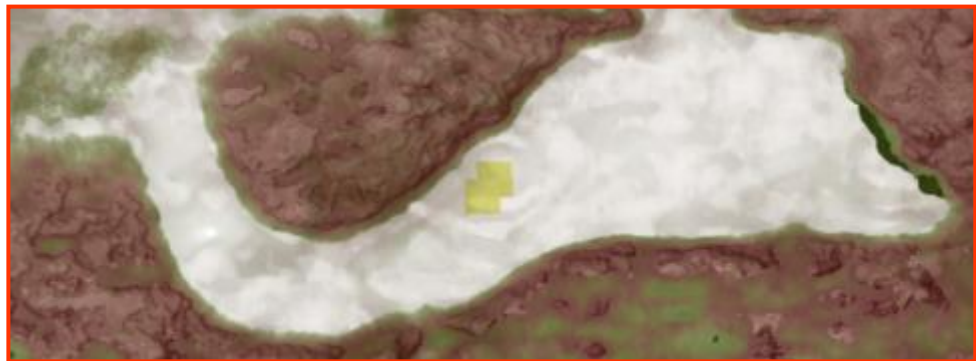
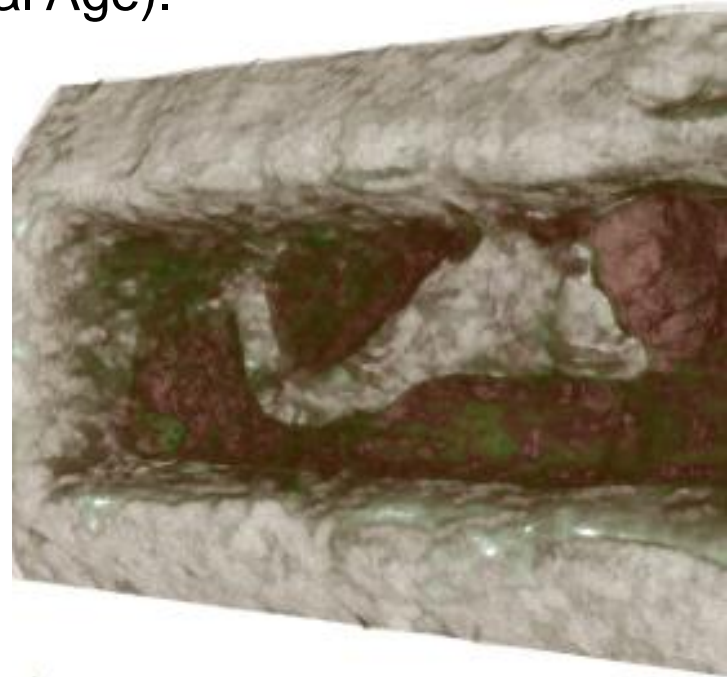
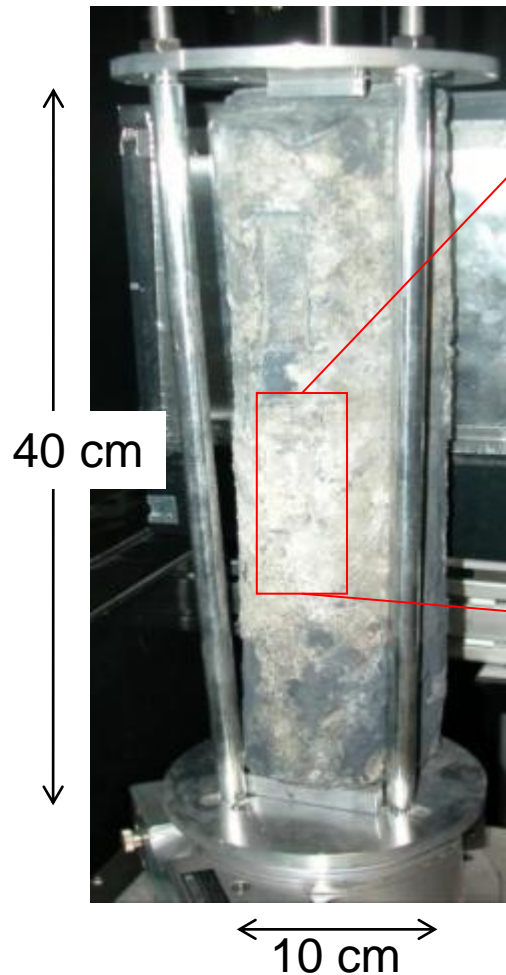
Lead blocks recovered near the UNESCO World Heritage Site Syracuse. Presumably I century B.C. (Roman Imperial Age).



Triolo, R. et al, Neutron tomography of ancient lead artefacts, *Anal. Methods* 6 (2014) 2390-2394

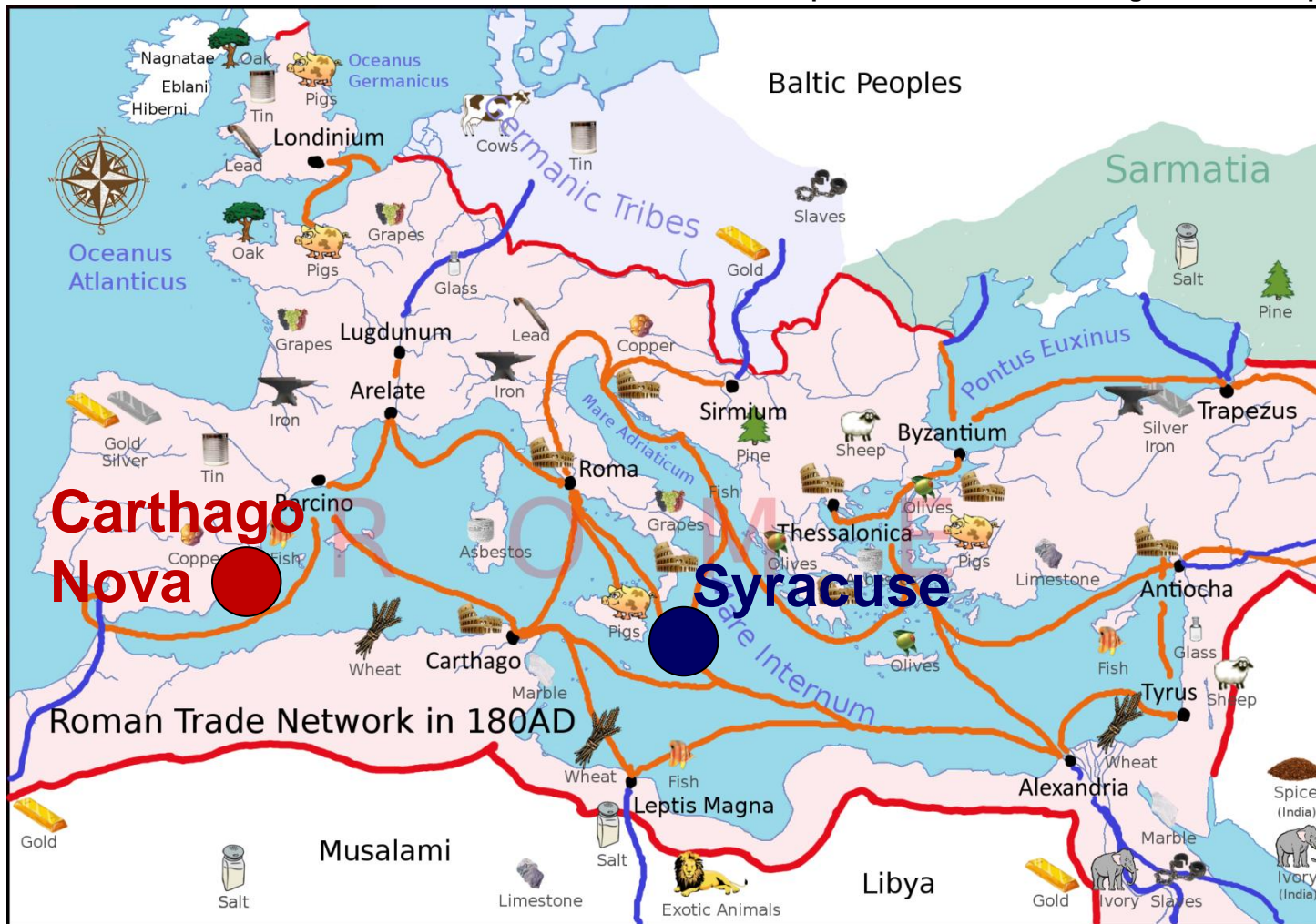
Attenuation Contrast

Lead blocks recovered near the UNESCO World Heritage Site Syracuse. Presumably I century B.C. (Roman Imperial Age).



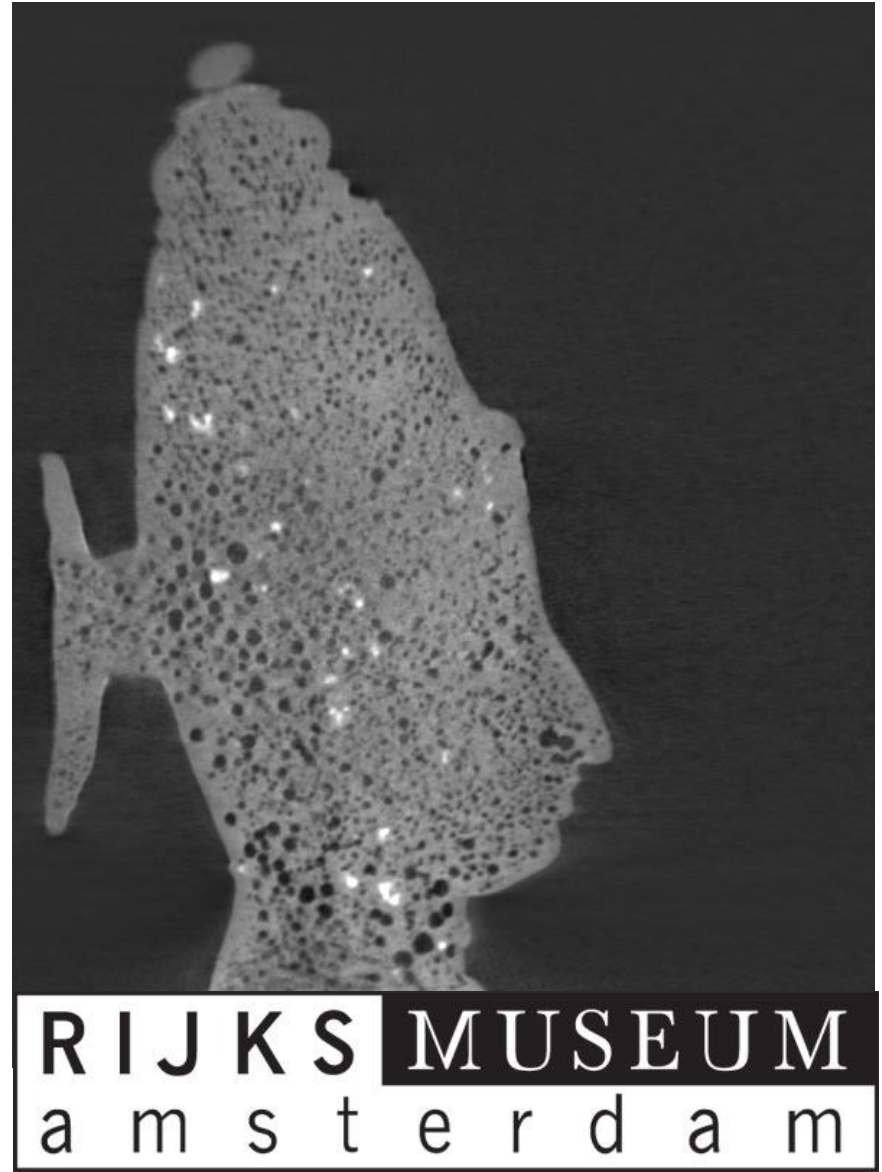
Attenuation Contrast

https://commons.wikimedia.org/wiki/File:Europe_180ad_roman_trade_map.png



Triolo, R., et al. *Analytical Methods* 6.7 (2014): 2390-2394.

Neutron tomography of bronze statues



Resolution

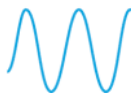
- Beam optimisation
- Detector development

Contrast

- Neutron interaction with matter



- absorption



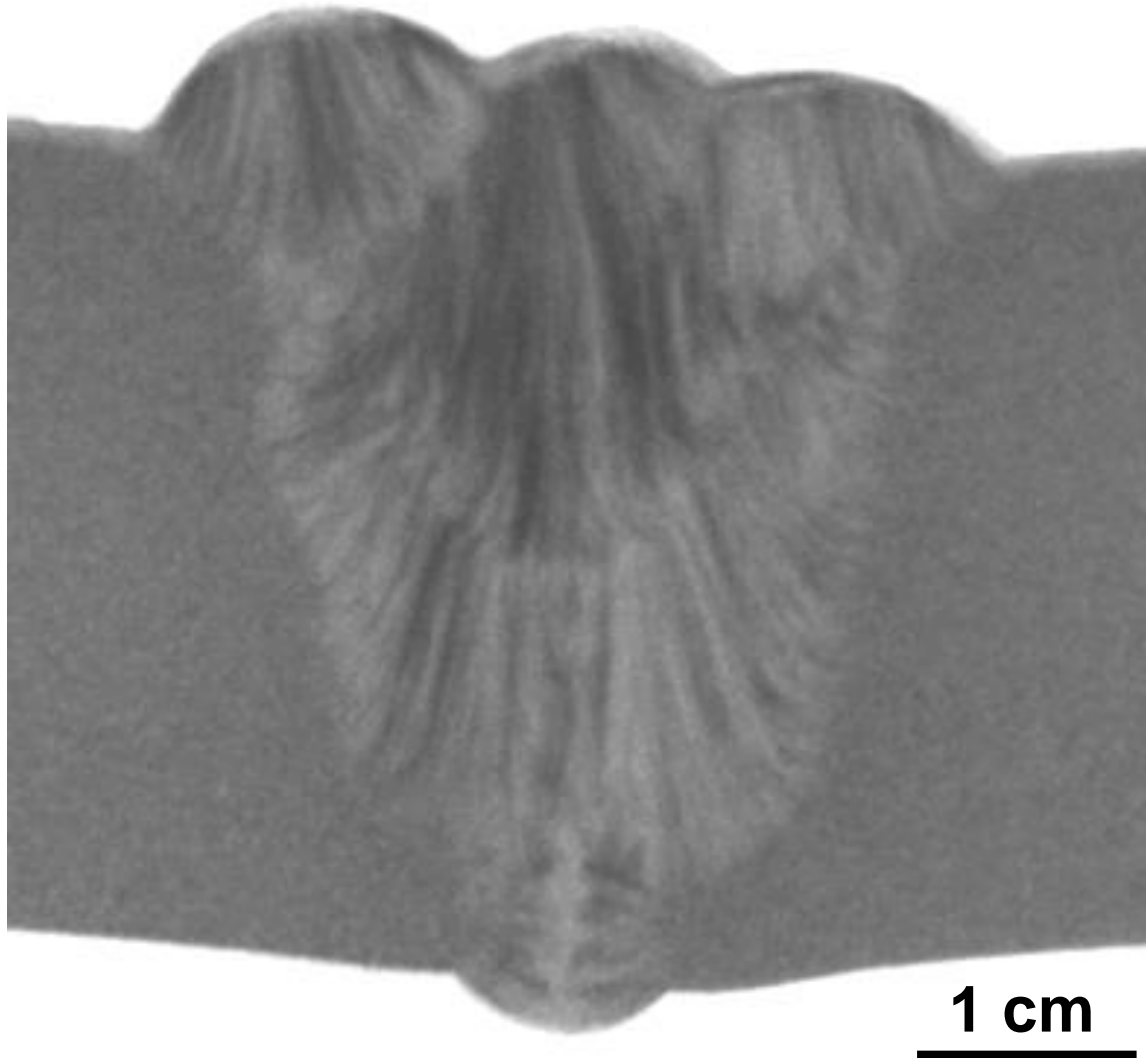
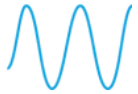
- scattering ←



- magnetic interaction

Diffraction Contrast

$$\lambda = 4.0 \text{ \AA}$$



Diffraction Contrast

Beam monochromatisation

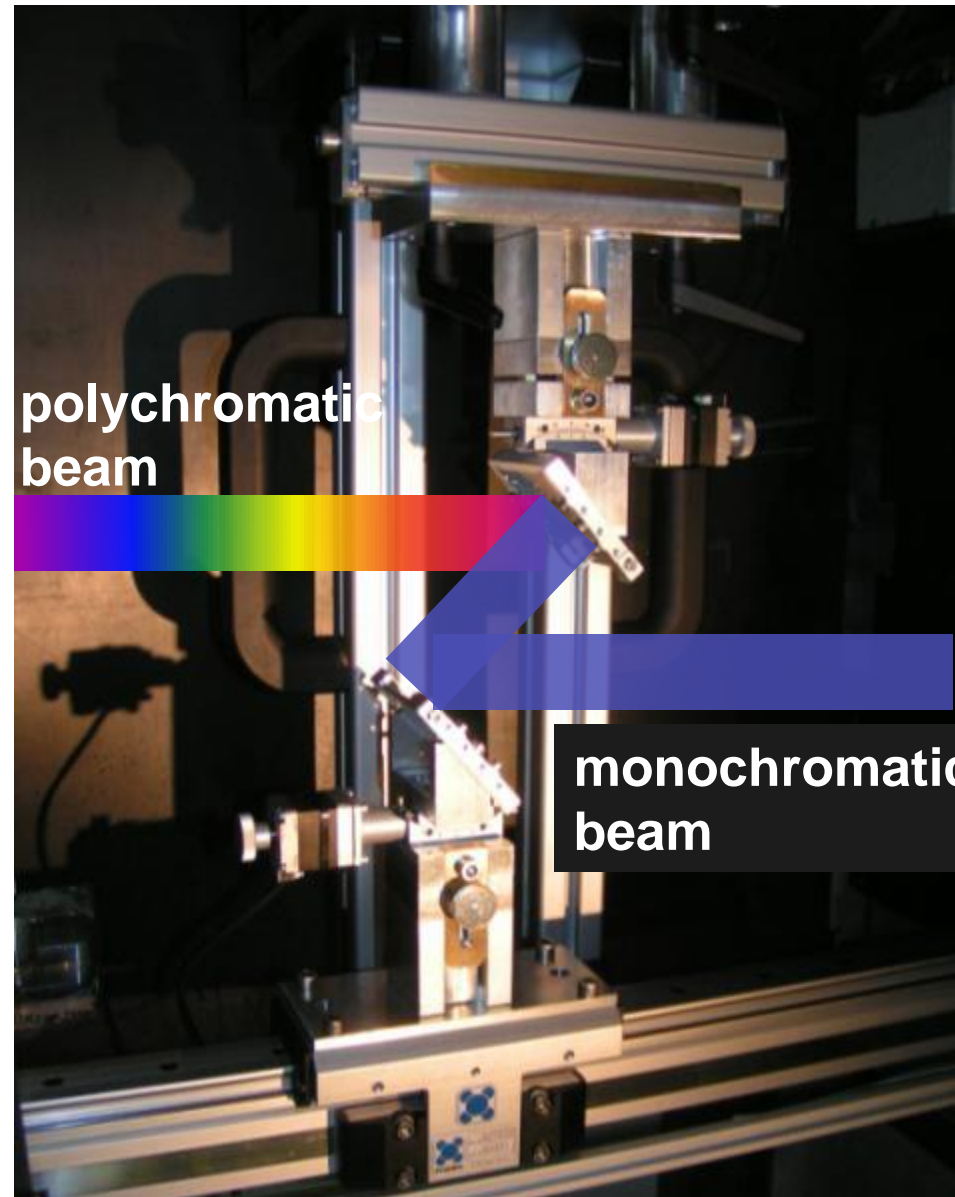
Double crystal monochromator:
PCG crystals (mosaicity of 0.8°)

Range: 2.0 – 6.5 Å

Resolution ($\Delta\lambda/\lambda$): $\sim 3\%$

Neutron flux: $\sim 4 \times 10^5$ n/cm²s
(at $\lambda=3.0$ Å)

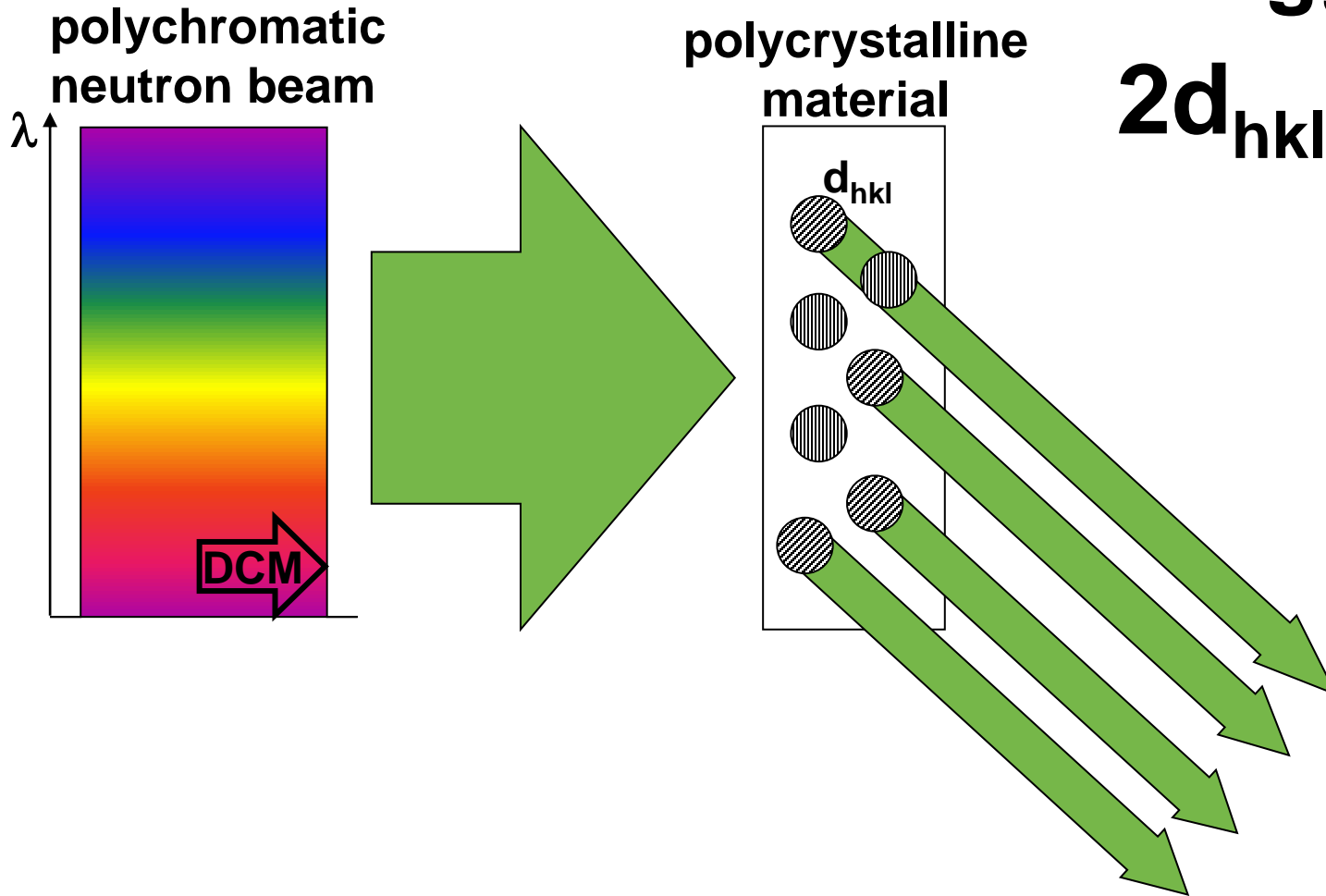
Beam size: 5 x 20 cm²



N. Kardjilov, et al. NIMA 605.1 (2009), 13-15.

Diffraction Contrast

Coherent scattering – Bragg edges

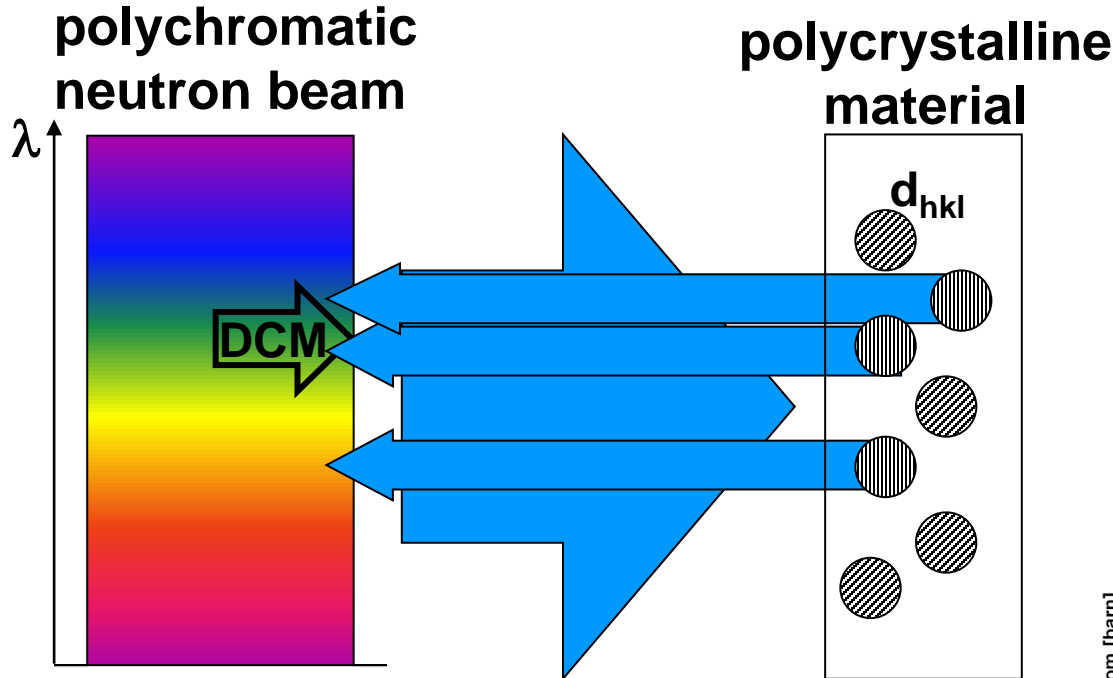


Bragg's law

$$2d_{hkl}\sin\theta = \lambda$$

Diffraction Contrast

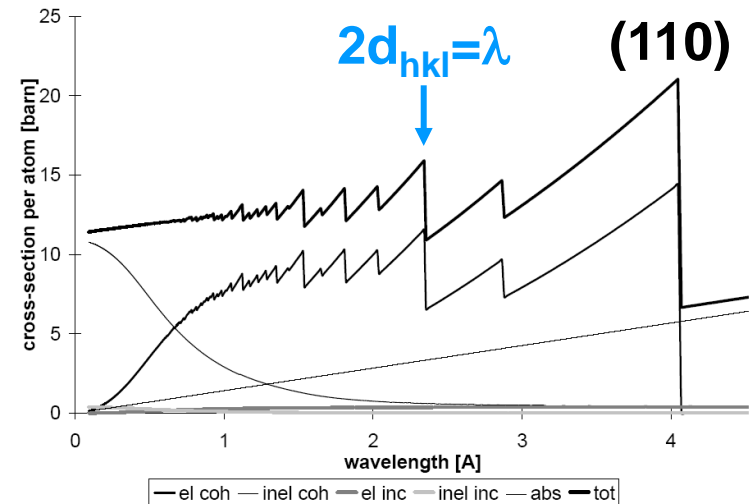
Coherent scattering – Bragg edges



Bragg's law

$$2d_{hkl}\sin 90^\circ = \lambda$$

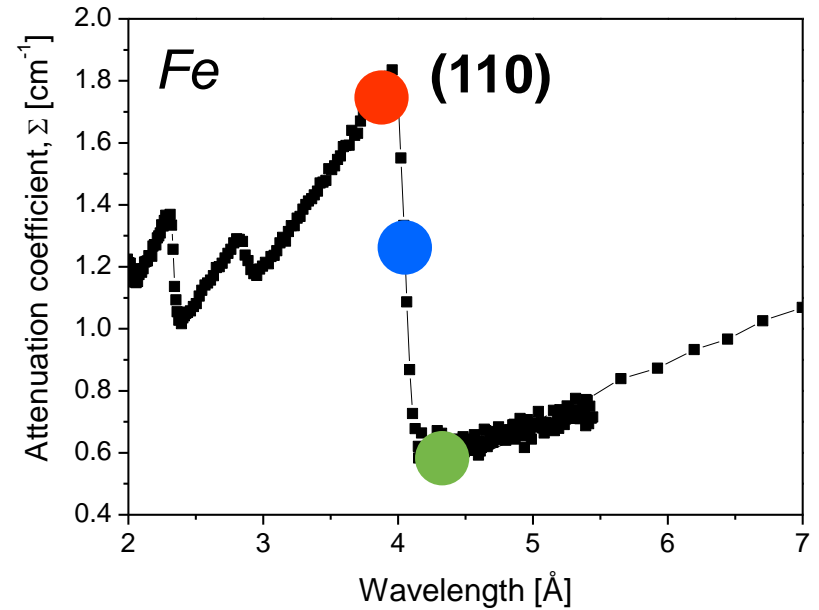
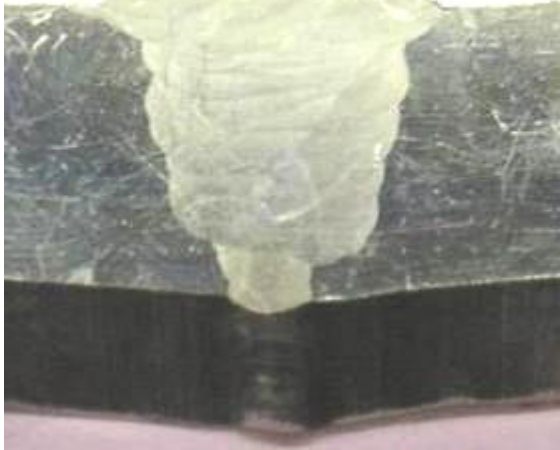
Cross-sections of iron per atom



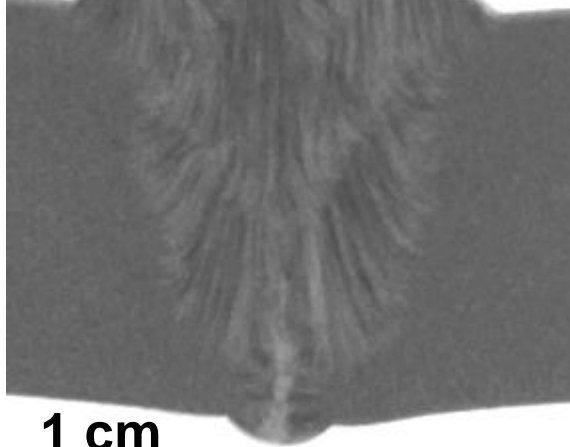
Neutron imaging

Energy-selective radiography

Weld (photo)



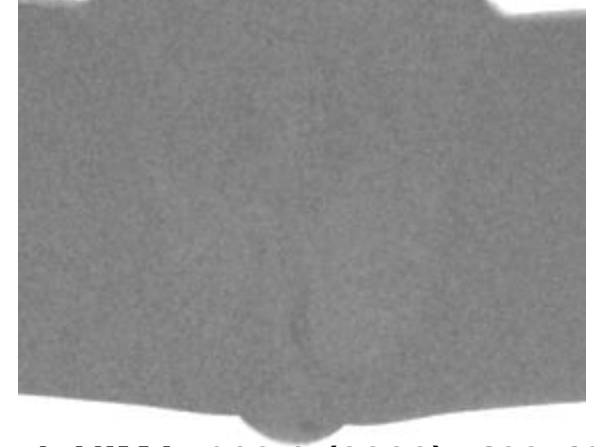
3.8 \AA



4.0 \AA



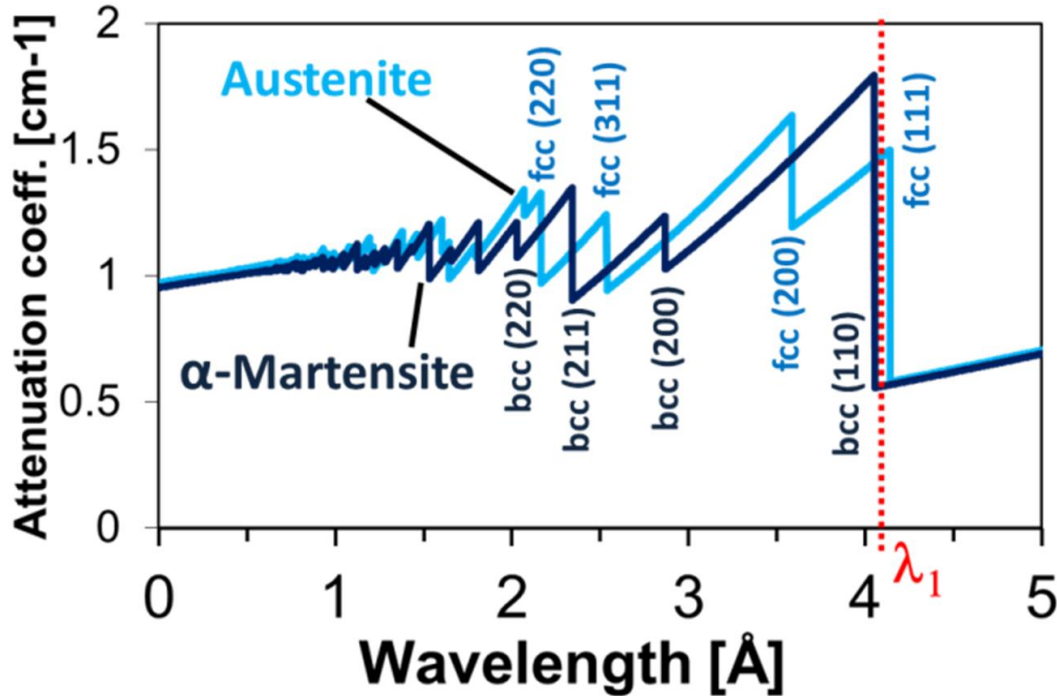
4.2 \AA



1 cm

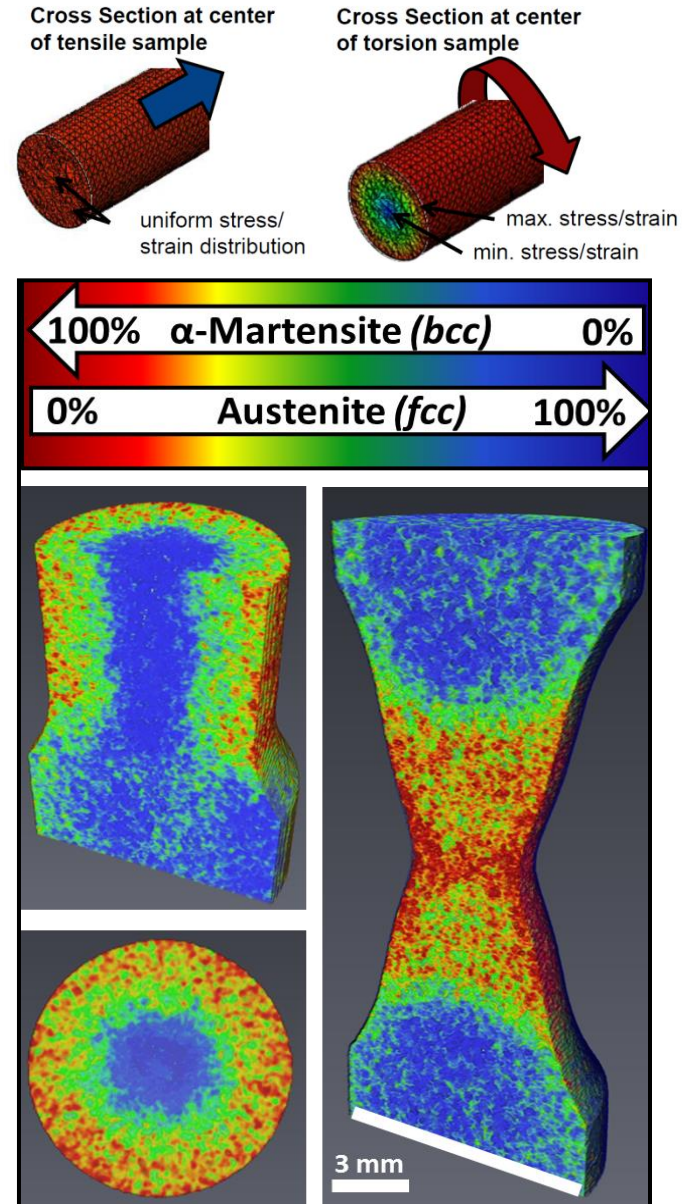
Lehmann, E. H., et al. NIMA 603.3 (2009): 429-438.

3D Phase mapping in metals



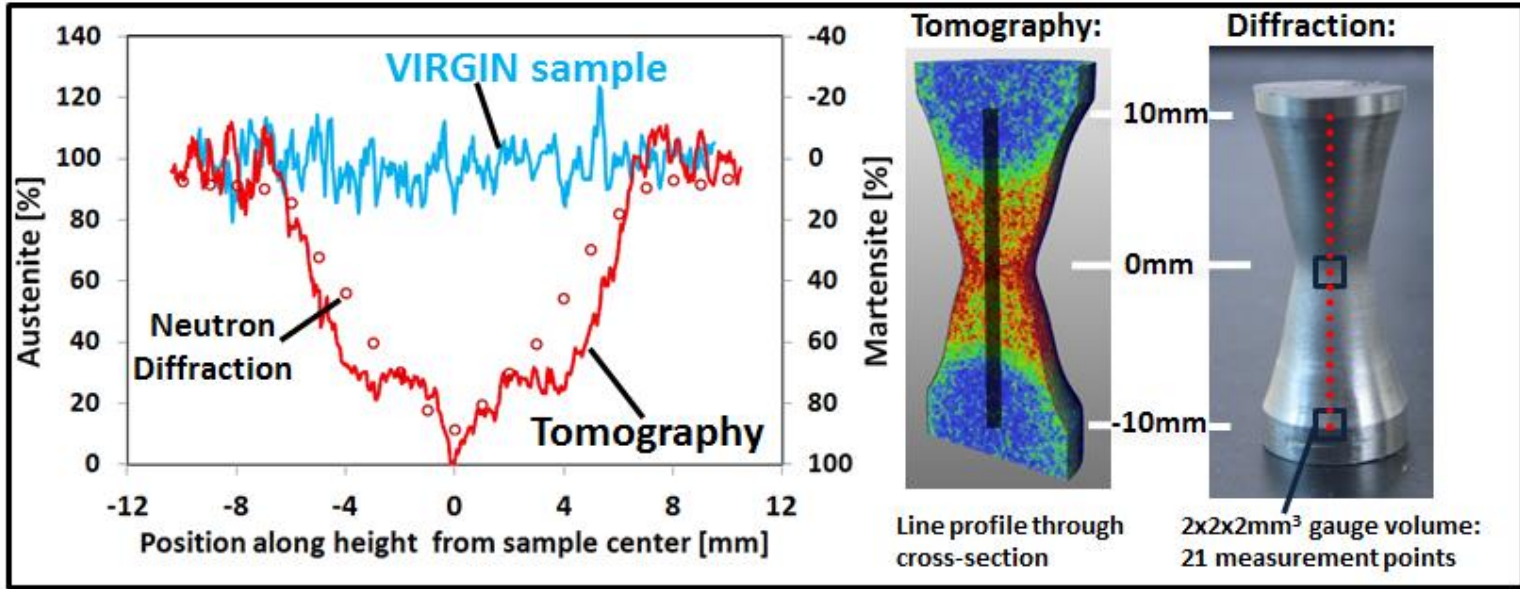
Energy-selective neutron tomography of TRIP-steel

R. Woracek et al., *Advanced Materials* 26 (2014)

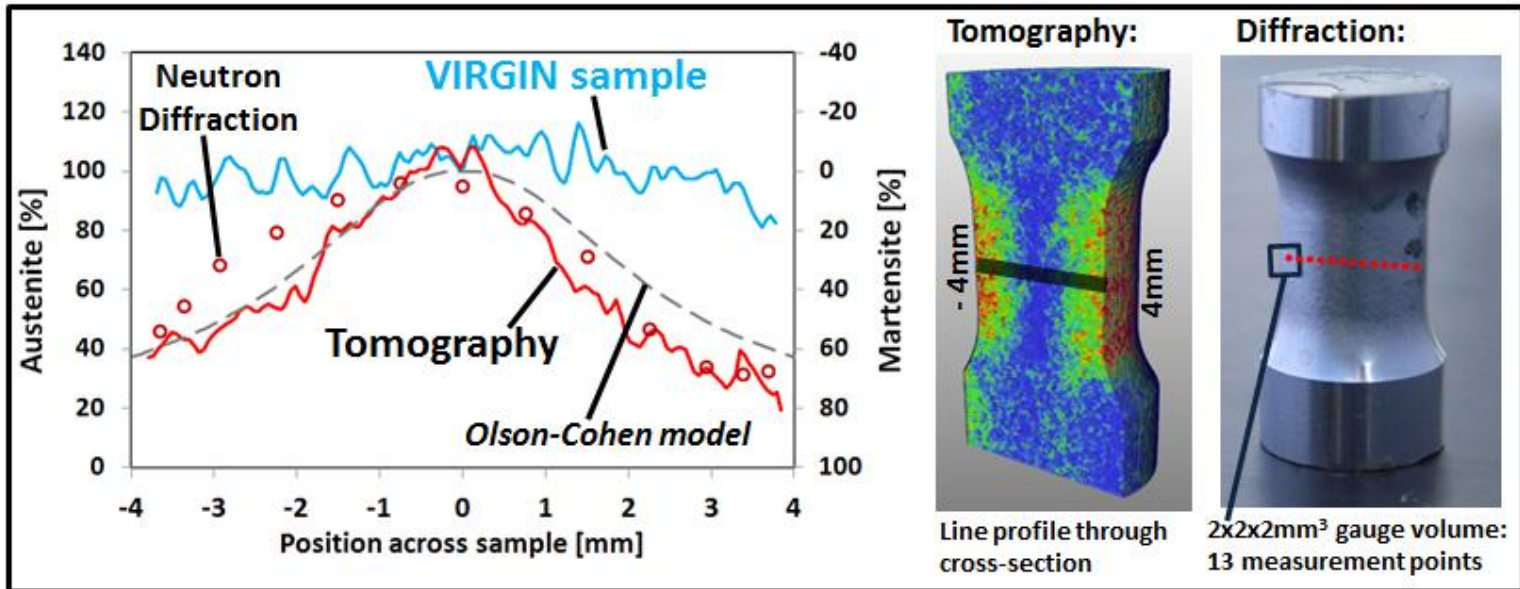


Diffraction Contrast

Tensile sample



Torsion sample



Resolution

- Beam optimisation
- Detector development

Contrast

- Neutron interaction with matter

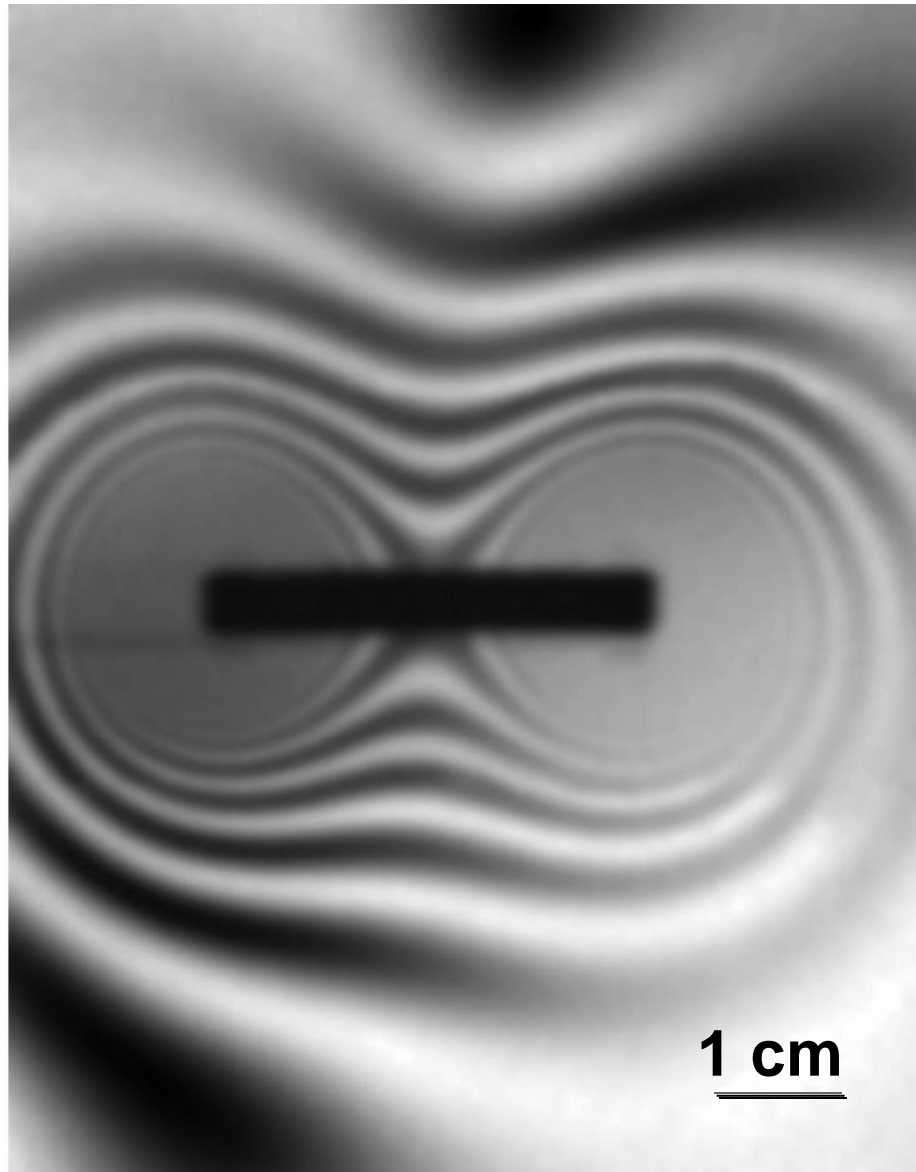
 - absorption

 - scattering

 - magnetic interaction 

Imaging with polarized neutrons

Radiography image of a bar magnet taken with polarized neutrons

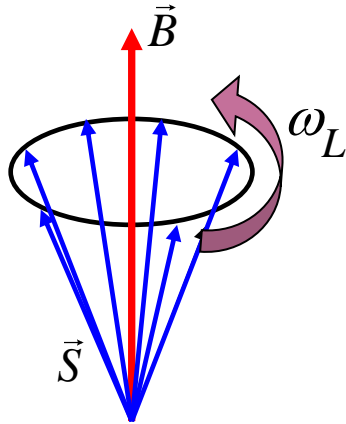


N. Kardjilov, et al,
Nature Physics 4, 399-403, (2008)

Imaging with polarized neutrons

Interactions of neutron spin with magnetic fields

Spin precession around external magnetic field



Larmor precession with a frequency:

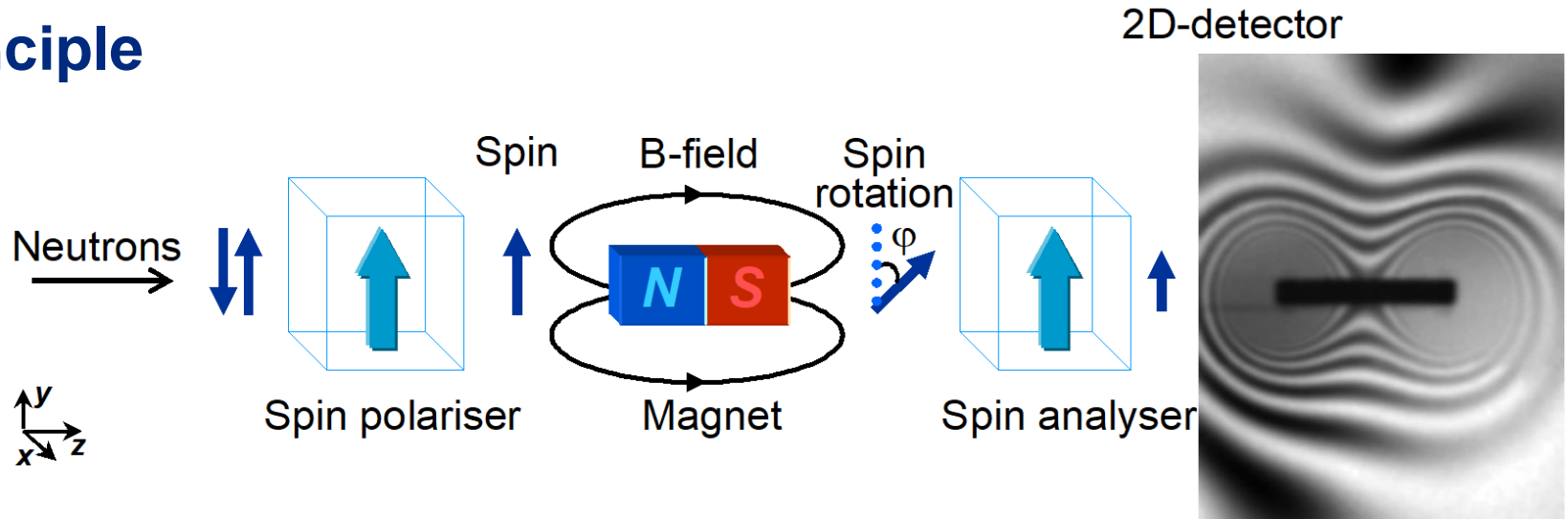
$$\omega_L = \gamma B$$

$$\gamma = 1.83 \cdot 10^8 \frac{rad}{s \cdot T} \text{ (gyromagnetic ratio)}$$

The magnetic moment is antiparallel to the internal angular momentum of the neutron described by a spin S with the quantum number $s = 1/2$.

Imaging with polarized neutrons

Principle



$$\varphi = \omega_L t = \frac{\gamma_L}{v} \int_{path} H ds$$

For the imaging setup, a polariser and analyser are used to select a defined neutron polarisation or orientation of the magnetic moment and to convert the precession angle φ of the neutron spin after transmission through the magnetic field or sample to imaging contrast, respectively.

N. Kardjilov, et al, Nature Physics 4, 399-403, (2008)

Imaging with polarized neutrons

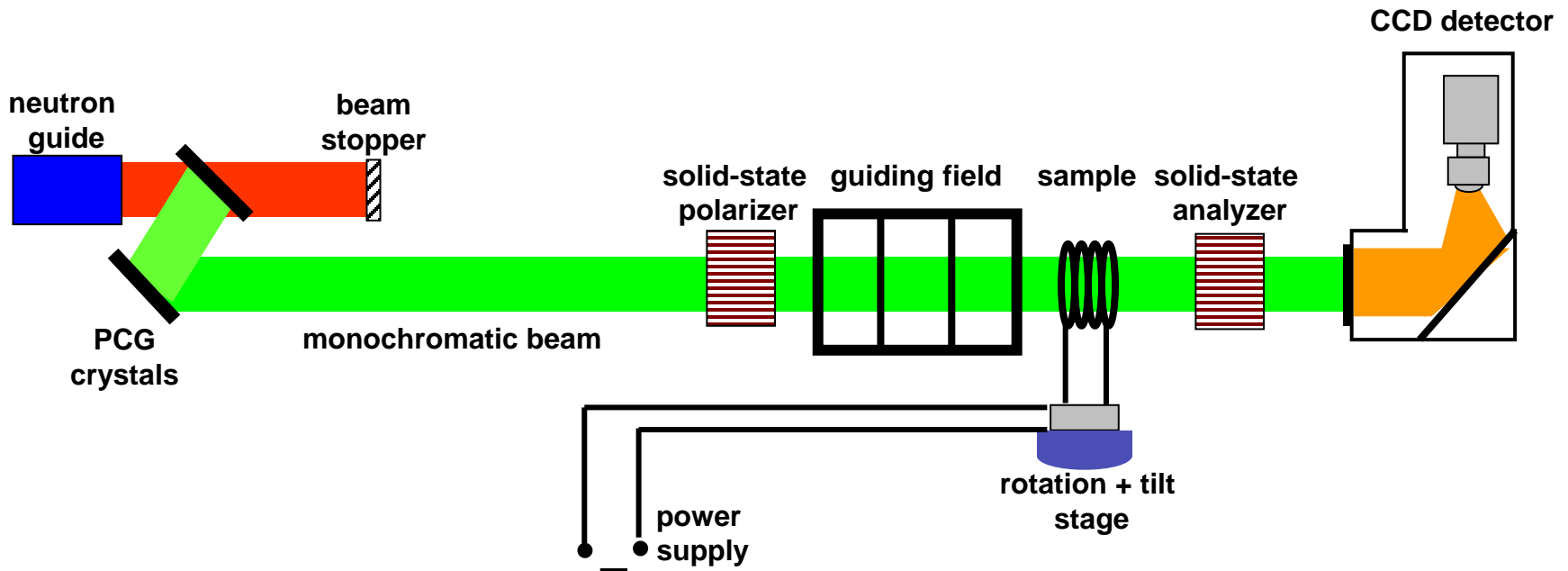
Example

Instrument: V7 (CONRAD) at HZB, Berlin

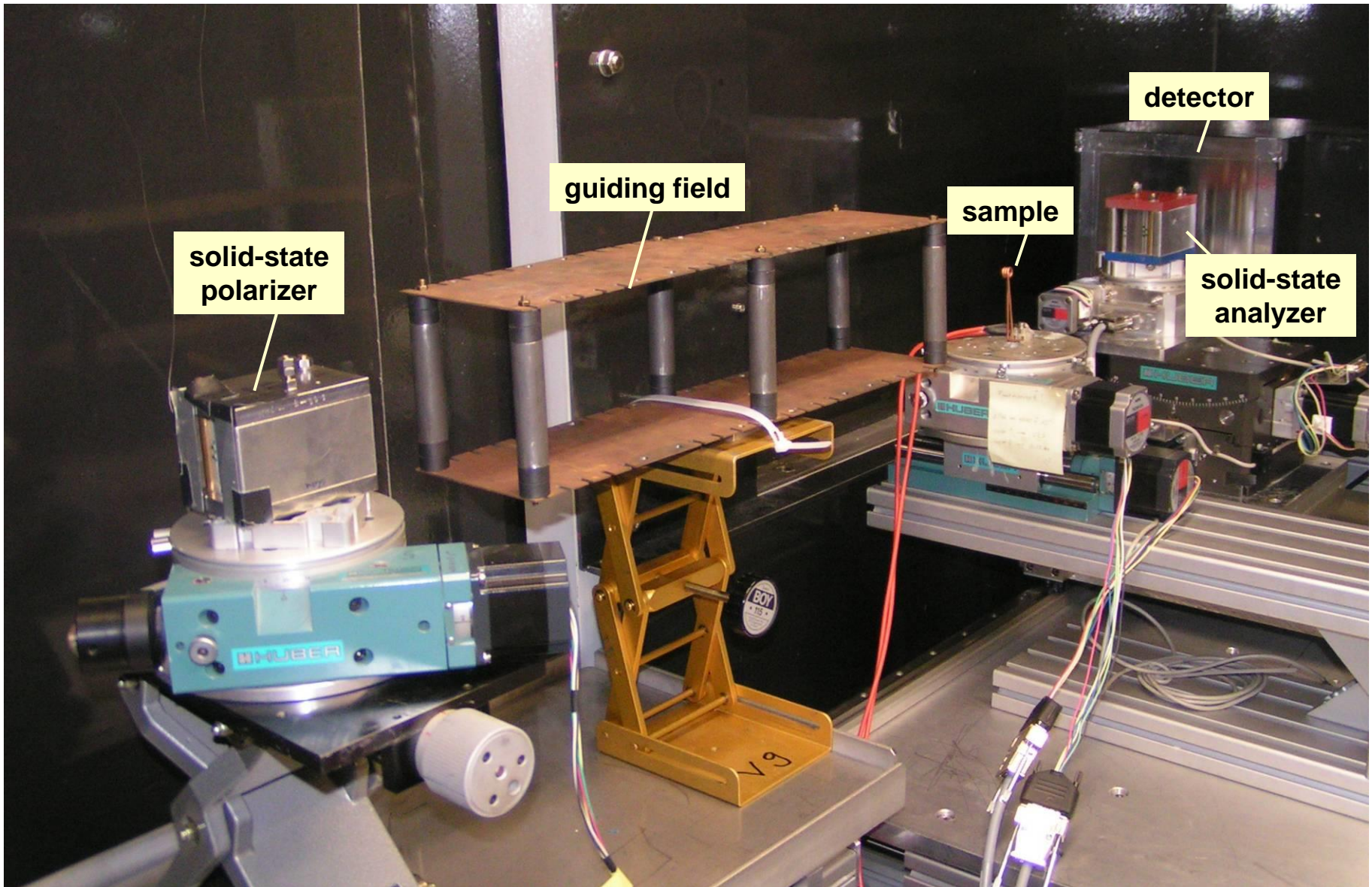
Monochromatic beam with wavelength of 4.2 \AA

Spatial resolution: 0.2 mm/pixel

Experimental sketch:

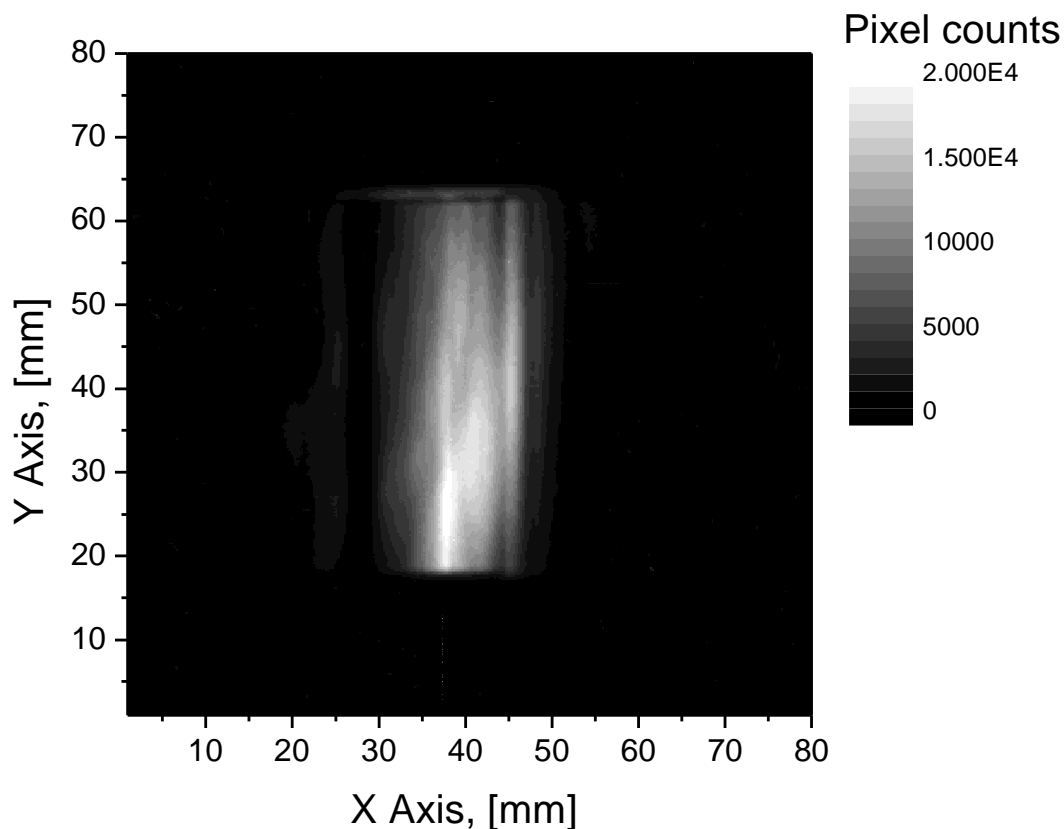


Imaging with polarized neutrons



Imaging with polarized neutrons

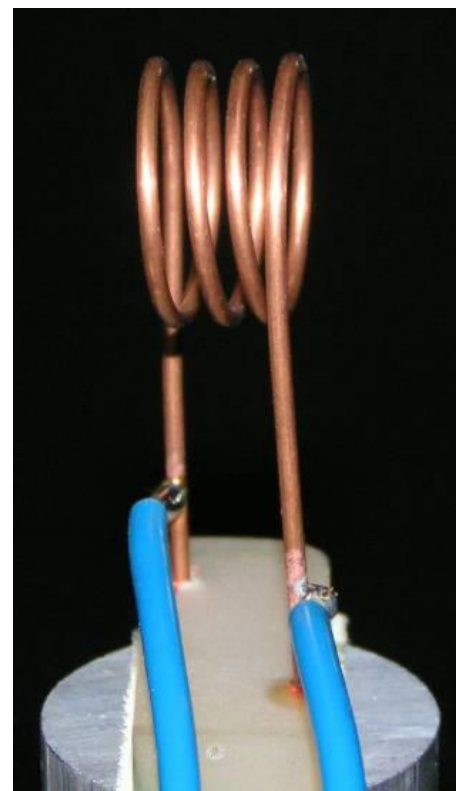
Open beam (without sample)



Exposure time: 300 s

Binning: 2x2

Sample

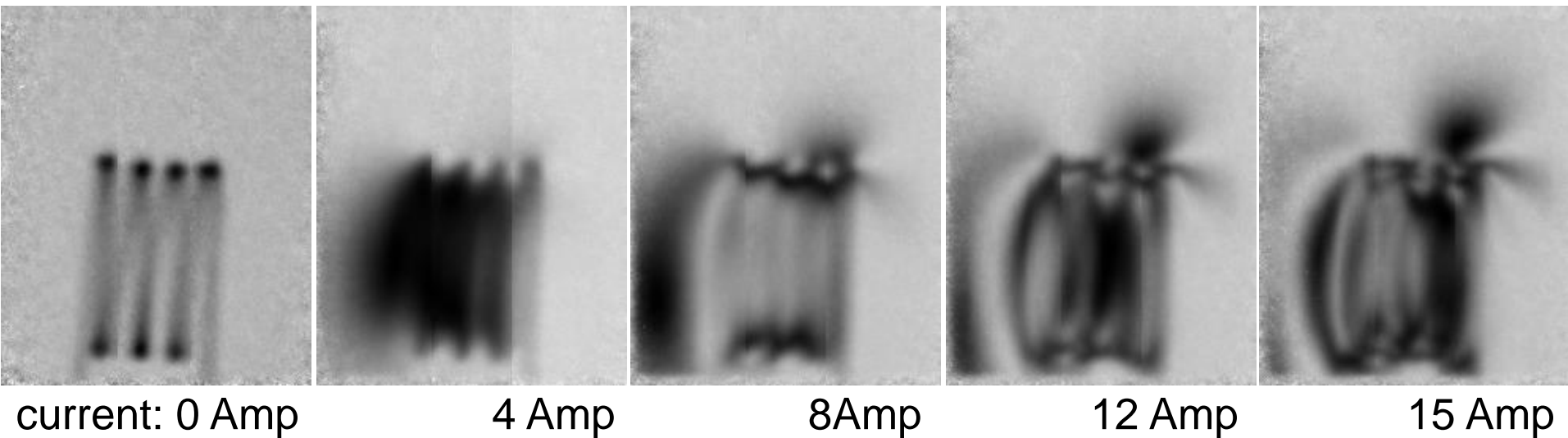


Copper coil

Wire thickness: 2 mm

Imaging with polarized neutrons

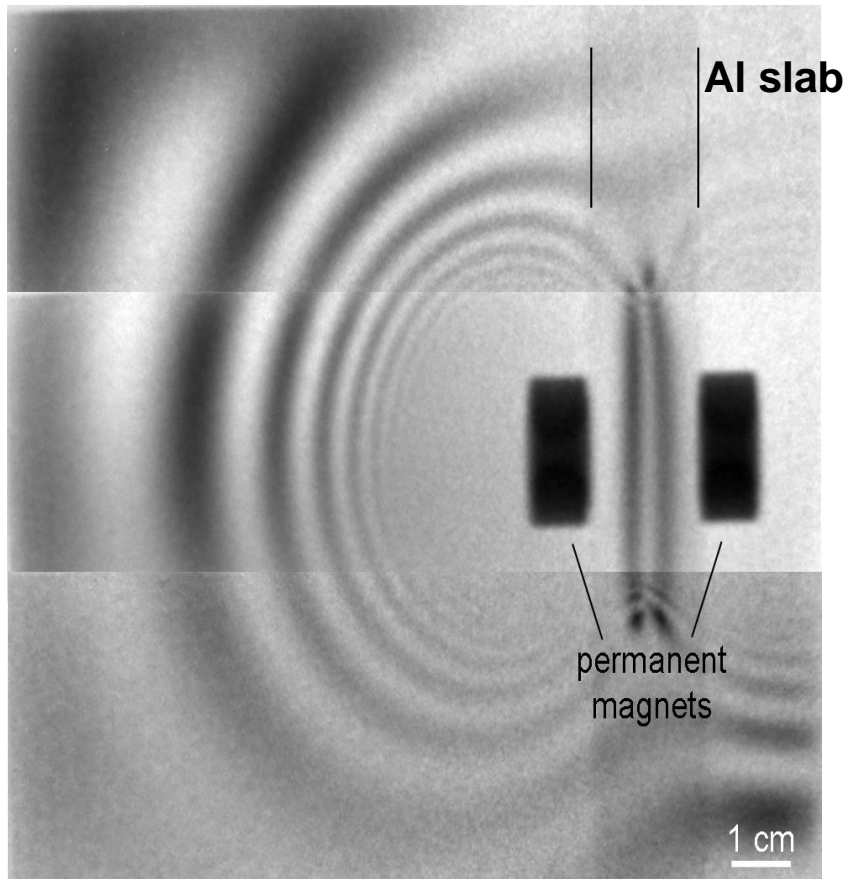
Radiography of magnetic field produced by a copper coil applying different currents using polarised neutrons



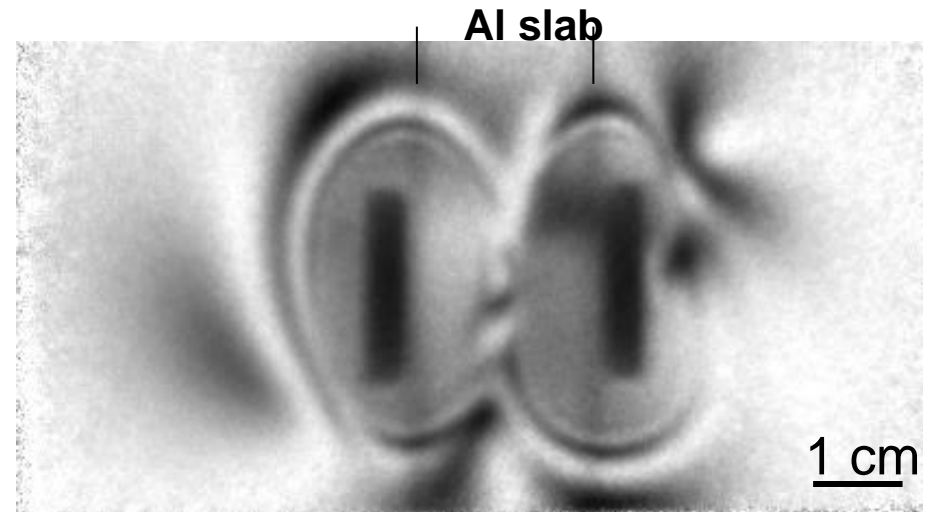
For the imaging setup, a polariser and analyser are used to convert the precession angle φ of the neutron spin after transmission through the magnetic to imaging contrast, respectively.

Imaging with polarized neutrons

Radiography of magnetic field produced by permanent magnets using polarised neutrons



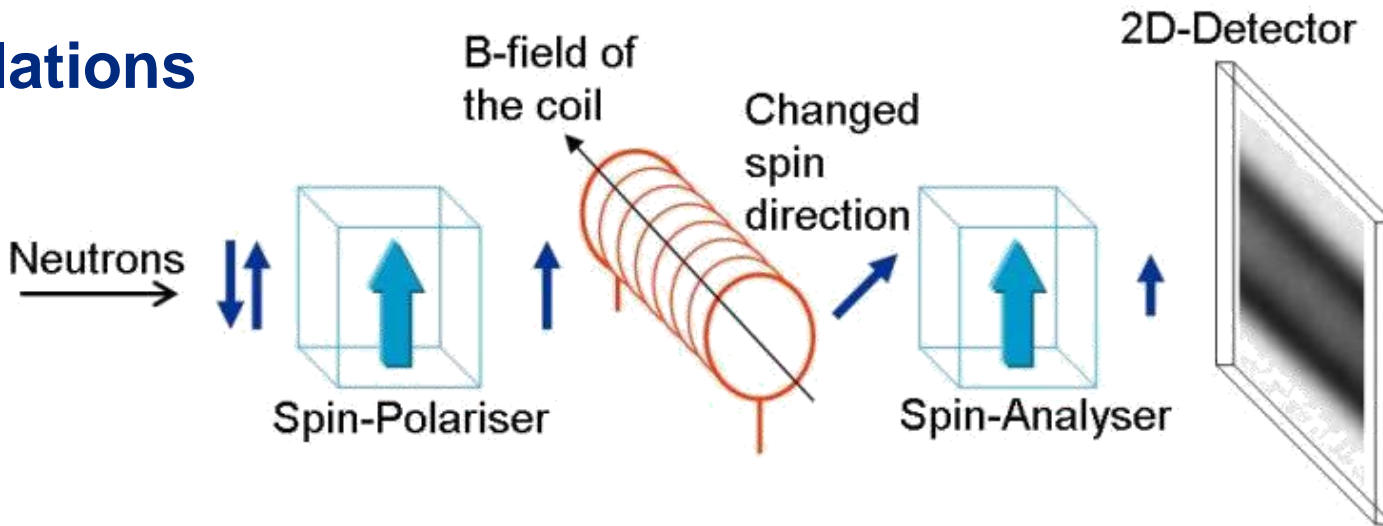
dipole magnets



non-dipole magnets

Imaging with polarized neutrons

Simulations

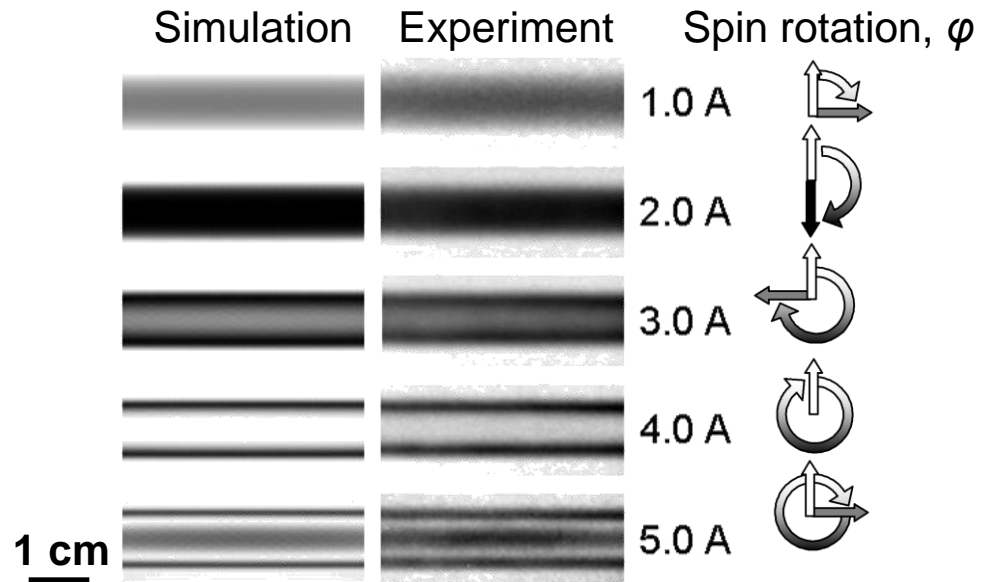


Biot-Savart law

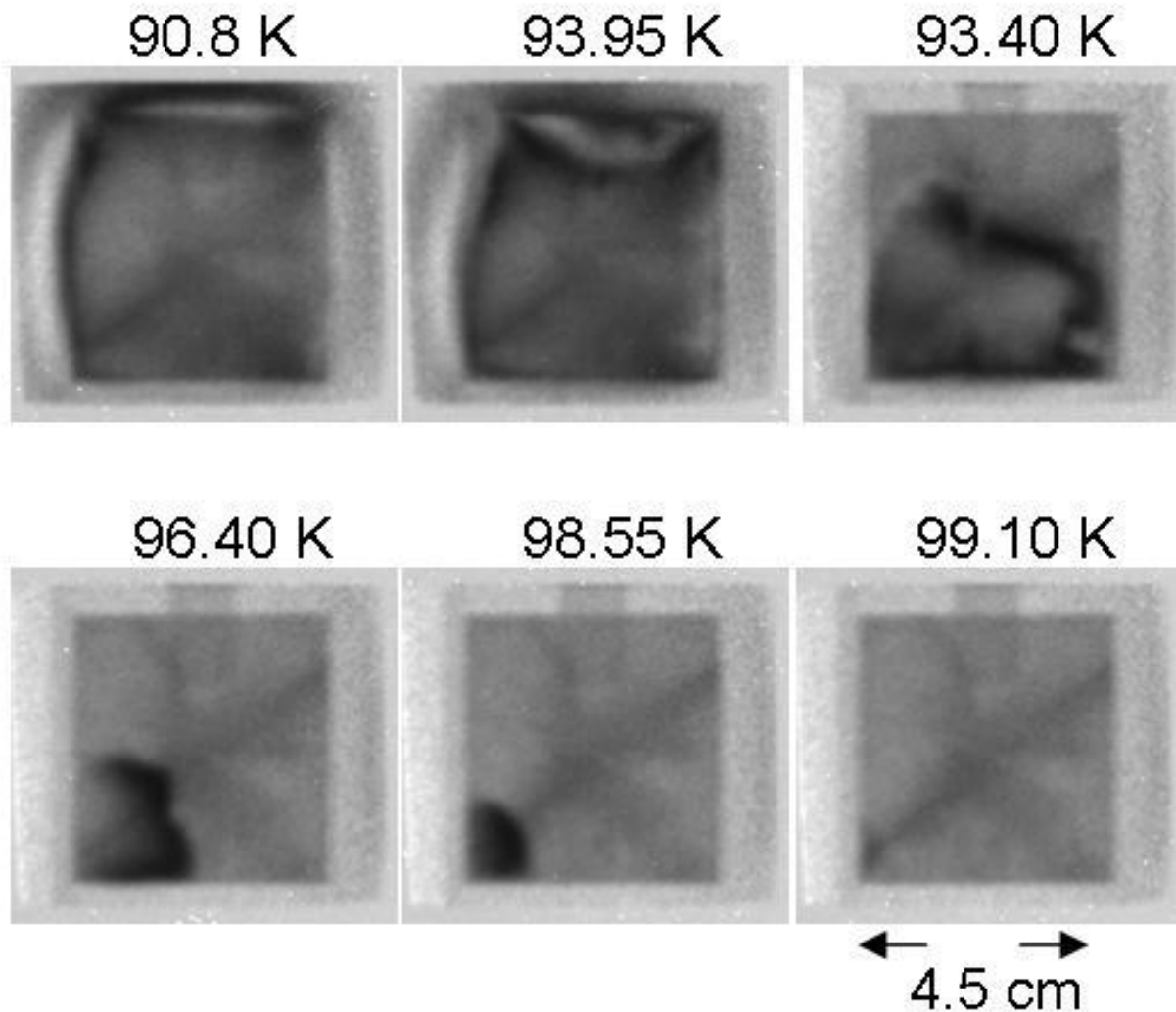
$$d\vec{B} = \frac{\mu_0}{4\pi} \frac{Id\vec{l} \times \hat{r}}{r^3}$$

$$\phi = \frac{\gamma_L}{v} \int_{path} B ds$$

Spin rotation

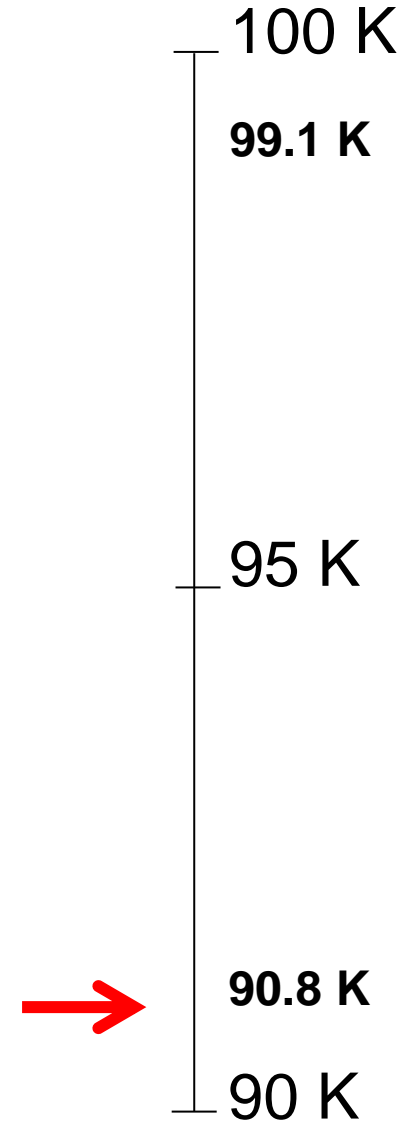


Magnetic Contrast



Flux trapping in a 45x45x12 mm² bulk YBCO sample.

Magnetic Contrast

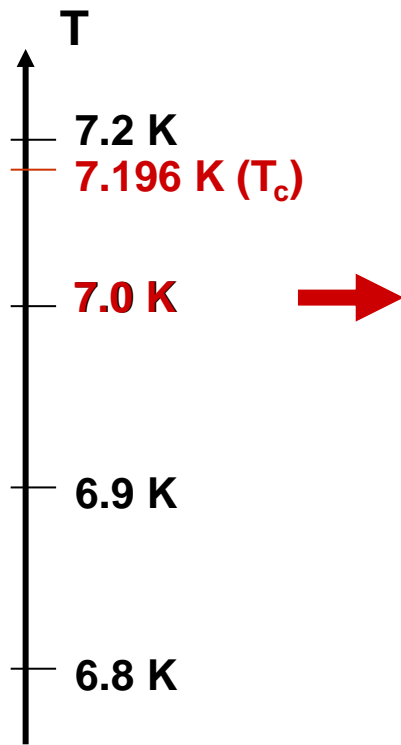
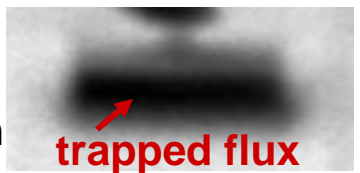
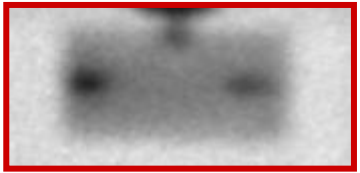
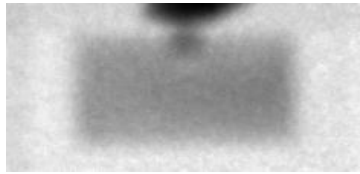


Flux trapping in a 45x45x12 mm² bulk YBCO sample.

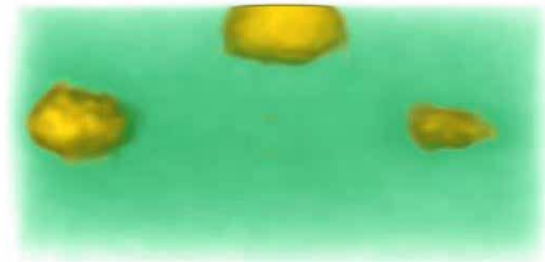
Magnetic Contrast

Example: Flux pinning

Pb cylinder
(polycrystalline)



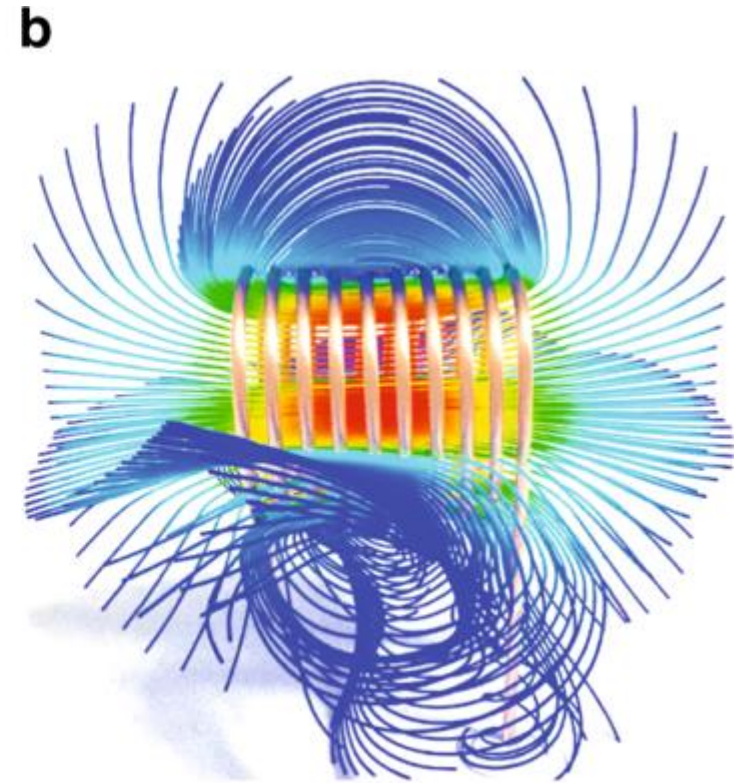
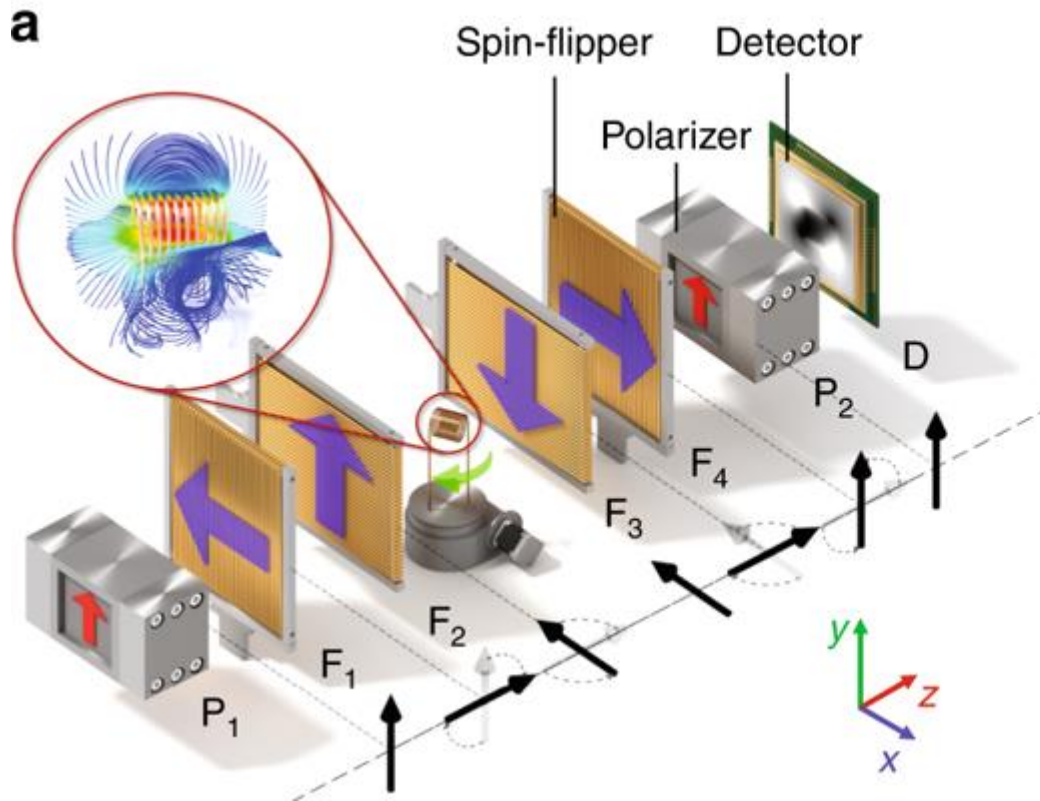
Tomography



Flux pinning at cooling down below T_c while applying a homogenous magnetic field of 10 mT perpendicular to the beam.

The images were recorded after switching off the magnetic field.

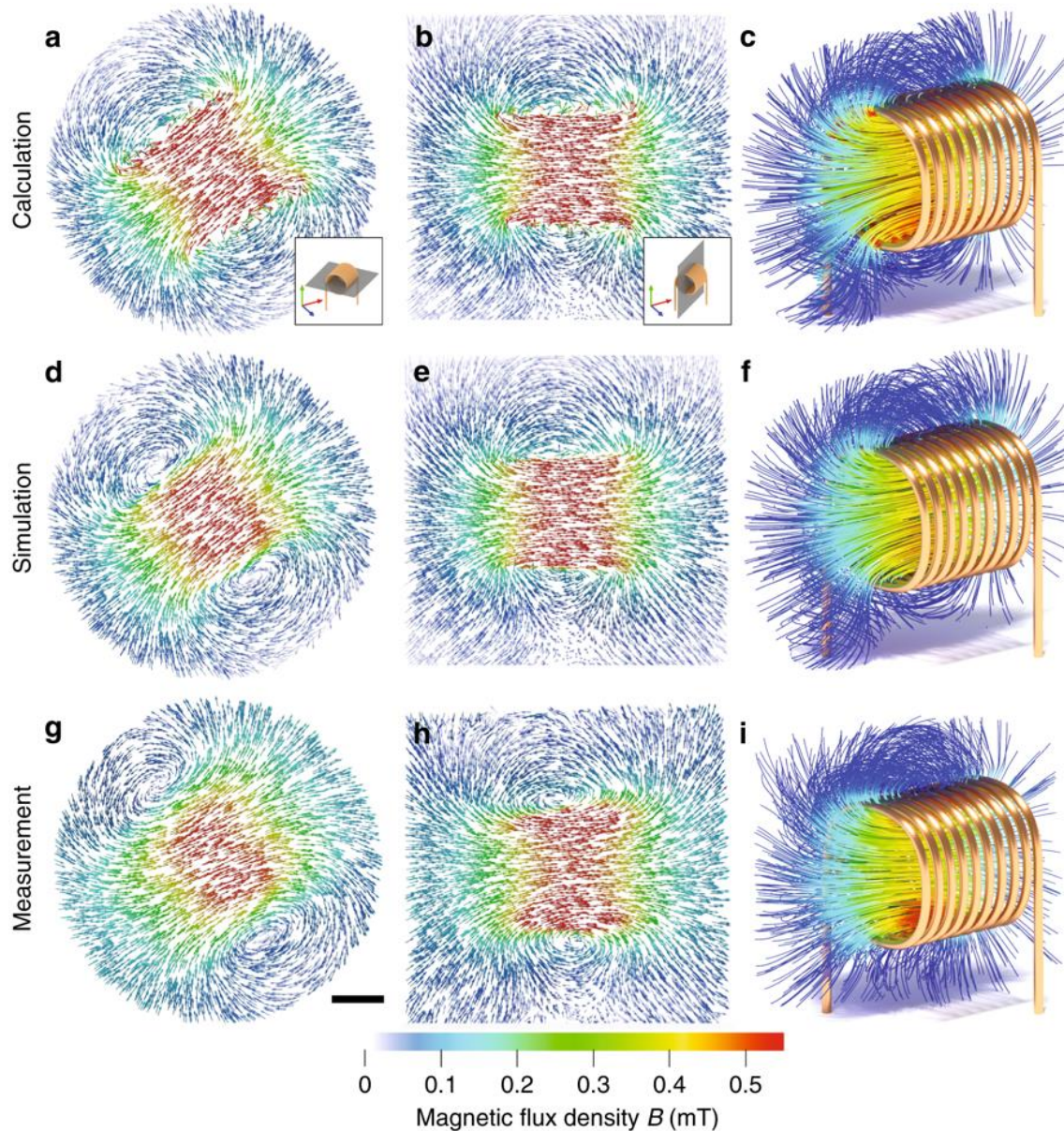
Experimental setup



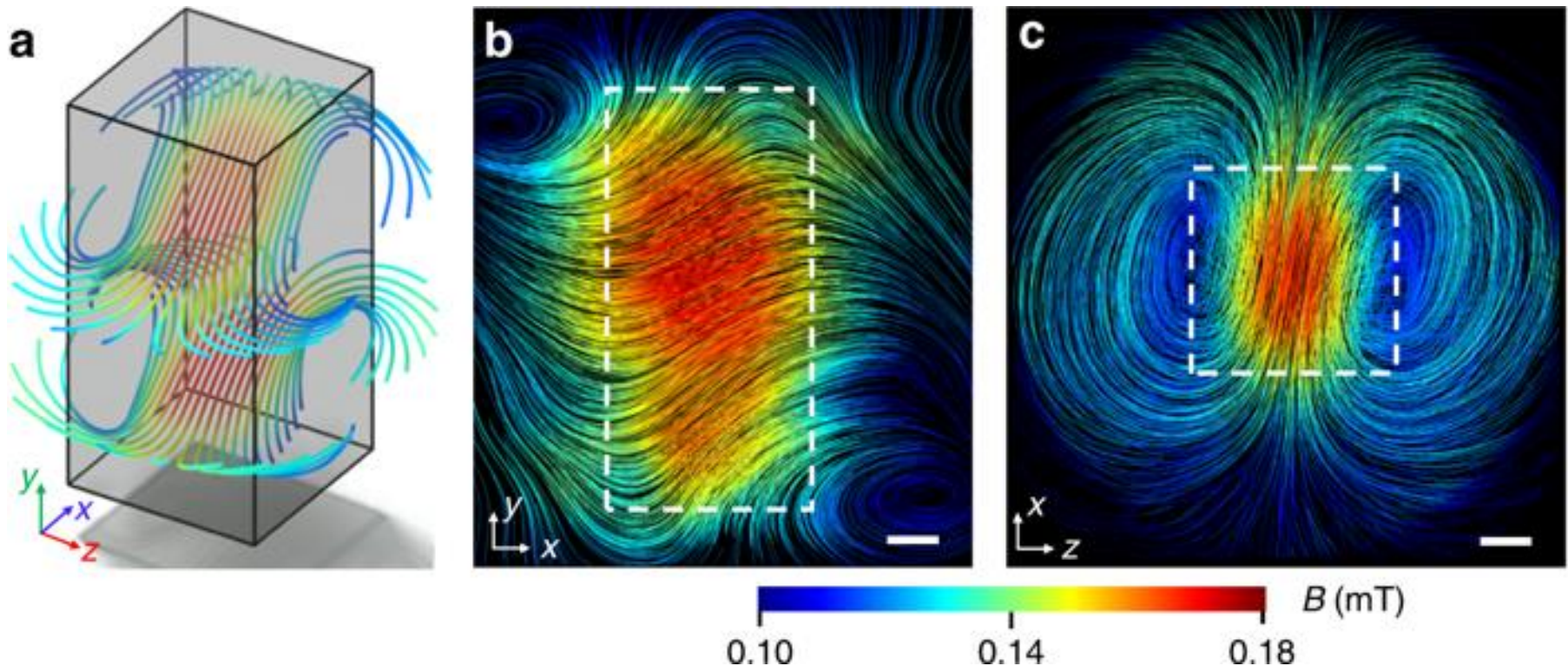
Tensor tomography. **a** Schematic drawing of the setup used for tensor tomography with spin-polarized neutrons, comprising spin polarizers (P), spin flippers (F) and a detector (D). **b** Selected magnetic field lines around an electric coil (calculation)

A. Hilger, et al, *Nature Communications* 9.1 (2018): 4023

Tensorial reconstruction



Quantitative magnetic tomography



Magnetic vector field inside a superconducting lead sample measured at $T = 4.3$ K. **a** Some selected magnetic field lines show the location of the magnetic field inside the sample indicated by the cuboid. **b** Magnetic field lines in a selected xy plane (silhouette of the lead sample marked by dotted lines). Scale bar, 5 mm. **c** Magnetic field lines in a selected xz plane. Scale bar, 5 mm.

A. Hilger, et al, *Nature Communications* 9.1 (2018): 4023

Neutron Imaging (NI)

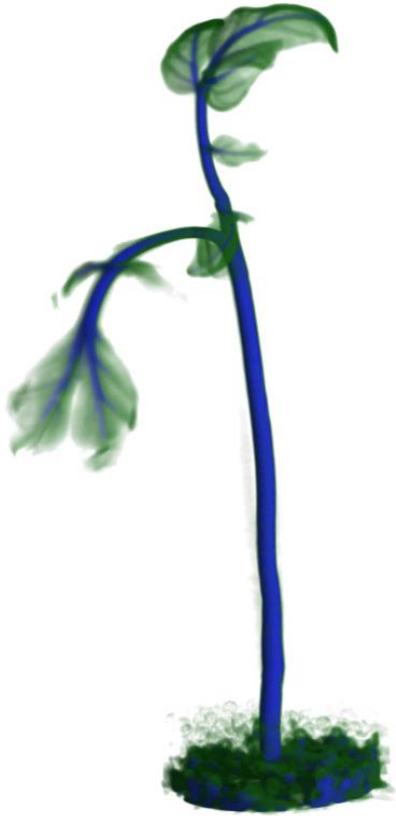
- is a technology to produce visible information of objects and structures by using beams of free neutrons
- due to the high penetration power of neutrons for most of the observed materials also inner features can be visualized
- NI is therefore a suitable tool for non-destructive testing and for applied research

ADVANTAGES

- no charge: often deeper penetration
- magnetic moment: magnetic interaction with nuclei → polarized neutrons
- high sensitivity for light elements
- different isotopes can be distinguished (D:H, B-10:B-11, Li-6: Li-7, U-235:U-238)
- energy selection using time-of-flight (at pulsed sources)

DISADVANTAGES

- neutron intensity limited
- no direct detection – a secondary process is needed (limiting spatial resolution)
- no charge: no focusing and guiding by el.-magnetic fields possible
- risks of samples activation



Thank you !

<https://www.helmholtz-berlin.de/>